SSI Ref: 1076

NONLINEAR GLOBAL STABILITY ANALYSIS OF COMPRESSOR STALL PHENOMENA

NASA Lewis Research Center

Contract No. NAS3-24089

Hamid Razavi
Scientific Systems, Inc.
54 Rindge Avenue Extension
Cambridge, MA 02140

June, 1985

This material is based upon work supported by NASA Lewis Research Center under Contract NAS3-24089. Any opinions, findings, and conclusions or recommendations expressed in this publication are those of the author and do not necessarily reflect the views of the National Aeronautics and Space Administration.

TABLE OF CONTENTS

Preface 1
1. Summary 2
2. Introduction 4
3. Pertinent Background in Bifurcation Techniques 8
   3.1 Introduction 8
   3.2 Hyperbolic Fixed Points and Linearization 8
       Result 1 10
       Result 2 11
   3.3 Center Manifolds 11
       Result 3 12
   3.4 Hopf Bifurcations 14
       Result 4 16
4. Three Interlocking Models 18
   4.1 Introduction 18
   4.2 State Space Relations for Positive Flow Stalled Dynamics (PS) ... 19
   4.3 State Space Relations for Unstalled Dynamics (US) 20
   4.4 State Space Relations for Reverse Flow Stalled Dynamics (RS) 21
   4.5 Typical Output Relations 22
   4.6 Linking the Models 25
5. Equilibrium Loci 26
   5.1 Introduction 26
   5.2 (RS) Model Contains No Equilibria 26
   5.3 Generation of Equilibria By Continuation 27
   5.4 BISTAB: Computational Tool for Bifurcation and Stabiity Analysis 28
   5.5 Equilibrium Solutions for (US) and (PS) 28
6. Bifurcation - Catastrophe Loci 36
   6.1 Introduction 36
   6.2 Bifurcation of Solutions and Stall/Recovery 36
   6.3 Hopf Bifurcation 45
   6.4 Global Bifurcation of Limit Cycles 52
   6.5 Time Simulations 56
7. Domains of Attraction for Off-Design Stability, Stall/Recovery, and Sensitivity Analysis 63
   7.1 Introduction 63
   7.2 First Stage, Second Stage, Third Stage Stall/Recovery 63
   7.3 Domains of Attraction 66
   7.4 Transient Analysis and Corrected Flow 67
   7.5 Domain of Attraction as Stability Set and Criterion for Stall ... 69
   7.6 Some Experimental Results for Stall/Recovery and Sensitivity Analysis 71
8. Concluding Remarks and Suggestions for Further Research 75

Bibliography 77

Appendix A A-1
Appendix B B-1
Appendix C C-1
Appendix D D-1

PREFACE

This work was performed by Scientific Systems, Inc. from December, 1983 to February, 1985 under NASA Award No. NAS3-24089. The work represents an initial investigation into the applicability of bifurcation-catastrophe techniques to the compressor stall phenomena. Dr. Leon Wenzel was the contract monitor for NASA.

Dr. R.K. Mehra was the project supervisor. Dr. H. Razavi was the principal investigator. Partial computing support was provided by Mr. S. Negahdaripouri. Special thanks goes to Ms. Alina Bernat for her skillful supervision of the documentation.

1. SUMMARY

Compressor stall phenomena are analyzed from a nonlinear control theory viewpoint, based on bifurcation-catastrophe techniques. This new approach appears promising and offers insight into such well known compressor instability problems as **surge** and **rotating stall**; furthermore it suggests strategies for recovery from stall. More specifically, three interlocking dynamic nonlinear state space models are developed. The models, which are based on Wenzel, Bruton (1982), represent compressor operation under normal **unstalled** conditions (US), and **stalled** compressor operation under **normal** and **reverse** flow conditions (PS and RS, respectively). It is shown that the problem of rotating stall can be viewed as an induced bifurcation of the solution of the (US) model. Both equilibrium and bifurcation loci are generated in the state-parameter space, based on parameter continuation techniques combined with catastrophe/singularity theory. **Hysteresis** effects are shown to exist in the stall/recovery process. Surge cycles (of about 50 cycles/sec) are observed for some critical parameter values. It is shown that the oscillatory behavior is due to development of **limit cycles**, generated by **Hopf bifurcation** of solutions. More specifically it is observed that at certain critical values of parameters a family of **stable** limit cycles with growing and then diminishing amplitudes is generated, then giving rise to an **unstable** family of limit cycles. This unstable family in turn bifurcates into other unstable families (as indicated in the diagrams). The quantitative approach adopted for generation and continuation of limit cycles employs a number of notions from topology, differential calculus, and singularity theory. (Unstable limit cycles can not be detected by simulation techniques, though their presence vastly influences the system dynamics.) To further illustrate the usefulness of the methodology some partial computation of **domains of attraction** of (US) and (PS) equilibria is carried out, though this objective is clearly beyond the scope of this investigation. This provides a global picture, suitable to address the non-steady state 'off-design' instability conditions which are present before the onset of stall.

The domains of attraction of equilibria help define the 'position' of system trajectories in a global sense, and in this way provide a natural

classification of trajectories with respect to their stall/recovery characteristics. Three types of trajectories are defined according to the 'severity' of their stall/recovery action: 1st stage recoverable, 2nd stage recoverable, and 3rd stage recoverable. Finally, it is argued that the use of corrected flow (e.g. a scalar output variable), as the sole indicator of stall behavior may lead to incorrect conclusions with respect to recoverability of trajectories. In particular it is argued that neither the corrected flow rate nor the turbine area (or any other single scalar variable) can provide an unambiguous measure of stability. The use of the domain of attraction of some normal operating point(s) is proposed as a useful mechanism for stall detection, and recovery. By varying the parameters over their feasible range, the size and shape of the domains of attraction change, leading to the determination of those trajectories which may be recovered by appropriate control actions. Furthermore this approach provides a natural framework for carrying out parameter **sensitivity analysis** yielding the impact of various parameter changes on recovery from stall. Some sample sensitivity computations are also offered.

2. INTRODUCTION

Stability of aircraft engines over their operating envelopes is a primary design consideration. The degree of stability varies due to a number of factors such as engine operating condition, inlet flow conditions, age, and control tolerance and is generally a trade-off with performance; that is, for a given engine, increases in performance are attained at the expense of reduced stability margin. As a result, gas turbine engines have experienced stalls or surges throughout their history as aircraft power plants.

The stall problem has been receiving increasing attention in recent years. It was the subject of a recent NASA Lewis Workshop (1983). The major aircraft engine manufacturers such as GE and Pratt & Whitney are developing complex simulation models, whereas research at universities (MIT, Cornell) is aimed at developing a more basic understanding of the problem.

Most stalls result in momentary disturbances to engine operation and recover without any active intervention. Some stalls are of more serious nature and require **engine shutdown** to restore normal engine operation. Such stalls are typically characterized by low engine speed and high turbine temperatures together with low thrust; these stalls are referred to as **nonrecoverable, stagnation,** or **hung stalls.** Prolonged operation in nonrecoverable state can result in turbine damage due to over-temperature; in this state the engine is not responsive to scheduled inputs. Indeed, as expressed in Stetson (1983), "one of the most critical functional problems that a high technology turbine engine encounters is nonrecoverable stall."

In recent years, the incidence rate of nonrecoverable stall has increased by a great deal. This is mainly due to the increased use of augmented, mixed-flow, turbofan engines in modern aircraft due to their wide performance range, compact size, and flexibility. In these aircraft the engine is a highly interactive system. This interaction between components can directly affect the stall/surge characteristics through complicated feedback paths (Patterson (1983)).

In the following paragraphs we discuss the above issues in some more detail.

Typically, multimission aircraft experience a wide range of Mach numbers, Reynolds numbers, angles of attack, side slip angles and dynamic motions in longitudinal and lateral planes. However, aircraft, including the propulsion system, have historically been designed for steady conditions with minimum attention to the effect of distorted flow. Actual operation of the aircraft is in an environment which is unsteady, and in which the propulsion system experiences distorted flows.

The propulsion system, consisting of the gas turbine engine, is particularly sensitive to these "off design" operating conditions. In particular, it is the compressor which has a narrow operating range. If one exceeds the limits of the operating range, the compressor operation becomes unstable. Such instabilities may affect the flow in the entire engine. The combustor or afterburner may discontinue burning, resulting in loss of thrust for the aircraft.

The result of many of these instabilities is only a temporary disruption (less than a second, say) of the unstalled operation of the engine. In some cases, however, the consequence of the initial instability is a situation in which the engine will not recover to unstalled operation and will have to be shut down and restarted in flight, and this has an obvious implication for the effectiveness of the aircraft.

If such a non-recoverable stall occurs the sequence of events is that the turbine inlet temperature will rise and the engine speed will fall. The rate at which the former occurs is determined from the interactions of the fuel control and the compression, burner and turbine system. The drop in speed arises due to the mismatch of turbine and compressor work, because of the very low compressor efficiencies in this regime. The danger from non-recoverable stall is that the combustor exit temperature (turbine inlet temperature) will exceed the allowable limits for the turbine and/or that the rotor speed will fall below the level that the gas turbine power cycle is self-sustaining. If so, it is generally necessary to shut the engine down and cool it before restarting.

As stated this problem has received a great deal of attention in recent years, and there has been much work on the topic, at levels ranging from examination of the detailed fluid mechanics of unsteady boundary layers on compressor blades to analysis and experiments which attempted to consider a description of the overall system. These latter results have proved to be of significant help in understanding the overall phenomenon.

A basic analysis of this type was presented in Greitzer (1976) in which the nonlinear behavior of a model compression system was examined. Experiments were also carried out to validate system modeling. Since that study, system models have also been carried out by many other investigators.

At NASA Lewis, Wenzel and Bruton (1982) have developed a lumped parameter simulation model of the TF34 engine to study the nonrecoverable stall phenomenon. This study, in fact, forms the basis of the models presented in this report. Other relevant NASA reports include: Szuch and Seldner (1975), Szuch, Seldner and Cwynar (1977), Szuch (1978); and Seldner, Mihaloew and Blaha (1972). A major theoretical contributor is Frank Moore (1983). Another contribution to the subject is the classic work of Emmons et al. (1955), which appears to have laid the foundation for much of the current research in the compressor stall area.

Though, as the bibliography indicates, there has been considerable interest in the subject of stall, the phenomenon is still not well understood, especially with regard to the system behavior **subsequent** to the onset of instability, i.e., the **post stall** response of the system. This is true not only as far as tests and/or experiments are concerned, but also as far as modeling and analytical understanding are concerned. This is in part due to the fact that the post-stall transients involve very complicated nonlinear interactions and feedback mechanisms -- a heavily mathematical subject. In particular, up until the present there has not been an attempt to bring to bear on this problem some of the modern mathematical techniques employed in nonlinear control theory. This report presents such an analysis.

This work addresses the application of bifurcation-catastrophe theory to the problem of nonlinear compression system stability. It is thus an attack on the problem from a different viewpoint than existing work in this area. Hence it provides a complementary perspective for analyzing the strongly nonlinear dynamics of compression systems.

The report is organized as follows. Chapter 3 presents some background information on bifurcation theory used in subsequent chapters. Chapter 4 presents three state space models of compressor dynamics: one for the unstalled compressor, and two for the stalled compressor — corresponding to normal flow and reverse flow conditions. (Appendices B, C, and D present a derivation of the models based on the modified Wenzel-Bruton (1982) results.) In Chapter 5, generation of equilibrium surfaces is discussed. Chapter 6 is devoted to the analysis of bifurcation-catastrophe points of the models; Hopf bifurcation points are discussed. Issues regarding stall recovery are discussed in Chapter 7; three types of trajectories corresponding to their stall/recovery behavior are defined. Finally, Chapter 8 contains some concluding remarks.

3. PERTINENT BACKGROUND IN BIFURCATION TECHNIQUES[1]

3.1 Introduction

While linear control theory is well developed by now, the same assertion cannot be made about the nonlinear theory. The problem is even more frustrating if one is interested in obtaining computable results in particular. This is due to the fact that nonlinear theory tends to be more qualitative.

One of the most exciting developments in the field of nonlinear stability theory has been that of bifurcation theory -- pioneered by the work of Poincare, and later refined by Andronov (1937, 1966), Hopf (1942), and others. The importance of this theory is in its practical applicability. For example, in elastic stability, bifurcation is called **buckling**, and in hydrodynamic stability bifurcating solutions are referred to as transitions. It has numerous applications in many other physical systems.

Another important feature of the theory is in its ability to provide a global picture. That is, it gives information about all of the "turning points" of the solutions. This is in contrast to linearization procedures, in which only local stability is characterized. In fact, in a certain sense, bifurcation theory takes over when linearization fails.

3.2 Hyperbolic Fixed Points and Linearization

We shall use the above remarks to motivate our discussion. Consider the nonlinear differential equation

$$\frac{dx(t)}{dt} = f(x,\mu) \tag{3.1}$$

[1]This chapter is based on SSI's Progress Report (Jan. 1 - May 1, 1984) to NASA Lewis.

in which $x \in X \subseteq R^n$

$\mu \in U \subseteq R^m$.

We shall refer to x as the state vector and u as the control vector (or sometimes as the parameter). For the purposes of illustration let $\mu \equiv 0$, i.e., consider the system

$$\frac{dx}{dt} = f(x), \quad x \in X \subseteq R^n \tag{3.1)'}$$

Assume that the point $x_0 \in R^n$ is a stationary point of f in (3.1)':

$$0 = f(x_0) \tag{3.2}$$

and let the Jacobian matrix of partial derivates of f at x_0 be denoted as $\nabla f(x_0)$.

Consider the linear system

$$\frac{dz}{dt} = \nabla f(x_0) z \tag{3.3}$$

where

$$z = x_0 + \varepsilon, \quad \varepsilon << 1 \tag{3.4}$$

The major question to be addressed is what we can say about the solutions of (3.1)' based on our knowledge of (3.3)? This question is of interest since the solutions of (3.3) are given by:

$$z(t) = e^{t\nabla f(x_0)} z(0) \tag{3.5}$$

To relate (3.5) and solutions of (3.1)' let $\phi_t(x)$ denote the flow generated by f, i.e., a smooth function defined for all $x \in X$ and $t \in (a,b) \subseteq R$ such that

$$\frac{d}{dt}(\phi_t(x)) = f(\phi_t(x)) \tag{3.6}$$

for all $x \in X$ and $t \in (a,b)$. We now state a fundamental result in nonlinear system theory which provides the answer.

Result 1 (Hartman (1964))

Provided that $\nabla f(x_0)$ has no purely imaginary or zero eigenvalues, there is a continuous mapping with a continuous inverse (i.e., a homeomorphism), say, g, defined on some neighborhood of x_0 in R^n locally taking trajectories of the nonlinear flow ϕ_t of (3.1)' to those of the linear flow $e^{\nabla f(x_0)t}$. The homeomorphism preserves the direction of the trajectories.

We will not provide the proof of this result here. The interpretation is that roughly speaking, as long as the linearized system has no purely imaginary or zero eigenvalues, it provides a good local picture of the nonlinear system. (It is possible to strengthen this result in the sense that the linear and nonlinear system solutions may be related via a **diffeomorphism.** But this requires certain "resonance" conditions among the eigenvalues. We shall not discuss the matter here.) The important point for our purposes is that when $\nabla f(x_0)$ has no eigenvalues with zero real parts it is acceptable to linearize. A stationary point x_0 at which $\nabla f(x_0)$ has the above property is known as being **hyperbolic.** (But of course bifurcating solutions occur precisely when this condition is **not** met!) The following result will further characterize hyperbolic fixed points (or stationary points). But first we need the following definitions. Define the **local stable** and **unstable** manifolds of x_0,

$$M^s(x_0) = \{x \in X \text{ such that } \phi_t(x) \to x_0 \text{ is } t \to \infty \text{ and } \phi_t(x) \in X \text{ for all } t \geq 0\}$$
$$M^u(x_0) = \{x \in X \text{ such that } \phi_t(x) \to x_0 \text{ as } t \to -\infty \text{ and } \phi_t(x) \in X \text{ for all } t \leq 0\}$$

Let E^s and E^u denote the eigenspaces associated with stable and unstable eigenvalues. They are respectively said to be stable and unstable eigenspaces.

Result 2 (Hyperbolic Fixed Points)

Let x_0 be a hyperbolic fixed point of (3.1)'. Then there exist local stable and unstable manifolds $M^s(x_0)$, $M^u(x_0)$, which are, respectively, of the same dimensions d_s and d_u as those of the eigenspaces E^s and E^u of the linear system (3.3). Furthermore, the manifolds $M^s(x_0)$ and $M^u(x_0)$ are tangent to the eigenspaces E^s and E^u, respectively. The manifolds are as smooth as the function f.

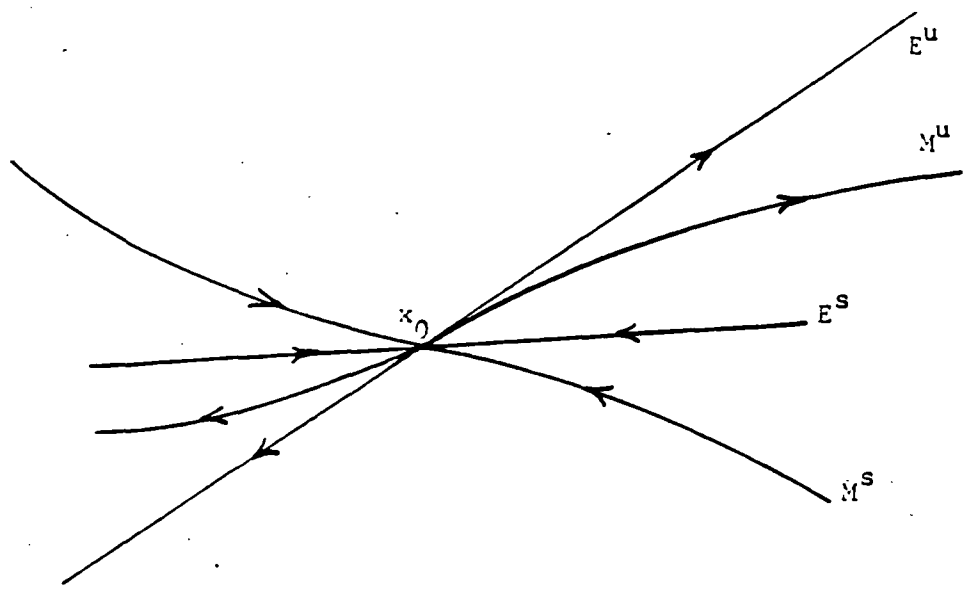

Figure 3.1 Manifolds M^s, and M^u; Eigenspaces E^s and E^u.

3.3 Center Manifolds

As mentioned previously, in bifurcation problems we are specifically interested in equilibria at which we have purely imaginary eigenvalues. On the complex plane these eigenvalues are located on the imaginary axis and separate the stable eigenvalues (e.g., those with negative real parts) from the unstable ones, (e.g., those with positive parts). Hence they are located in the "center". Thus in the linear analysis attention is focused on this center subspace associated with the purely imaginary eigenvalues. In nonlinear problems we are interested in center manifolds. The other two

manifolds are referred to as stable and unstable manifolds. By focusing on this manifold we will in fact reduce the dimension of the problem in a systematic manner.

The center manifold concept isolates the complicated asymptotic behavior by pinning down an invariant manifold tangent to the subspace spanned by the generalized eigenspace of eigenvalues on the imaginary axis. But one problem here is that center manifolds are in general not unique. This is in contrast to the stable manifolds.

The above discussion is made more precise in the following statement.

Result 3 (Center Manifolds)

Let f be k times differentiable (denoted by C^k) with $f(0) = 0$. (This may be accomplished by a shift of origin.) Thus the Jacobian in (3.3) becomes the square matrix $\nabla f(0)$. Split the spectrum of $\nabla f(o)$ into σ_s, σ_c, σ_u such that

$$\text{Re } \lambda > 0 \text{ if } \lambda \in \sigma_u$$

$$\text{Re } \lambda = 0 \text{ if } \lambda \in \sigma_c$$

$$\text{Re } \lambda < 0 \text{ if } \lambda \in \sigma_s$$

with E^s, E^u, and E^c denoting the respective eigenspaces of σ_s, σ_u, and σ_c. Then there exist C^k stable and unstable invariant manifolds M^s and M^u tangent to E^s and E^u at zero. Also there exists a C^{k-1} center manifold M^c tangent to E^c at zero. Both the stable and the unstable manifolds are unique. But in general M^c may not be unique.

The following example, due to Kelley (1967) illustrates this point. Consider the differential equation

$$\begin{aligned} \dot{x}_1 &= x_1^2 \\ \dot{x}_2 &= -x_2 \end{aligned} \tag{3.7}$$

It is easily verified that the solutions to this system are

$$x_1(t) = \frac{c_1}{1 - t_{c^1}}$$

$$x_2(t) = c_2\, e^{-t}$$

Eliminating t yields

$$x_2(x_1) = c_2\, e^{\frac{-1}{c_1}}\, e^{\frac{1}{x_1}}$$

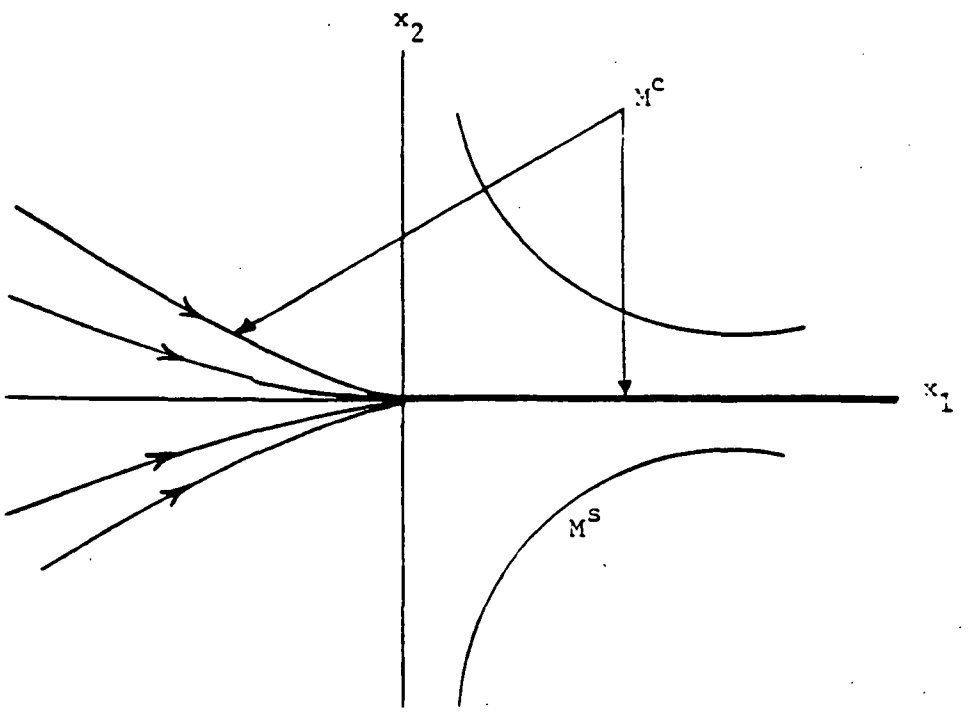

Figure 3.2 Center Manifold Is Not Unique

It is clear that for $x > 0$ the only solution approaching the origin is $x = 0$. But for $x < 0$, any solution with zero slope at the origin is acceptable. For example, the entire x_1 axis is one such solution, and in fact the only **analytic** one. This is illustrated in Figure 3.2. (Note that a center manifold is an invariant manifold tangent to the center eigenspace. Hence this tangency condition at zero can be satisfied by many center manifolds: take any solution curve with $x_1<0$ pieced together with the positive half of the x_1 axis; the resulting curve will be a center manifold.)

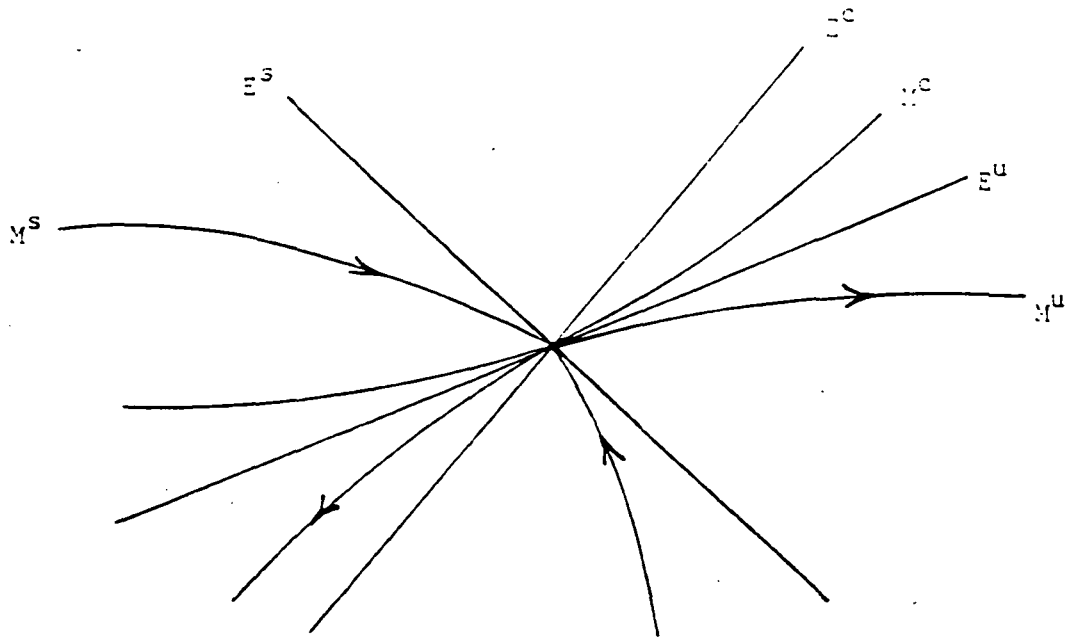

Figure 3.3 Stable, Unstable, and Center Manifolds

3.4 Hopf Bifurcations

The simple equilibria that we have discussed so far are examples of point equilibria. It is possible, for example, to have situations in which the state of a system hovers around in the state space without ever reaching any stationary point. One such situation arises in the following example.

$$\begin{bmatrix} \dot{x}_1 \\ \dot{x}_2 \end{bmatrix} = \begin{bmatrix} \alpha_1 & -\alpha_2 \\ \alpha_2 & +\alpha_1 \end{bmatrix} \begin{bmatrix} x_1 \\ x_2 \end{bmatrix} \tag{3.8}$$

The solutions to (3.8) are of the form

$$\begin{bmatrix} x_1(t) \\ \\ x_2(t) \end{bmatrix} = e^{\alpha_1 t} \begin{bmatrix} \cos \alpha_2 t & -\sin \alpha_2 t \\ \\ \sin \alpha_2 t & \cos \alpha_2 t \end{bmatrix} \begin{bmatrix} x_1(0) \\ \\ x_2(0) \end{bmatrix} \tag{3.9}$$

For $\alpha_1 > 0$ the trajectories spiral away from the origin; for $\alpha_1 < 0$ the opposite occurs. Bur for $\alpha_1 = 0$ the solutions become periodic — never expanding or contracting. The Hopf theory is a body of results which generalize this observation. Note that the eigenvalues of the matrix

$$A = \begin{bmatrix} \alpha_1 & -\alpha_2 \\ \alpha_2 & \alpha_1 \end{bmatrix}$$

are $\alpha_1 \pm j\alpha_2$ and become purely imaginary for $\alpha_1 = 0$.

Let's slightly generalize the form of (3.8):

$$\begin{aligned} \dot{x}_1 &= (d\alpha_1 + a(x_1^2 + x_2^2))\, x_1 - (\alpha_2 + c\alpha_1 + b(x_1^2 + x_2^2))x_2 \\ \dot{x}_2 &= (\alpha_2 + c\alpha_1 + b(x_1^2 + x_2^2)x_1 + (dx_1 + a(x_1^2 + x_2^2))x_2 \end{aligned} \tag{3.10}$$

or expressing (3.10) in polar coordinates

$$\begin{aligned} \dot{r} &= (d\alpha_1 + ar^2)r \\ \dot{\theta} &= (\alpha_2 + c\alpha_1 + b\, r^2) \end{aligned} \tag{3.11}$$

where

$$r = \sqrt{x_1^2 + x_2^2}$$

$$\theta = \tan^{-1} \frac{x_1}{x_2}$$

In equation (3.11) the radius r is independent of θ and therefore $\dot{r}=0$ in (3.11) yields the steady state trajectories -- which are circles of constant r.

In a fundamental sense, equation (3.11) captures the essence of the Hopf bifurcation in that the addition of higher order terms will not make a qualitative difference in the behavior of solutions near the origin:

Result 4 (Hopf Bifurcation)

Consider the nonlinear control system (3.1), and assume that it has a steady state solution x_0 corresponding to $\mu = \mu_0$ with the property (P1): $\nabla_x f(x_0,\mu_0)$ has a simple pair of purely imaginary eigenvalues and no other eigenvalues with zero real parts.

Then there is a smooth curve of equilibria $(x(\mu),\mu_0)$ such that $x(\mu_0) = x_0$. The imaginary eigenvalue pairs $\lambda(\mu)$ and $\bar{\lambda}(\mu)$ vary smoothly with μ. Furthermore, if

$$\frac{d}{d\mu}(\mathrm{Re}\ \lambda(\mu)) = d \neq 0 \tag{3.12}$$

Then there is a three dimensional center manifold which passes through (x_0,μ_0) in the product space $R^n x R$. Furthermore, when (3.12) is satisfied, there is a smooth coordinate system in which the Taylor series expansion of degree 3 on the center manifold is given by (3.10) (with the new notation μ replacing α_1). In addition, if $a \neq 0$, there is a surface of periodic solutions in the center manifold tangent to the eigenspace of $\lambda(\mu_0)$ (and

$\bar{\lambda}(\mu_0))$ which agrees to the second order with the paraboloid $\mu = -\frac{a}{d} r^2$. For $a < 0$, these periodic solutions are **stable** limit cycles -- while for $a > 0$ the limit cycles are diverging. The proof of this well known result can be found in any standard text on nonlinear dynamic systems (c.f. Marsden and McCracken (1976)).

We will see in Section 6.3 that, for some critical parameter values, the unstalled compressor exhibits surge cycles corresponding to Hopf bifurcation points; also in that section a more quantitative discussion of Hopf solution points will be carried out. Many ~~Much~~ of the stationary operating points of the compressor models will turn out to be of the Hyperbolic Stable or Unstable type (e.g. Section 5.5)

4. THREE INTERLOCKING MODELS

4.1 Introduction

In this chapter three separate state space models of a compressor rig are developed. One corresponds to the compressor operation under normal unstalled conditions (US); the other two are developed for the stalled compressor - corresponding to the normal (positive) flow and reverse flow conditions ((PS) and (RS), respectively). The reverse flow and normal flow stall conditions are modeled separately to account for the different (e.g., opposite) heat and mass flow conditions in the compressor. Wenzel and Bruton (1982) describe these conditions and provide explanations for the approach; their work forms the basis of the models presented here.

The (simplified) Wenzel-Bruton model reported in Appendix A is used exclusively in our development of the state space models. The reader is assumed to be familiar with the related fluid mechanic terminology and vocabulary as described in Wenzel and Bruton (1982) or similar treatments. Refering to Appendix A (and Wenzel and Bruton (1982) for definitions) we begin with defining the state vector x as

$$x = \begin{bmatrix} W_2 \\ (WT)_2 \\ \dot{\omega}_2 \\ W_3 \\ (WT)_3 \end{bmatrix} \tag{4.1}$$

our objective is to derive from the relations of Appendix A, three state space formulations of the form

$$\frac{dx}{dt} = f_i(x(t),\ \theta(t),\ u(t)) \tag{4.2}$$

$$i = 1,\ 2,\ 3,$$

in which x, θ, and u represent the state vector, the parameter vector, and the control vector, respectively. In addition a set of output relations of the form

$$y_i = g_i(x, \vartheta, u) \tag{4.3}$$

$$i = 1, 2, 3,$$

are also obtained.

A typical element of the control vector may be the area A determining the flow rate downstream of the compressor. A typical parameter would be the fractional corrected speed PN, or some design parameter such as install compressor performance at positive (or negative) flow KP (or KN). The elements of the state vector are defined in (4.1). The first two elements denote the mass and (thermal) energy stored upstream of the compressor; $\dot{\omega}_2$ represents the mass flow rate through the compressor; and the last two elements are the downstream mass and energy variables.

4.2 State Space Relations for Positive Flow Stalled Dynamics (PS)

Keeping in mind the definition of the state x as described by Equation 4.1, Appendix B shows how the integral relations of Appendix A can be used to derive a state space model of the stalled compressor rig in normal (positive) flow condition. They are summarized below.

Summary of State Space Systems for Positive Flow Stalled Dynamics (PS)

$$\dot{x}_1 = \frac{P_1}{R_0} - \frac{R}{R_0 V_2} x_2 - x_3 \tag{PS1}$$

$$\dot{x}_2 = \gamma \frac{P_1}{R_0} T_1 - \frac{R}{R_0 V_2} T_1 x_2 - x_2 \frac{x_3}{x_1} \tag{PS2}$$

$$\dot{x}_3 = \frac{1}{L} g_3 g_1^2 KP \frac{x_3^2}{x_1} + \frac{1}{L} g_2(PN) x_2 - \frac{1}{L} \frac{R}{V_3} x_5 \tag{PS3}$$

$$\dot{x}_4 = x_3 - A \frac{R}{V_3} \sqrt{x_5 x_4} \tag{PS4}$$

$$\dot{x}_5 = \gamma \frac{x_2 x_3}{x_1}\left(1 + \frac{1.19 + 0.925\ KP\ \frac{(g_1\ x_3)^2}{519\ x_1 x_2} + 0.33\ PN^2\ ^{0.286} - 1}{\eta_0 + F_4(PN,\eta_0)\frac{g_1}{PN}\ \frac{x_3}{\sqrt{519\ x_1 x_2}}}\right)$$

$$- \frac{\gamma AR}{V_3} x_5 \quad \frac{x_5}{x_4} \tag{PS5}$$

where g's are defined in Appendixes B, C, D,

4.3 State Space Relations for Unstalled Dynamics (US)

Recalling from Appendix A that

$$F_1\left(\frac{\dot{\omega}_2\sqrt{\theta_2}}{\delta_2},\ PN\right) = \frac{P_3^*}{P_2} \tag{4.4}$$

$$F_2\left(\frac{\dot{\omega}_2\sqrt{\theta_2}}{\delta_2},\ PN\right) = \frac{T_3^*}{T_2} \tag{4.5}$$

we now summarize the state space model derived in Appendix C for the unstalled compressor.

Summary of State Space Systems for Unstalled Dynamics (US)

$$\dot{x}_1 = \frac{P_1}{R_o} - \frac{R}{R_o V_2} x_2 - x_3 \tag{U1}$$

$$\dot{x}_2 = \gamma \quad \frac{P_1}{R_o} - \frac{R}{R_o V_2} x_2 \quad T_1 - x_3 \quad x_2/x_1 \tag{U2}$$

$$\dot{x}_3 = \frac{R}{L}\left[\frac{x_2}{V_2} \cdot F_1\left(g_4\ \frac{x_3}{x_1 x_2},\ PN\right) - \frac{x_5}{V_3}\right] \tag{U3}$$

$$\dot{x}_4 = x_3 - \frac{AR}{V_3}\ \sqrt{x_4 x_5} \tag{U4}$$

$$\dot{x}_5 = \gamma\left[\frac{x_3 x_2}{x_1} \cdot F_2\left(g_4\ \frac{x_3}{\sqrt{x_1 x_2}}, PN\right) - \frac{AR}{V_3} x_5 \quad \frac{x_5}{x_4}\right] \tag{U5}$$

where

$$g_4 = \frac{14.7\ V_2}{R\sqrt{T_1}}$$

and corrected flow $h_1 = g_4 \dfrac{x_3}{\sqrt{x_1 x_2}}$.

4.4 State Space Relations for Reverse Flow Stalled Dynamics (RS)

The major distinction between the (PS) case and the present one is that in the latter the flow through the compressor reverses — thus, roughly speaking, the exit and inlet conditions are switched. In this case the compressor flow is corrected by downstream conditions. However, the correction to compressor speed is not switched, to preserve continuity at zero flow. The detailed derivation of the relations are given in Appendix D. Here we summarize the relations.

Summary of Reverse Flow Stalled Dynamics (RS)

$$\dot{x}_1 = \frac{P_1}{R_0} - \frac{R}{R_0 V_2} x_2 - x_3 \tag{RS1}$$

$$\dot{x}_2 = \gamma\left(\left(\frac{P_1}{R_0} - \frac{R}{R_0 V_2} x_2\right)\frac{x_2}{x_1} - \frac{x_3 x_5}{x_4}\left(1 - \frac{g_8}{PN}\frac{x_3}{\sqrt{x_4 x_5}}\right)\right) \tag{RS2}$$

$$\dot{x}_3 = \frac{R}{L}\left(\frac{x_2}{0.837\ V_2}\left(g_9 + KN\ g_{10}\frac{x_3^2}{x_4 x_5}\right) - \frac{x_5}{V_3}\right) \tag{RS3}$$

$$\dot{x}_4 = x_3 - \frac{AR}{V_3}\sqrt{x_4 x_5} \tag{RS4}$$

$$\dot{x}_5 = \gamma \left(x_3 \frac{x_5}{x_4} - \frac{AR}{V_3} x_5 \quad \overline{\frac{x_5}{x_4}} \right) \tag{RS5}$$

where

$$\text{corrected flow } h_r = g_6 \frac{x_3}{\sqrt{x_4 x_5}}$$

$$g_6 = \frac{P_1 \; V_3}{R \sqrt{T_1}} \; .$$

(Other g's are defined in Appendix D.)

4.5 Typical Output Relations

The dynamic relations (US), (PS), and (RS) describe the compressor in unstalled and stalled conditions. The state vector x in each case completely summarizes the past history of the variables and can be used to generate future conditions under alternative input scenarios. In general, the state variables are not all measurable -- they represent "internal" variables of the system. More often some other related variables, typically represented by a combination of the state variables, are measurable or physically significant. They may be labled as output variables. The output variables y_i may be written in the general form

$$y_i(t) = g_i(x(t), \theta(t), u(t))$$

where i varies over the set of output relations of the models (US), (PS), and (RS).

In the context of our work, typical output variables are the various pressures and temperatures -- both in absolute and relative terms. Another important variable that is interpretable as an output variable is the

corrected flow $\frac{\dot{\omega}_2\sqrt{\theta_2}}{\delta_2}$. This variable plays a crucial role in our analysis, as will later be described. Here we cite some typical output relations (derived in Appendices B, C, and D).

$$P_2 = \frac{R}{V_2} x_2 \tag{4.6}$$

$$T_2 = \frac{x_2}{x_1} \tag{4.7}$$

$$P_3 = \frac{R}{V_3} x_5 \tag{4.8}$$

$$T_3 = \frac{x_5}{x_4} \tag{4.9}$$

$$hl: = \frac{\dot{\omega}_2\sqrt{\theta_2}}{\delta_2} = g_4 \frac{x_3}{\sqrt{x_2 x_2}} \qquad \text{(US,PS)} \tag{4.10}$$

$$hr: = \frac{\dot{\omega}_2\sqrt{\theta_2}}{\delta_2} = g_6 \frac{x_3}{\sqrt{x_4 x_5}} \qquad \text{(RS)} \tag{4.11}$$

$$\frac{P_3^*}{P_2} = F_1(hl,PN) \qquad \text{(US)} \tag{4.12}$$

$$\frac{T_3^*}{T_2} = F_2(hl,PN) \qquad \text{(US)} \tag{4.13}$$

$$\phi = g_1 \frac{x_3}{\sqrt{T_1\ x_1\ x_2}} \qquad \text{(PS)} \tag{4.14}$$

$$\frac{P_3^*}{P_2} = 1.194 + 0.925\ KP\ \frac{(g_1 x_3)^2}{T_1\ x_1\ x_2} + 0.33\ PN^2 \qquad \text{(PS)} \qquad (4.15)$$

$$\frac{T_3^*}{T_2} = 1 + \frac{1.19 + 0.925\ KP\ \frac{(g_1\ x_3)^2}{519\ x_1 x_2} + 0.33\ PN^2 \quad {}^{0.286} - 1}{\eta_0 + F_4(PN,\eta_0)\frac{g_1}{PN}\ \frac{x_3}{\sqrt{519\ x_1 x_2}}}$$

$$\text{(PS)} \qquad (4.16)$$

$$\phi = \frac{g_7}{PN}\ \frac{x_3}{\sqrt{x_4 x_5}} \qquad \text{(RS)} \qquad (4.17)$$

$$\frac{P_3^*}{P_2} = 1.194\left(1 + 0.2556\ PN^2 + 0.7746\ KN\ \frac{(g_7 x_3)^2}{x_4 x_5}\right)$$

$$\text{(RS)} \qquad (4.18)$$

$$\frac{T_3^*}{T_2} = 1 + \frac{1.19(1 + 0.2556\ PN^2 + 0.7746\ KN\ \frac{(g_7 x_3)^2}{x_4 x_5})\quad {}^{0.286} - 1}{\eta_0 + F_4(PN,\eta_0)\ \frac{g_7}{PN}\ \frac{x_3}{\sqrt{x_4 x_5}}}$$

$$\text{(RS)} \qquad (4.19)$$

Despite the seemingly complicated appearance of the above functions, it is clear that they are all of the basic (static) output form mentioned earlier.

4.6 Linking the Models

Having presented the three state space systems (US), (PS), and (RS), we now describe how they are linked.

The criterion used for switching the models is the magnitude and direction of the corrected flow through the compressor. For a given corrected speed PN, if the corrected flow falls below a certain positive threshhold value $t_s(PN)$, the compressor is assumed to enter into stall (PS). At a given speed PN, the requirement for recovery is for the corrected flow to exceed a certain threshhold $t_r(PN)$. At the time the flow reverses through the compressor, the (RS) dynamics are switched on; upon reentry into positive flow region, the (PS) dynamics are switched back on. This process is described graphically in Figure 4.1.

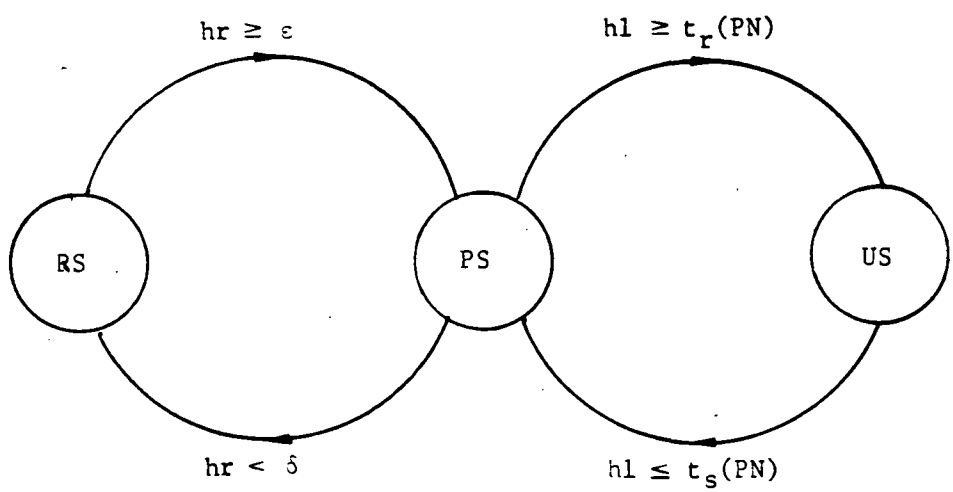

Figure 4.1: Linking of Models

In closing we note that the switching of the models is based on the value of the corrected flow, which is an output variable. There are some possible criticisms of this approach -- some of which we shall mention later.

5. EQUILIBRIUM LOCI

5.1 Introduction

In this chapter we will trace the equilibrium solutions of the systems (US) and (PS), continuously varying a parameter of interest. We will also show that (RS) has no equilibria — a result which turns out to be quite intuitive. Various types of fixed points such as hyperbolic stable and unstable points are encountered and discussed. The numerical results and plots are obtained by the use of our in-house software package BISTAB; a discussion of its features is also offered in this chapter.

5.2 (RS) Model Contains No Equilibria

In order to see that the in-stall reverse flow model (RS) can not have any equilibria let us assume on the contrary that it does. This means, in particular, that the left hand side of Equation (RS4) must equal zero, i.e.,

$$0 = x_3 - \frac{AR}{V_3}\sqrt{x_4 x_5}$$

with $x_3(t) < 0$ for all time $t \geq 0$. On the other hand, $x_4(t)$ and $x_5(t)$ being mass and energy, are both nonnegative quantities for all times $t \geq 0$. Furthermore, the quantities A, R, and V_3 are all positive scalars. Thus, the above assertion can not hold.

The above property of the in-stall reverse flow model is intuitively correct, as the reversal of the flow direction in a real world situation is only temporary and can not represent a steady state operating condition.

In this way when we speak of equilibria in this work we are referring to the steady state operation of the compressor (model) in normal unstalled operating conditions or in in-stall conditions with normal flow.

5.3 Generation of Equilibria By Continuation

Let's look at a stationary point of Equation (3.1). This makes the left-hand side equal to zero,

$$0 = f(x,\mu) \ . \tag{5.1}$$

Treating μ as a parameter to be varied, the vector x can be viewed as the dependent variable. Continuation methods deal with the problem of solving (5.1) for the state vector x as a function of the parameter μ; they do so by utilizing results from differential calculus and topology. In general $\mu \in R^m$ but here let's assume for the sake of simplicity that $\mu \in R^1$; as before assume $x \in R^n$.

Differentiating (5.1) with respect to μ yields

$$F(x,\mu)\frac{\partial x}{\partial \mu} + \frac{\partial f}{\partial \mu}(x,\mu) = 0 \tag{5.2}$$

where,

$$F: = \frac{\partial f}{\partial x} \tag{5.3}$$

It is clear that at a particular x as long as F is one-to-one, successive values of x can be obtained as μ is varied from some initial value μ_0. Typically the initial value of μ is chosen at any point which is computationally convenient; the desired value of (x,μ) is then arrived at by "continuation" of solution from (x_0,μ_0). (In the language of Chapter 3, the stationary points at which F is invertible are said to be **hyperbolic**. The points at which F becomes **singular** are called bifurcation points; at these points more than one x satisfies (5.2), for a given μ. Singular points at which the rank deficiency of F is one are referred to as **simple** bifurcation points — otherwise, they are called **general** bifurcation points.

5.4 BISTAB: Computational Tool for Bifurcation and Stability Analysis

In order to trace the equilibrium solutions of (5.1) for the compressor models (US) and (PS) the computational software package BISTAB was employed; the package was developed by Scientific Systems, Inc., specifically for this type of analysis. BISTAB contains three user interface FORTRAN V functions and a number of supporting functions and subroutines. They:

(i) Trace connected bifurcating branches of solutions to Equation (5.1), starting from some given initial point.

(ii) Provide stability analysis of the branch curves and report the linearized stability type.

(iii) Spot Hopf, simple, and general types of bifurcation. (At present only solutions starting from simple bifurcation points can be traced.)

(iv) Read in the files generated by the bifurcation and stability analysis routines, and sort the points into curves of different bifurcation or stability type, for plotting. We will not engage in any in-depth analysis of the BISTAB package here; instead the reader is referred to a recently published description of the package by E.F. Wood, J.A. Kempf, and R.K. Mehra (1984). In the following section the equilibrium loci generated by BISTAB are presented.

5.5 Equilibrium Solutions for (US) and (PS)

The unstalled system (US) equilibrium solutions are shown as a function of the parameter A, the downstream flow area in Figures 5.1 through 5.9. Each figure depicts a state variable x_i versus the parameter A. The symbols □ and * on the diagrams stand, respectively, for the stability and instability of the system (US). More precisely, the points labeled as □ and * correspond to hyperbolically stable and unstable equilibria, respectively.

As will be discussed later, the question of stall must be related to the stability of the underlying dynamic system. Thus we seek the stability

behavior of (US) as the parameter A varies. We show that the use of A as a proxy for system stability may lead to some inconsistencies. We illustrate the point by fixing PN at 60% (e.g., Figure 5.1).[2]

It can be seen from Figure 5.1 that the stability effects of the parameter A on the system (US) is dependent on the location of the state in the state space. Thus as the area A decreases, say, from 28 to 25, the stability status of the system changes **three times**: at points 12, 23, and 34. In the regions 1 and 3, the system is **stable**, and in the regions 2 and 4 it is **unstable**. The points 12, 23, and 34 represent "border" points.

This means that a decrease in the flow area may or may not be destabilizing -- at least in a local sense. For example at an (unstable) equilibrium point in region 3 which is "close" to the point 23, a "small" decrease in the flow area pushes the equilibrium point towards "inside" region 3. In this case a **decrease** in A is **stabilizing** -- or, conversely, an **increase** in A is **destabilizing**. The above example suggests that a higher setting for the flow area A is **not** always associated with a higher degree of stability. However, for (stable) equilibrium states in region 1, an increase in A is always (further) stabilizing -- as Figure 5.1 indicates.

In the same manner, (the stable) equilibrium points that are located in the neighborhood of the point 23 of region 2, are pushed toward **stability** by a "small" **decrease** in A; conversely, they are **destabilized** by a small **increase** in A. Changes in A have the **opposite** effect on the stability characteristics of the neighboring equilibria of the point 12 of the region 2. However for points in region 4 **decreases** in A do further **destabilize** the system -- and vice versa.

Now, it can be shown that the flow area A and the corrected flow h_1 move up and down together -- in this same region of interest. (In fact, the relationship is almost linear.) Thus the above discussion **applies**

[2]This discussion was presented in SSI report (June 1 - Aug. 30, 1984) to NASA Lewis.

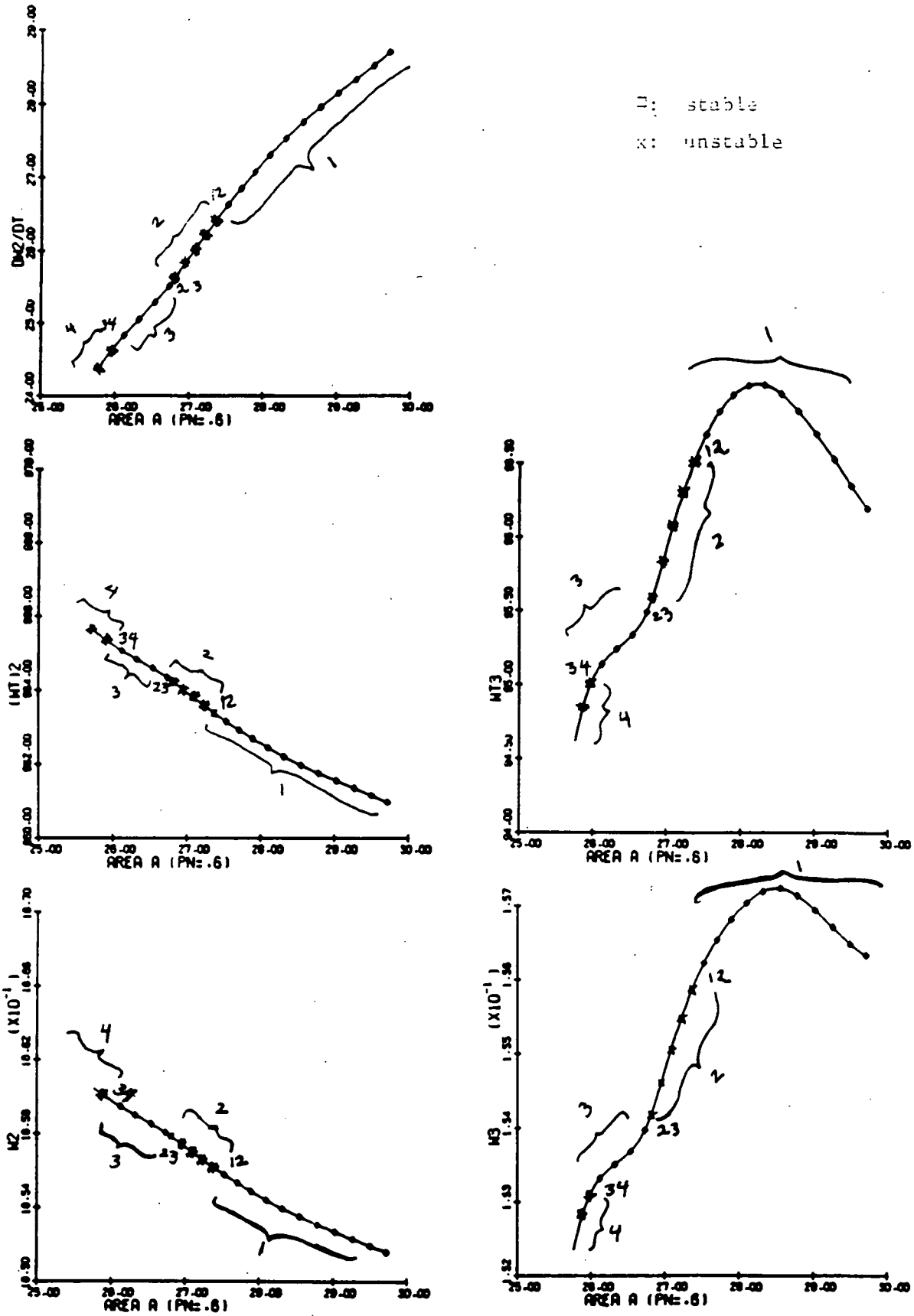

Figure 5.1 (US) Equilibrium Loci in (x_i, A) Plane i = 1,...,5
For Corrected Speed PN = 60%

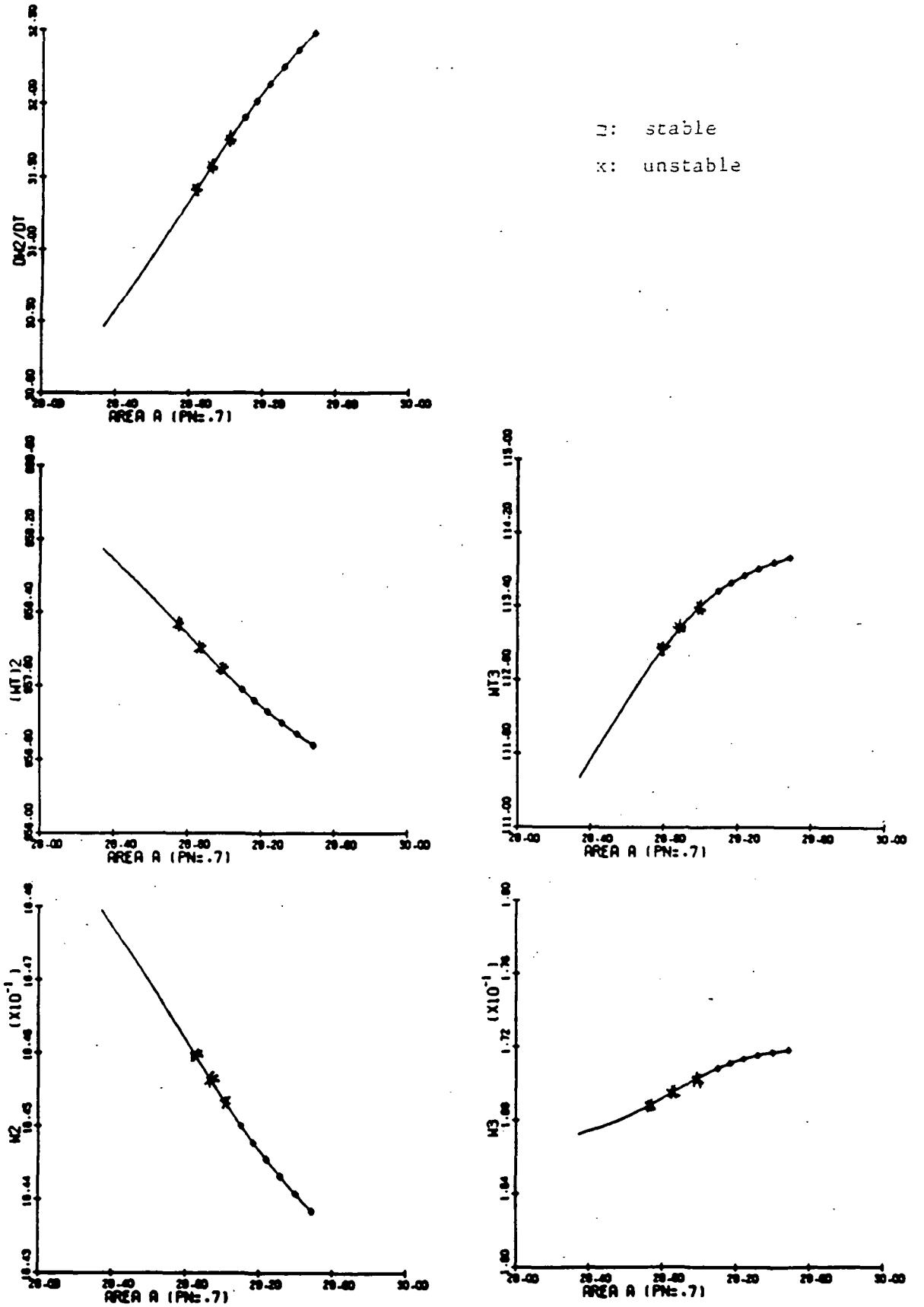

Figure 5.2 (US) Equilibrium Loci in (x_i, A) Plane $i = 1,\ldots,5$
For Corrected Speed PN = 70%

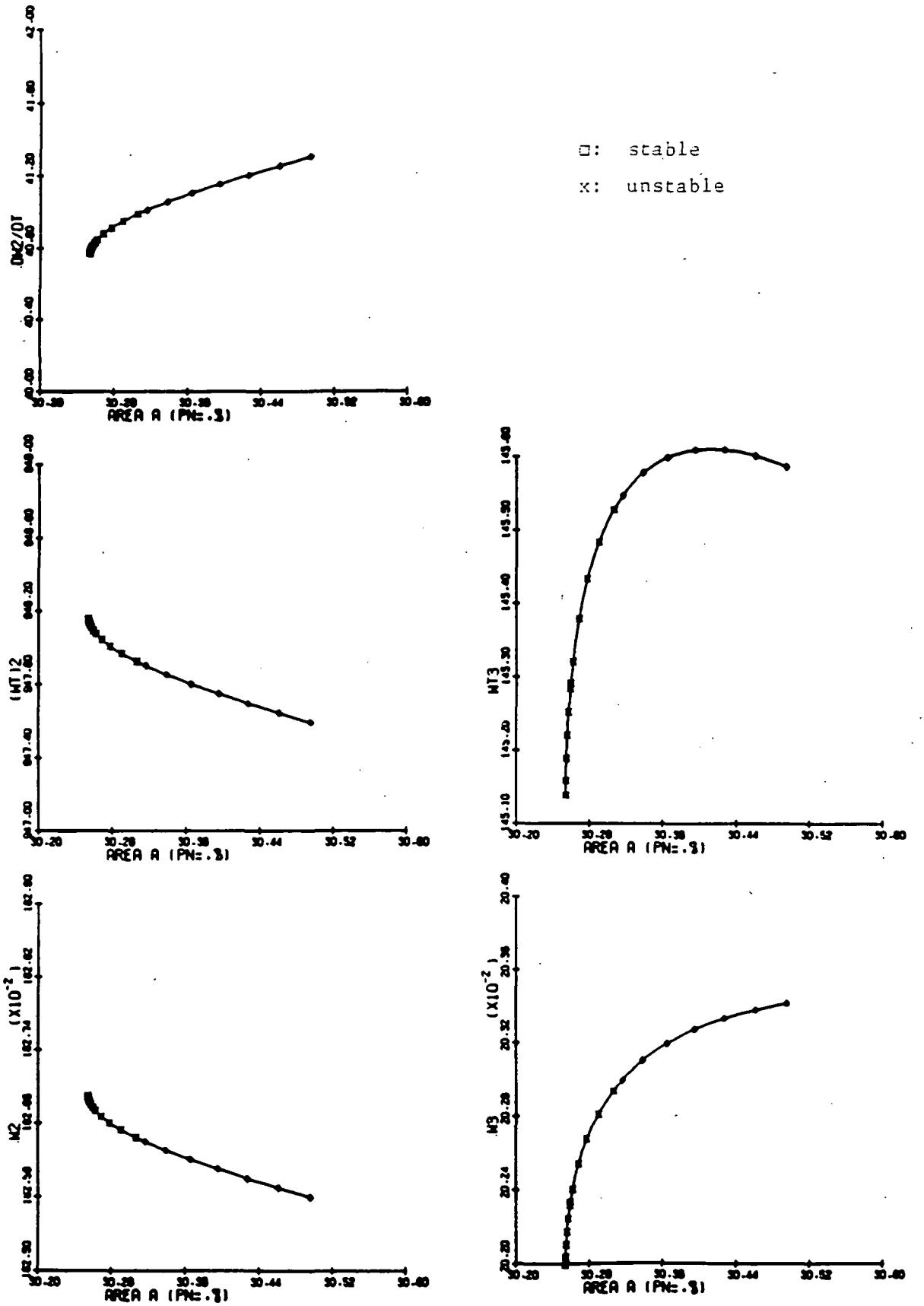

Figure 5.3 (US) Equilibrium Loci in (x_i, A) Plane $i = 1,\ldots,5$
For Corrected Speed PN = 80%

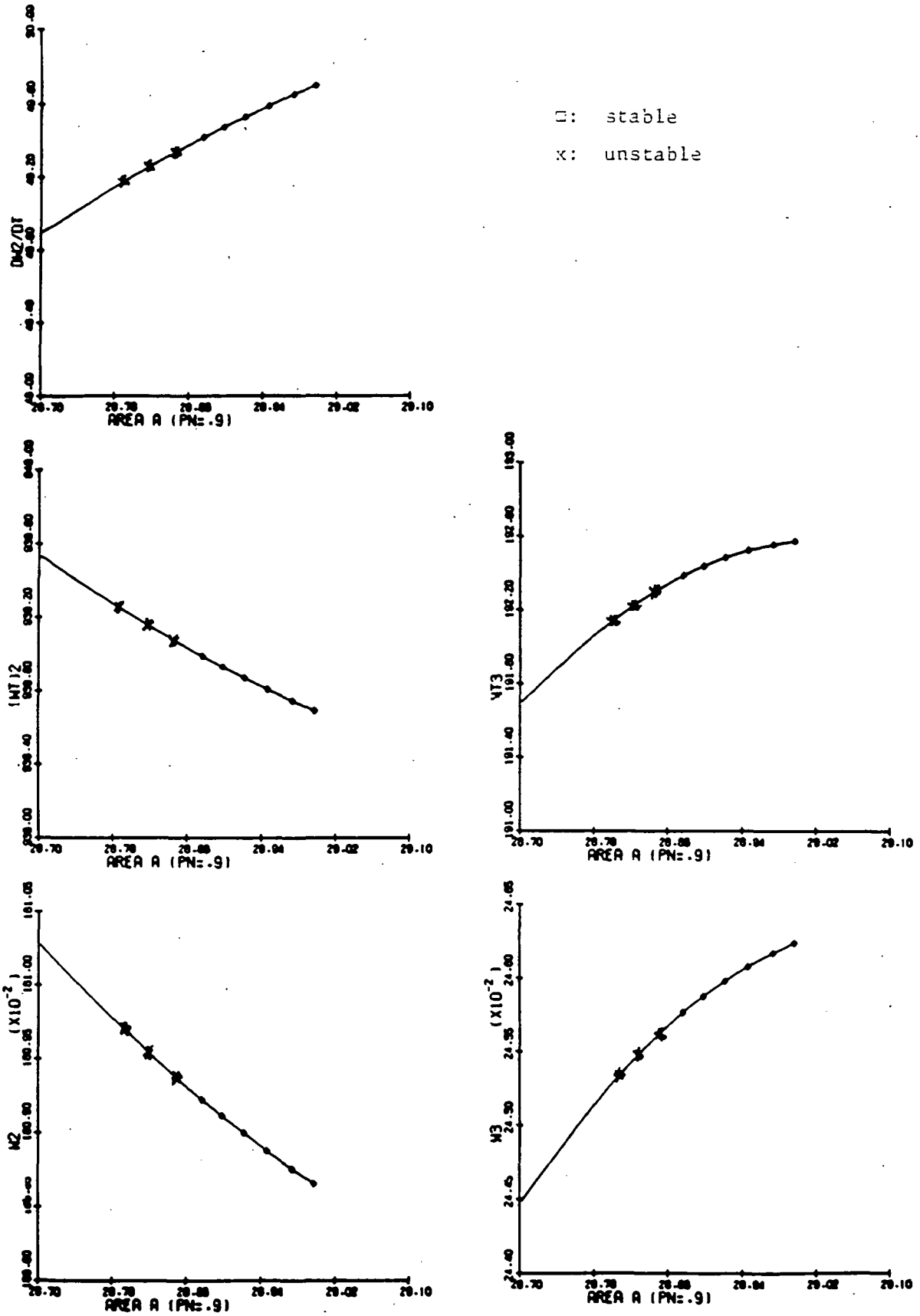

Figure 5.4 (US) Equilibrium Loci in (x_i, A) Plane $i = 1,\ldots,5$
For Corrected Speed PN = 90%

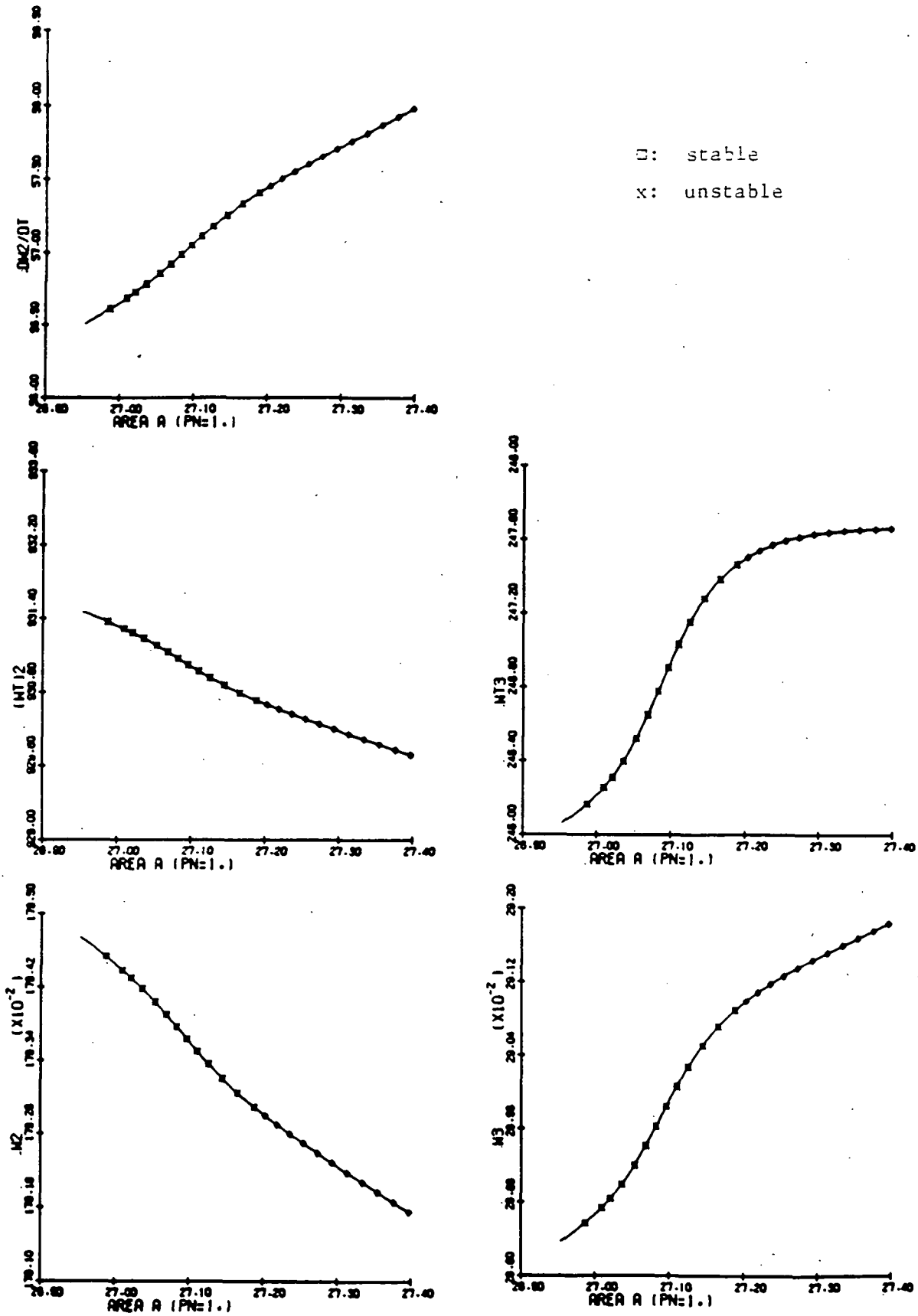

Figure 5.5 (US) Equilibrium Loci in (x_i, A) Plane $i = 1,\ldots,5$
For Corrected Speed PN = 100%

equally well with respect to the corrected flow -- viewed as a parameter. In this way, for example, an increase in the corrected flow is not necessarily associated with "more" stability and vice versa. Therefore, it seems clear that the observed (or computed) value of the corrected flow does not -- in a one-to-one manner — determine the system's stability rating.

We conclude our discussion of the subject by noting that the above reasoning applies equally well to the uncorrected flow $\dot{\omega}_2(= x_3)$. In Chapter 7 we show that the situation becomes even more complicated when we encounter non-steady state "off-design" conditions. We will suggest a more general approach to the problem which will alleviate the situation.

Finally, we wish to point out that the in-stall equilibria for this range of parameters turn out to be stable hyperbolic. The corresponding figures have not been included, for the sake of brevity. (Some equilibria are shown in Figures 6.1 through 6.3 in the next chapter.)

6. BIFURCATION - CATASTROPHE LOCI

6.1 Introduction

In the previous chapter **equilibrium** loci of the compressor model in (US) and (PS) modes were described. This chapter emphasizes the bifurcation loci. It is shown that the unstalled compressor exhibits Hopf bifurcation. The resulting family of limit cycle solutions are propagated by parameter continuation; both **stable** and **unstable** limit cycles are observed. Before the unstable family disappears, it further bifurcates into 3 families. Frequency, amplitude and centroids of the cycles are plotted in various state-parameter spaces. (The analysis is presented in Section 6.3.)

Section 6.2, however, presents bifurcation points of a different type: those corresponding to the switching of the models. Strictly speaking, such points should perhaps be labeled as "induced bifurcation" points since the jumps are induced by switching of the models. Hysteresis is shown to exist in the stall/recovery process.

6.2 Bifurcation of Solutions and Stall/Recovery

Let's recall from Section 4.5 that the overall compressor model consists of three interlocking models (US), (PS), and (RS). The models are switched based on the threshold values of the corrected flow: $t_r(PN)$, $t_s(PN)$, δ, and ε (e.g., Figure 4.1).

In our analysis we have taken $\delta = \varepsilon = 0$, indicating that at nearly zero but slightly negative flow the (PS) model is replaced by (RS); at zero flow (RS) is replaced by (PS). The values of $t_r(PN)$ and $t_s(PN)$ are given in Appendix A.

Figures 6.1 - 6.3 depict the loci of equilibria and jump points for the values of corrected fractional speed of 60%, 70%, and 100%, just to cite three examples. Let's note that for example in Figure 6.1(a), we have the bifurcation diagrams for the (state, parameter) combinations (x_i, A), $i = 1,5$; each x_i represents a state variable. For example, x_3 represents

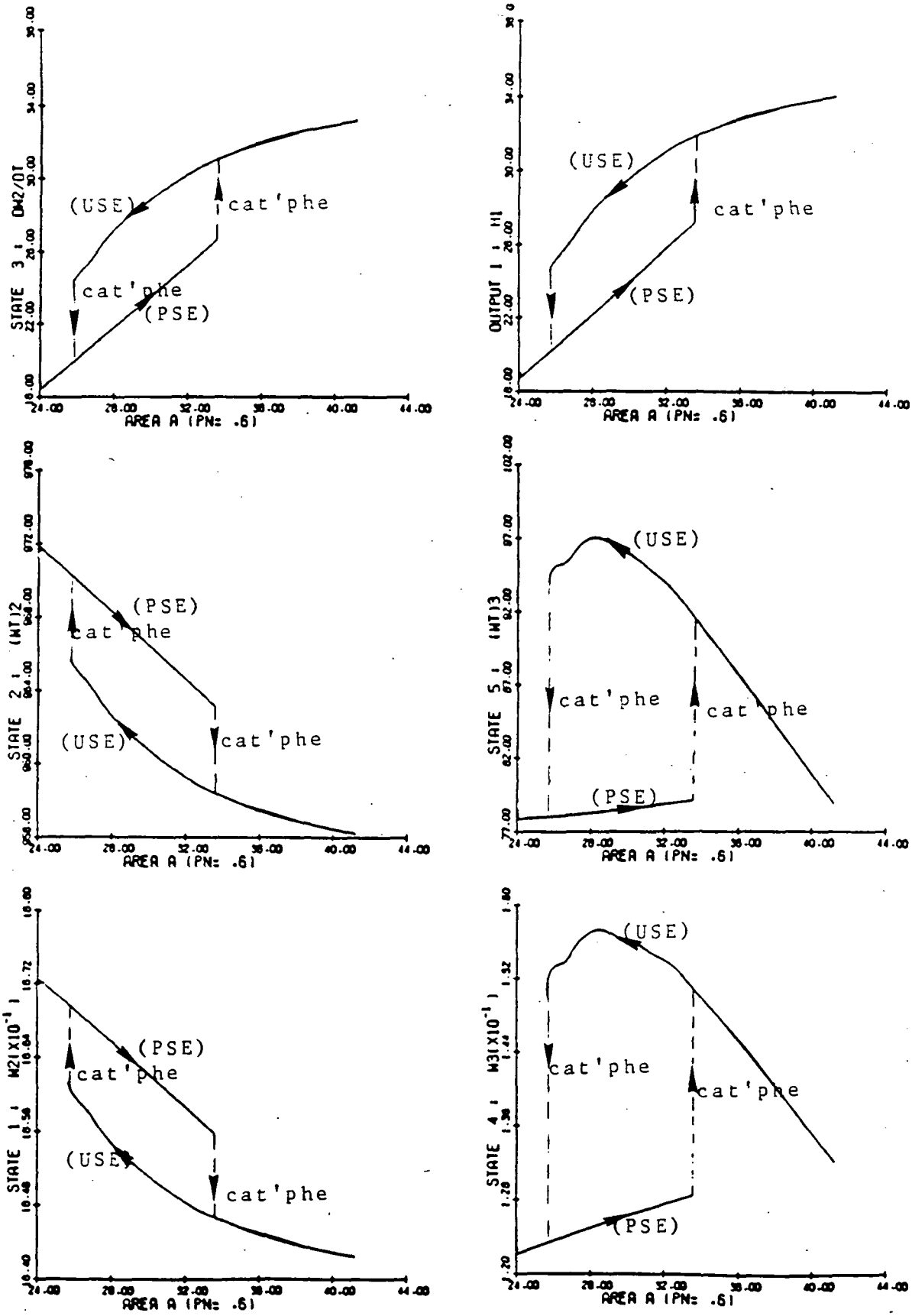

Figure 6.1(a) Bifurcation Diagrams in (x_i, A) Plane, $i = 1,5$. Bifurcation (catastrophe) points are indicated by dashed lines; they are labeled as "cat'phe". Arrows indicate direction of movement of the state; hysteresis is observed.

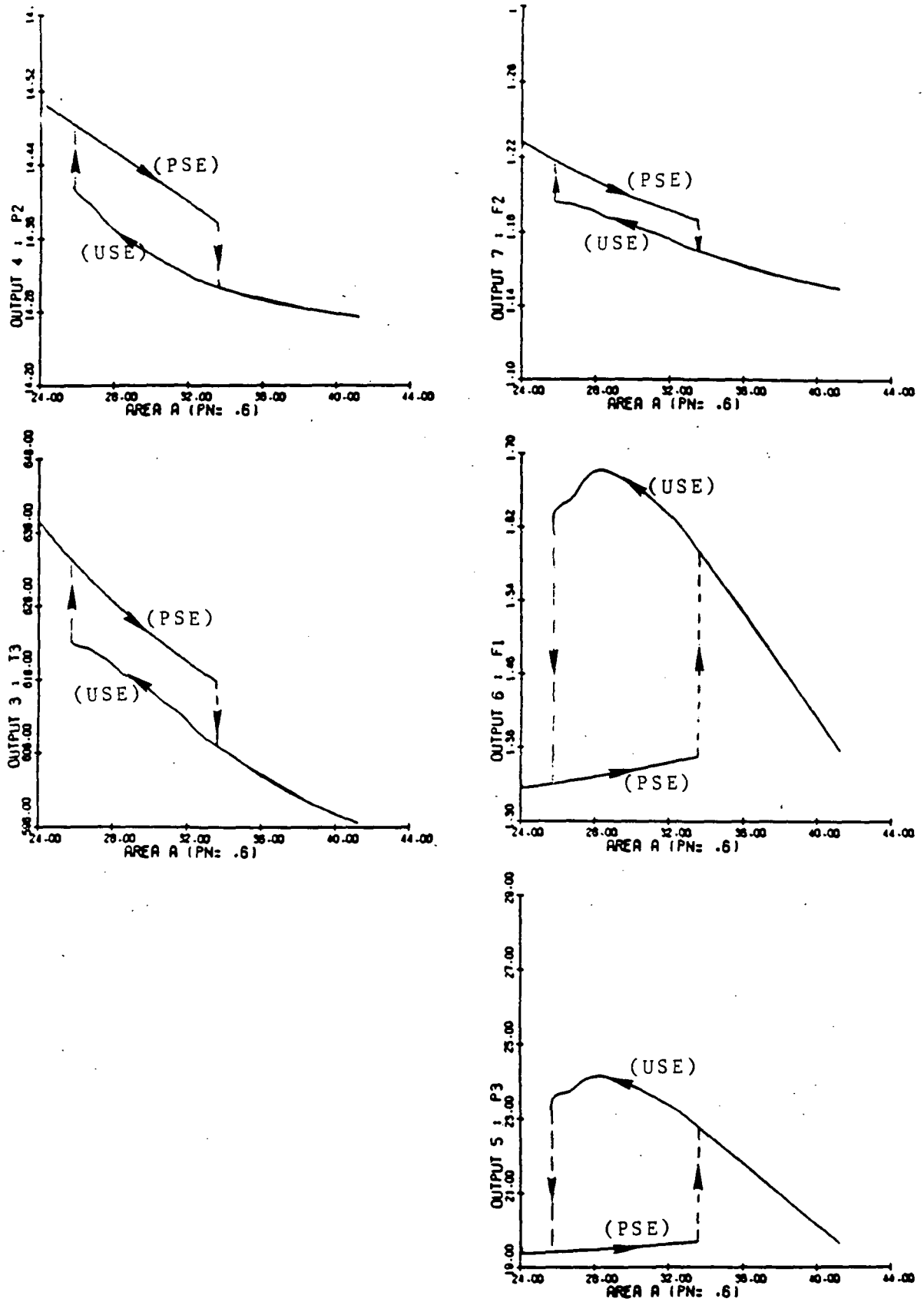

Figure 6.1(b). Some Output Variables Are Shown on (y_i, A) Planes for $i = 3,\ldots,7$; PN = .6. Arrows indicate direction of movement of outputs; hysteresis is observed.

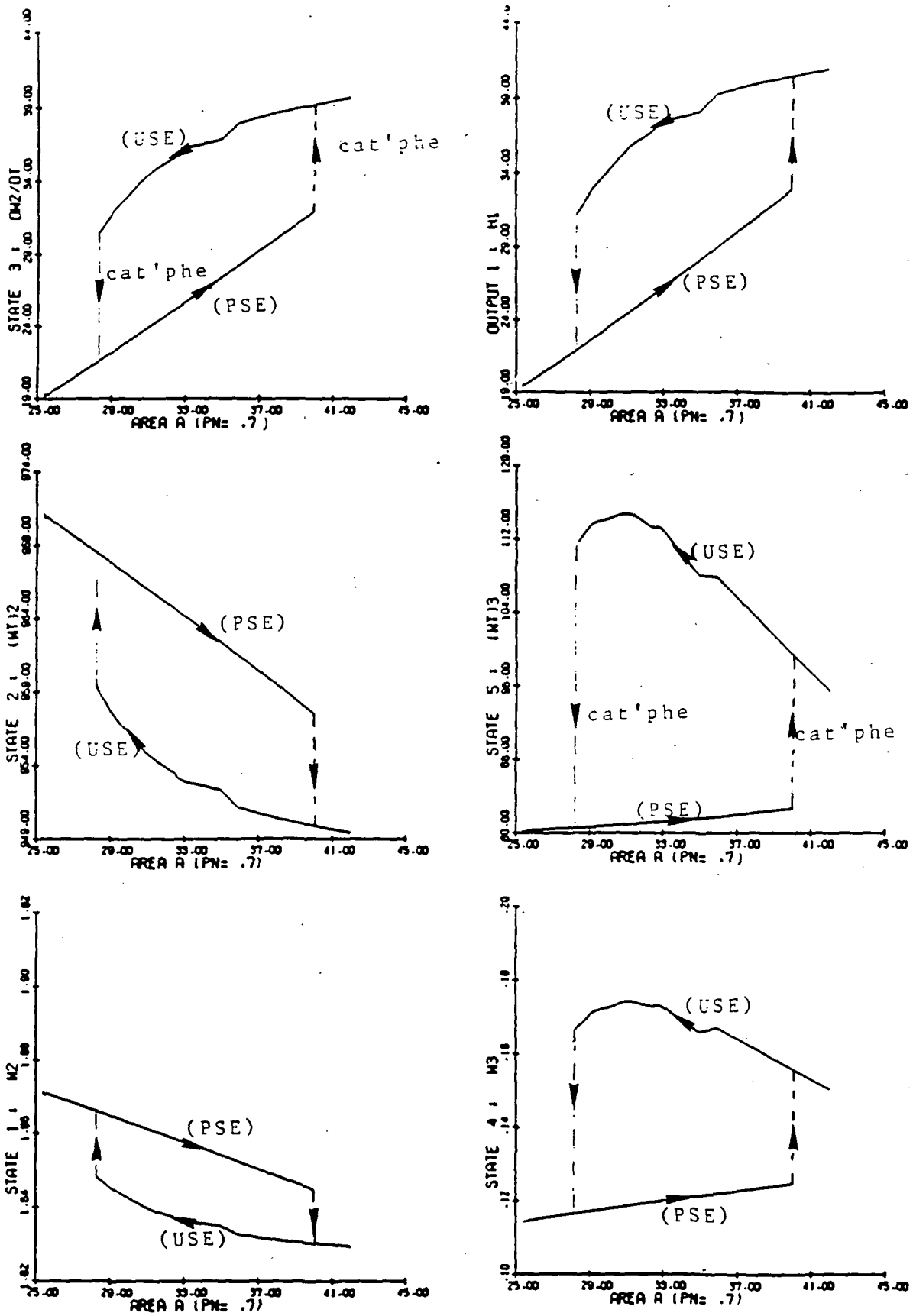

Figure 6.2(a) Bifurcation Diagrams in (x_i, A) Plane, $i = 1,5$ for PN = .7. Bifurcation (catastrophe) points are indicated by dashed lines.

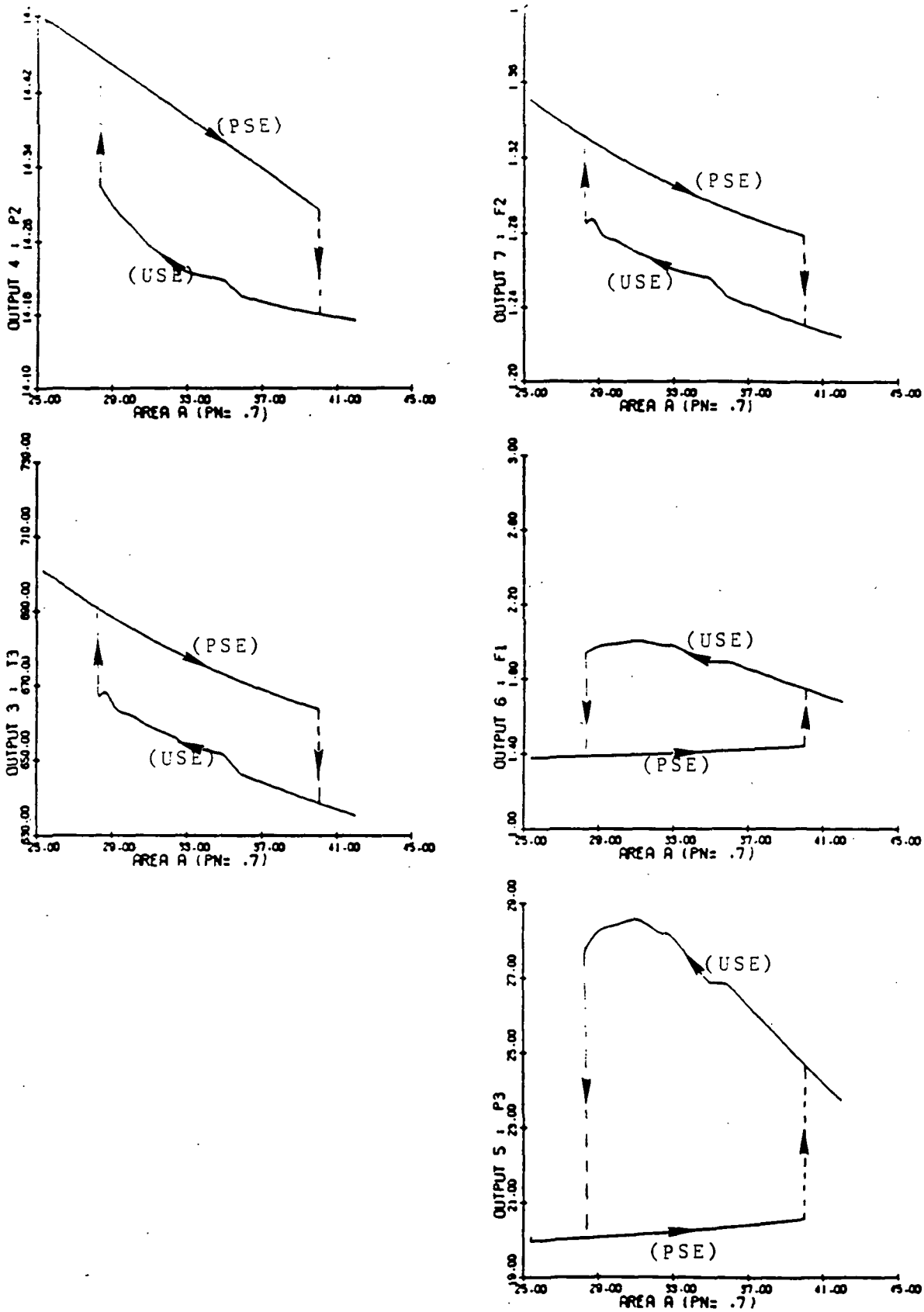

Figure 6.2(b). Output Variables y_i, i=3,...,7 versus area A, for PN = .7

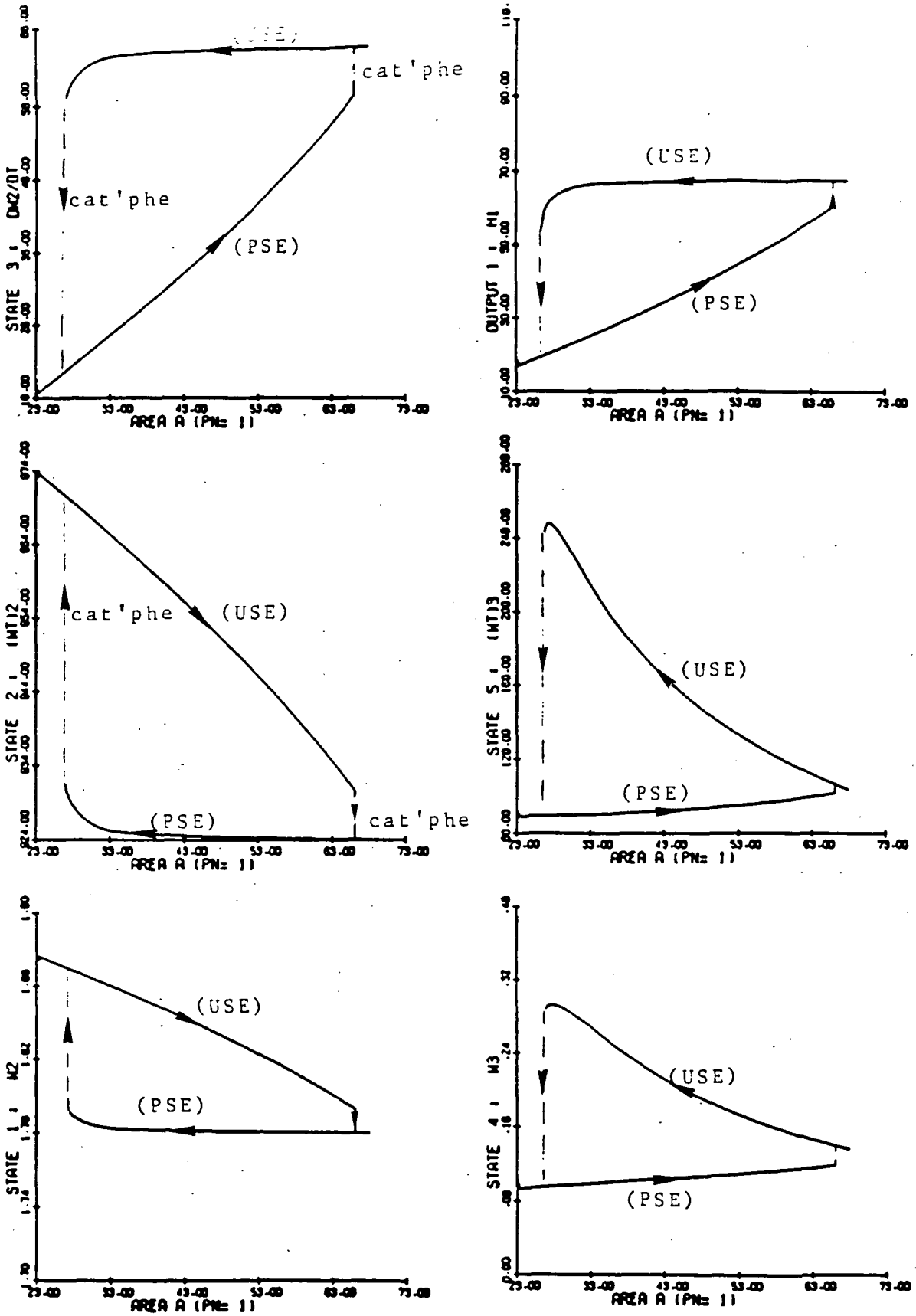

Figure 6.3(a). Bifurcation Diagrams in (x_i, A) plane, $i = 1,5$ and the Corrected Airflow $\bar{h}_1$, for PN = 1.0

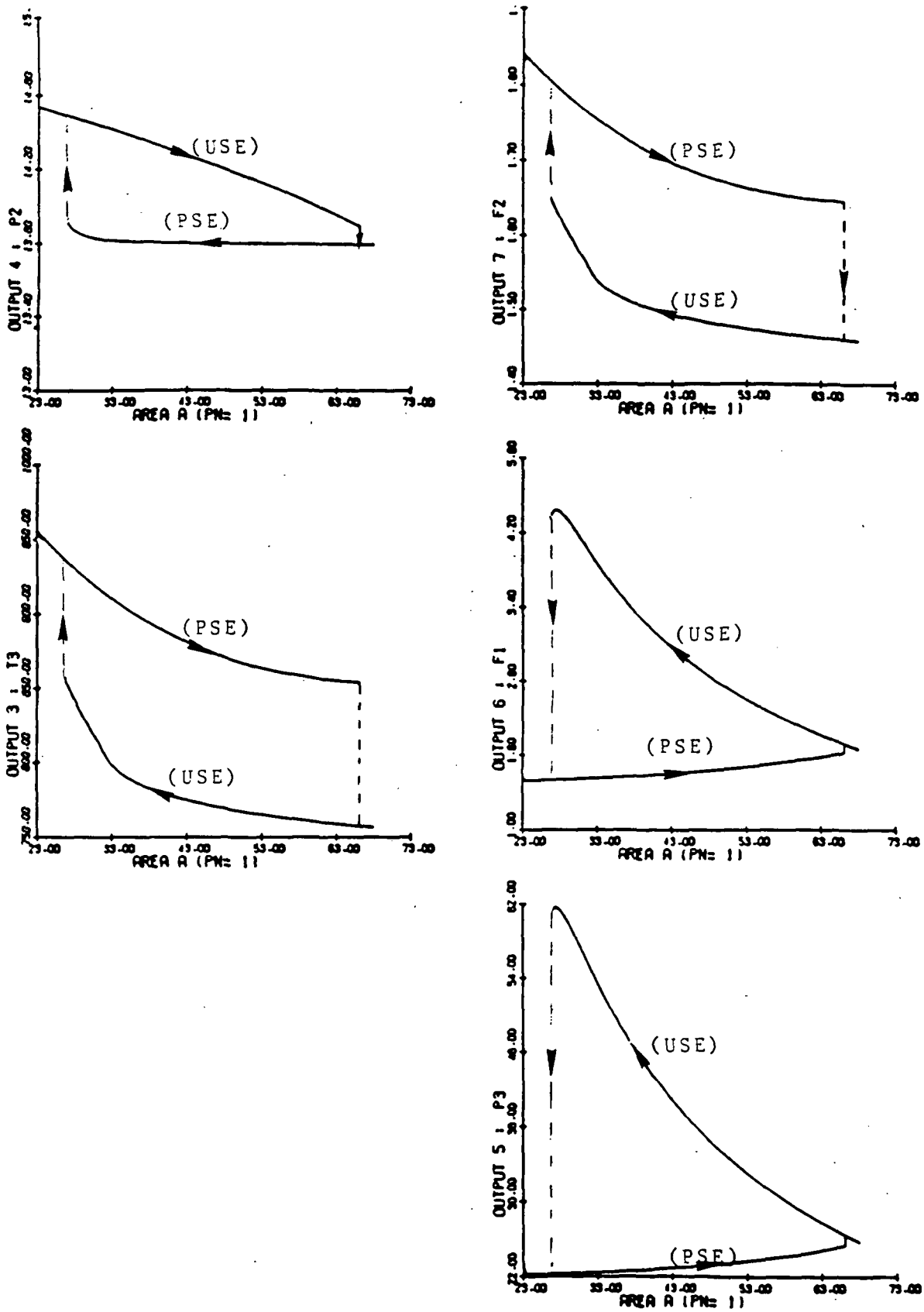

Figure 6.3(b) Some Output Variables y_i, $i = 3,\ldots,7$ for PN = 1.0.

the airflow rate $\dot{w}_2$ through the compressor.

Labels (USE) and (PSE) are used for indicating the equilibria of the unstalled and in-stall positive flow models, respectively. The dashed lines are the bifurcation points, and represent catastrophe points of the process using Thom's terminology (1974); the arrows indicate the direction of the movement of equilibria and jumps. Thus, for example, on the (x_3,A) diagram of Figure 6.1(a), as the downstream flow area A of the unstalled model is decreased from, say, 32, the flow x_3 continuously drops from a value of approximately 30 to that of 25 corresponding to $A \cong 25$. At this point there is a sudden drop in x_3 to the stalled value of $x_3 \cong 19$.

This process can also be described, for example, in terms of the compressor pressure ratio f_1 (output 6 of Figure 6.1(b)) and/or temperature ratio f_2 (output 7 of Figure 6.1(b)). Thus at the stall point corresponding to $A \cong 25$ the pressure ratio falls from approximately 1.63 to that of 1.34 and the temperature ratio rises from approximately 1.18 to that of 1.20.

Once the compressor enters the stall mode, recovery requires "extra effort" to take place. This is the result of hysteresis in the process. As A is now increased from the stall value of 25 it must reach the value of approximately 33 before recovery can take place. At this point the flow x_3 jumps from the stall value on (PSE) of about 27 to the unstalled value of about 31 on (USE). Or in terms of pressure and temperature ratios, the pressure ratio P_3^*/P_2 jumps from the stall value on (PSE) of about 1.38 to that of about 1.59 on (USE); the temperature ratio T_3^*/T_2 drops from the stall value of about 1.17 to that of 1.15. Figures 6.2 and 6.3 contain the same type of information for PN = .7 and PN = 1.0. (We did not feel it would be useful to include other speed values here — though they were computed.)

It is noted that the stall/recovery hysteresis loop grows as the corrected speed PN is increased. This is due to the fact that the stall thresholds increase with PN, while the in-stall characteristic remains relatively unaffected; this increases the unstall-to-stall gap at the point

of stall. However, the stall-to-unstall gap may or may not increase -- depending on which segment of the unstalled characteristic the recovery from stall to unstall takes place (e.g., compare gaps for PN = .6, .7, and 1 on Figures 6.1(a), 6.2(a), and 6.3(a)).

Figures 6.1 - 6.3 also illustrate that higher PN values require larger throttle variations, i.e., the width of the hysteresis loop increases with PN. In this way, for compressors with small allowable variations in throttle ares, recovery from rotating stall becomes a difficult problem. "Small" discontinuity in pressure change at stall is often associated with the compressor operating with one or more stall cells that do not cover the total height of the annulus. This is known as part span stall. For this type of stall the hysteresis effect is relatively small. On the other hand "large" pressure drops (associated with large hysteresis effects) characterize the full span stall. Figures 6.1 and 6.3 illustrate these cases.

We have been speaking of stall/recovery in the context of bifurcation of solutions. Figures 6.1 - 6.3 represent loci of equilibria and jumps. Thus the equilibrium loci describe the steady state behavior, not the transient. In other words the notion does not involve the so-called "off-design" situations. For this reason the stall and recovery process described above is perhaps best viewed as local (static) stall and local (static) recovery.

In order to capture the global transient or dynamic nature of the process, a different notion is required, namely, the domains of attraction of various equilibria and limit cycles. Though this subject is clearly beyond the scope of this investigation, we do nevertheless touch upon the subject. However, this is deferred until the following chapter in which the stall/recovery strategies are discussed; in that chapter parameter sensitivities are also discussed.

We note that the previously described local and global notions are intimately related — as the former provides the core for the latter. More specifically, the equilibrium loci provide the attracting and repelling poles for the trajectories of the dynamic process; thus they help shape the various zones.

We close by mentioning that the terms dynamic and static have been used in the literature of stall in different contexts. In particular, Greitzer (1980) discusses notions of static and dynamic stability. Roughly speaking, his description of dynamic stability corresponds to our definition of (local) static stability.

6.3 Hopf Bifurcation

Conditions for existence of Hopf bifurcation were given in Section 3.4. Here we describe the computational and algorithmic aspects of the problem, together with graphical illustrations.

Let's recall that we are interested in (oscillatory) solutions of the nonlinear dynamic systems

$$\frac{dx}{dt} = f(x,\mu) \tag{3.1}$$

with the property that

$$\phi_t(x_0,\mu_0) - \phi_{t+T}(x_0,\mu_0) = 0 \tag{6.1}$$

for some $x_0 \in R^n$ and $T \in [0,\infty)$, where we define $\phi_t(x_0,\mu_0)$ to be a solution to (3.1) starting from x_0, with the parameter μ set at μ_0.

Let's define $y \in R^{n+1}$ as

$$y = [x,\mu]' \tag{6.3}$$

and introduce an arc length parameter ℓ, giving

$$y(\ell) = [x(\ell),\mu(\ell)]'.$$

Then (3.1) and (6.1) become

$$f(y(\ell_0)) = \phi(y(\ell_0)) - \phi_{t+T}(y(\ell_0) = 0 \tag{6.4}$$

where $f \in R^n$.

We are interested in finding n+2 unknowns ($T(\ell_0)$, $y(\ell_0)$ satisfying (6.4). Suppose that for some μ_0 we know that there is a limit cycle solu-

tion; then we seek the (n+1) vector (x_0,T) satisfying n relations in (6.4); thus we need a further condition. Chua and Lin (1975) describe a procedure for fixing one element of x_0 to carry out the necessary predictor corrector iterations for homing in on the cycle.

The generic software package that we have developed contains a parameter continuation feature that generates a family of limit cycles as a function of the continuation parameter μ, starting from some easily obtained known solution corresponding to some initial parameter value μ_0.[3] (We will refer to this generic package as the Hopf package.) Thus starting from some initial point "near" a limit cycle, the Hopf routine will close in on the exact location and period of the cycle, for the particular value of the parameter μ that was selected. The continuation part of the routine consists of updating the continuation parameter μ and finding the corresponding new limit cycles that are created. (See Carroll and Mehra (1982) for a description of BACTM.)

Just as in the case of stationary equilibria, a limit cycle may or may not be stable. This means that in the case of a stable limit cycle, initial points beginning near the limit cycle will converge to it; the converse is true of unstable limit cycles. Hirsch and Smale (1974) present conditions for stability of limit cycles. The issue is related to the stability of the matrix G

$$G := \frac{\partial\ \phi_T(x_0,\mu_0)}{\partial\ x_0} \quad . \tag{6.5}$$

Here we are interested in the stability of the discrete mapping ϕ^n —as we wish to compare the values $x(t_0)$, $x(t_0 + T)$, $x(t_0 + 2T)$,... $x(t_0 + nT)$,... for various nonnegative integers n.[4] The precise condition for the stabi-

[3]This is the generic form of BACTM. BACTM is the acronym for Bifurcation Analysis and Catastrophe Theory Methodology. The software was developed by Scientific Systems, Inc. for the analysis of flight dynamics problems.

[4]ϕ^n is defined as the composite mapping $\phi.\phi.$ ..., repeated n times.

lity of a limit cycle is that all but one eigenvalues of G must be less than 1 in magnitude, while the remaining eigenvalue is always 1.

Unstable limit cycles are not easily observed in nature or in time simulation experiments. However, their presence does change the underlying dynamics. In the context of our investigation an unstable limit cycle can "carry" a trajectory into the in-stall (normal or reverse flow) region, or into the unstalled region — depending on the exact position of the cycle and the intervening control actions adopted.

Returning to our discussion of compressor stall, we are interested in determining whether the compressor exhibits any oscillation of the type described by the Hopf theory. This type of oscillation is often associated with surge in compressors (e.g., Greitzer (1982)). The present investigation appears to be the first published work indicating that such oscillations are due to Hopf bifurcation of solutions.

The unstalled compressor model (US) exhibits Hopf bifurcations at certain critical values of parameters. We have observed this behavior for every given corrected speed PN value (of course at different parameter settings). We have verified the oscillatory behavior by time simulations. Figures 6.4(a) through 6.4(f) show the development of a stable limit cycle for the corrected speed PN = 0.6. It can be seen that before the limit cycle disappears it becomes unstable. The stable limit cycle family reaches its peak amplitude for $A \cong 27.2$. Figure 6.4(f) indicates the period of the limit cycles as the parameter A varies. The peak period of the limit cycles is reached for $A = 27.32$; the corresponding period $T_{peak} \cong 16.6 \times 10^{-3}$ seconds. The minimum period of about 16.36×10^{-3} seconds is reached for $A = 26.9$.

As A is increased from the value of approximately 27.2, the stable limit cycle amplitudes decrease. For $A \cong 27.3892$ and beyond the stable limit cycles disappear and a family of unstable limit cycles is born.

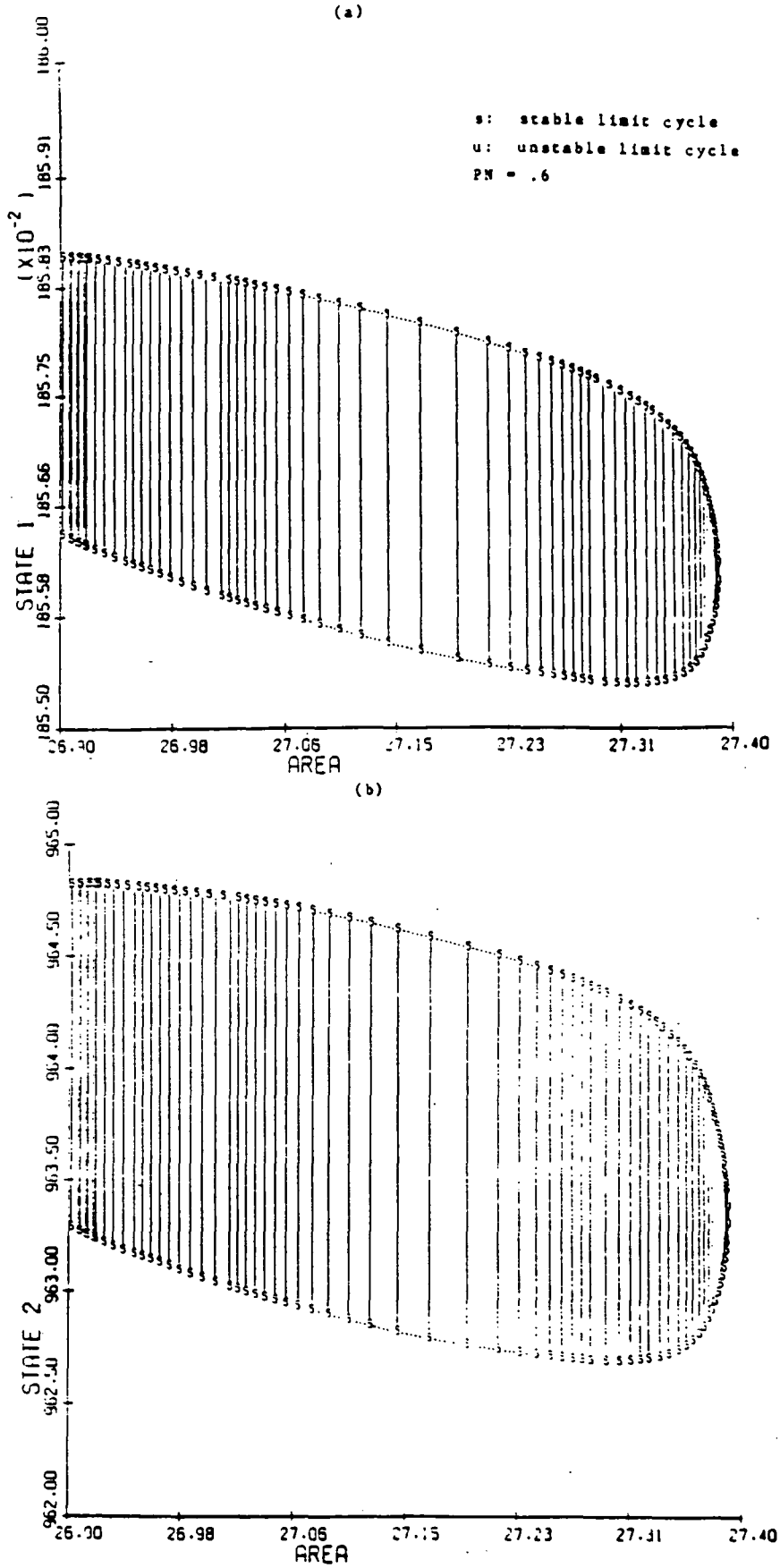

Figure 6.4(a),(b). Development and Disappearance of Stable Limit Cycle Projected on (x_i, A) Plane, $i = 1,2$. (State 1 = W_2, State 2 = $(WT)_2$)

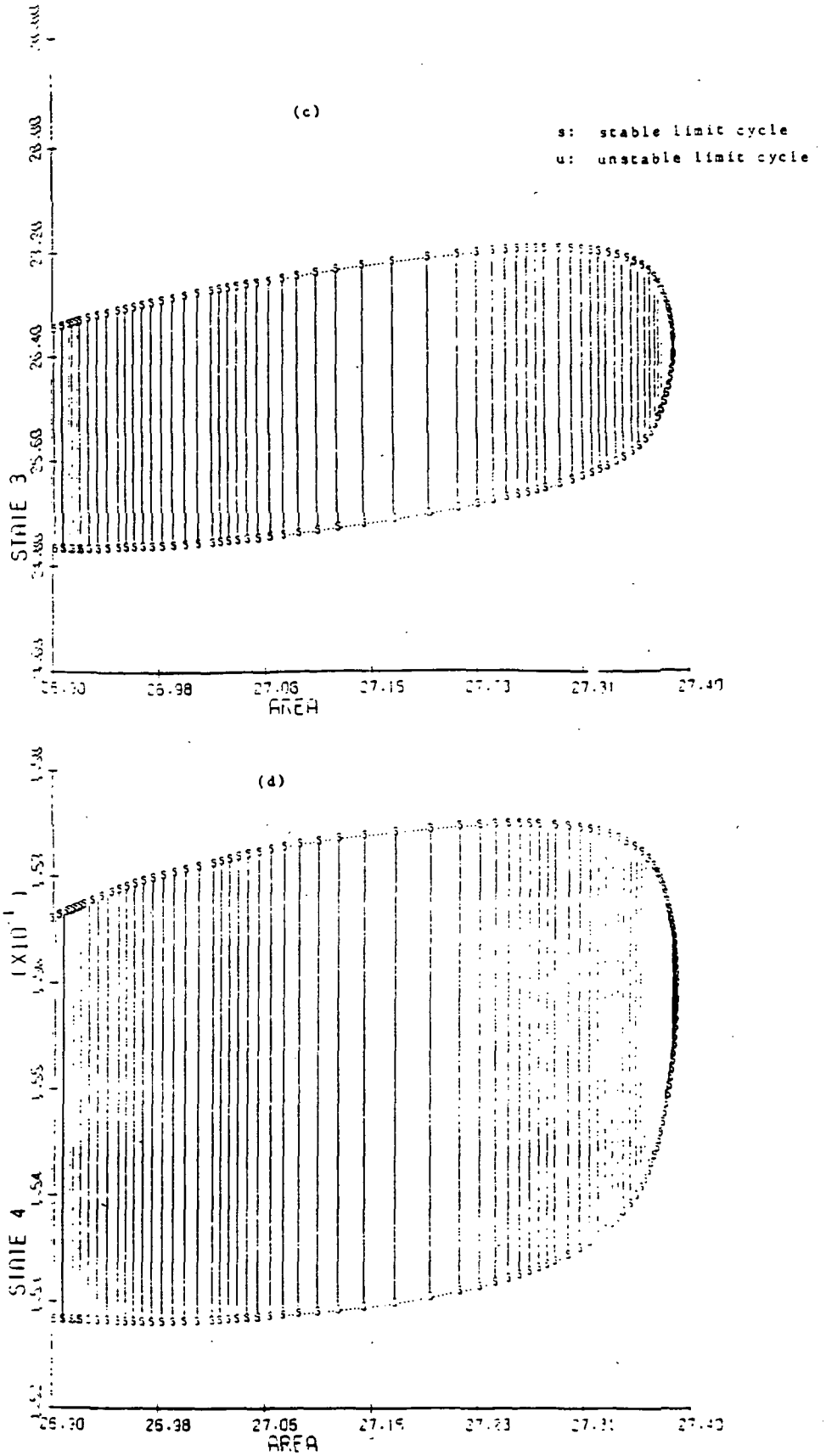

Figure 6.4(c),(d). Development and Disappearance of Stable Limit Cycle Projected on (x_i, A) Plane, i = 3,4. (State 3 = $\dot{\omega}_2$, State 4 = W_3)

s: stable limit cycle
u: unstable limit cycle
PN = .6

(e)

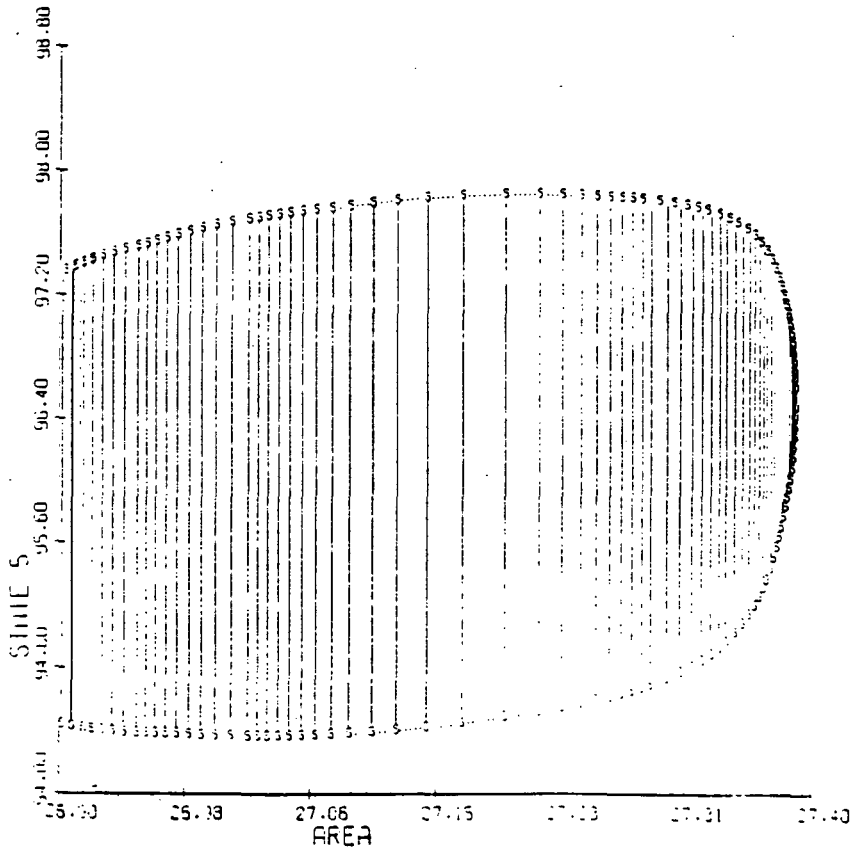

Figure 6.4(e). Development and Disappearance of Stable Limit Cycle Projected in (x_5,A) Plane. (State 5 = $(WT)_3$)

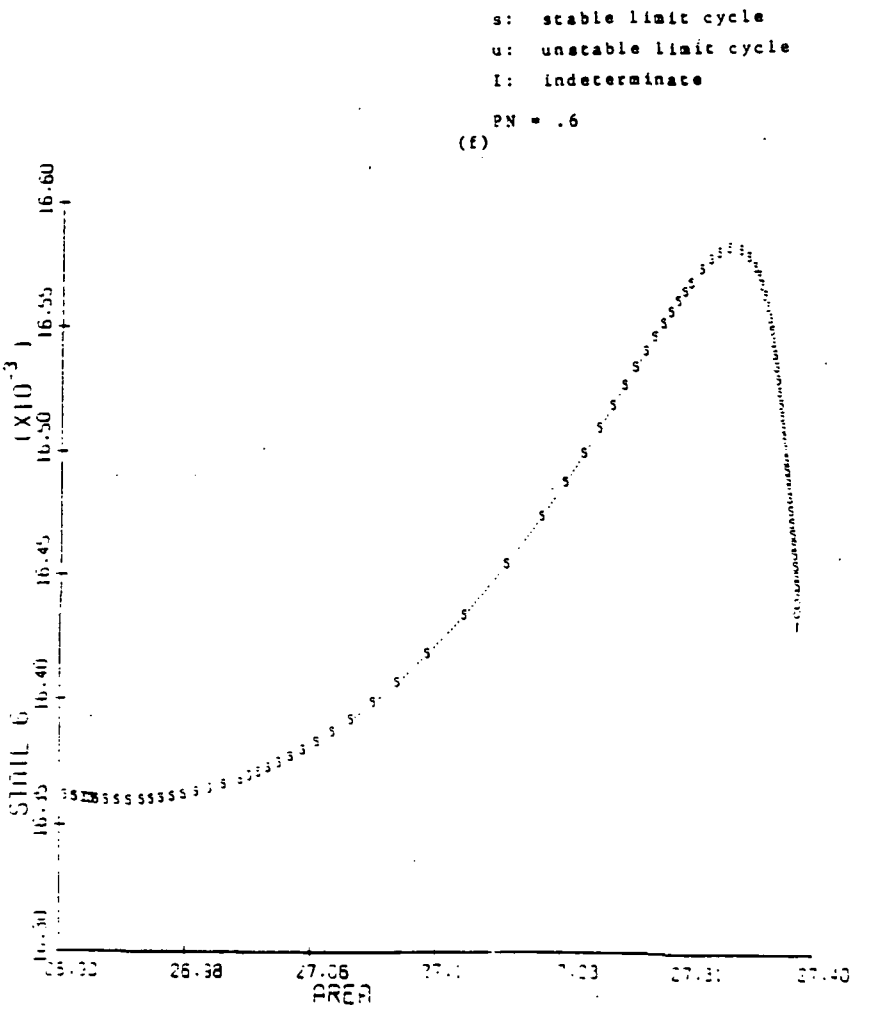

Figure 6.4(f). Period of Limit Cycles Versus A. (State 6 = T = period)

6.4 Global Bifurcation of Limit Cycles

Equation (6.1) of the previous section describes the property that limit cycle solutions must possess, namely, the existence of a pair (x_0,T) such that a trajectory of (3.1) satisfies

$$\phi_t(x_0,\mu_0) - \phi_{t+T}(x_0,\mu_0) = 0 \tag{6.1}$$

for all times $t > 0$. Equation (6.5) was used to describe the local stability of a limit cycle "starting" at x_0 and having the period T. Just as in the case of stationary equilibria, at some critical parameter value, say μ_0, Equation (3.1) may admit a multitude of solutions, say m of them, with the property

$$\phi_t^i(x_0^i,\mu_c) - \phi_{t+T_i}^i(x_0^i,\mu_c) = 0 \tag{6.6}$$

for "initial condition" x_0^i and period T_i, $i = 1,\ldots,m$.

Each limit cycle L_i would then have its local stability property as described by the corresponding stability matrix G_i, $i = 1,\ldots,m$

$$G_i = \frac{\partial\ \phi_t^i(x_0^i,\mu_c)}{\partial\ x_0^i} \quad . \tag{6.7}$$

If m represents the total number of limit cycles, then their determination represents a global solution to the problem. The situation is depicted in Figure 6.5. In this figure a total number of 3 limit cycles in the solution space X have been depicted for the parameter value μ_c.

Figures 6.6(a) - (b) depict the development and disappearance of a family of stable limit cycles — giving rise to an unstable family which subsequently bifurcates into three families of limit cycles; the continuation parameter is A, as before. Only 4 of 6 state variables are shown -- for the sake of brevity. Vertical bars indicate the amplitude of the limit cycles. As can be seen from Figures (a),(b),(c), and (d) as the

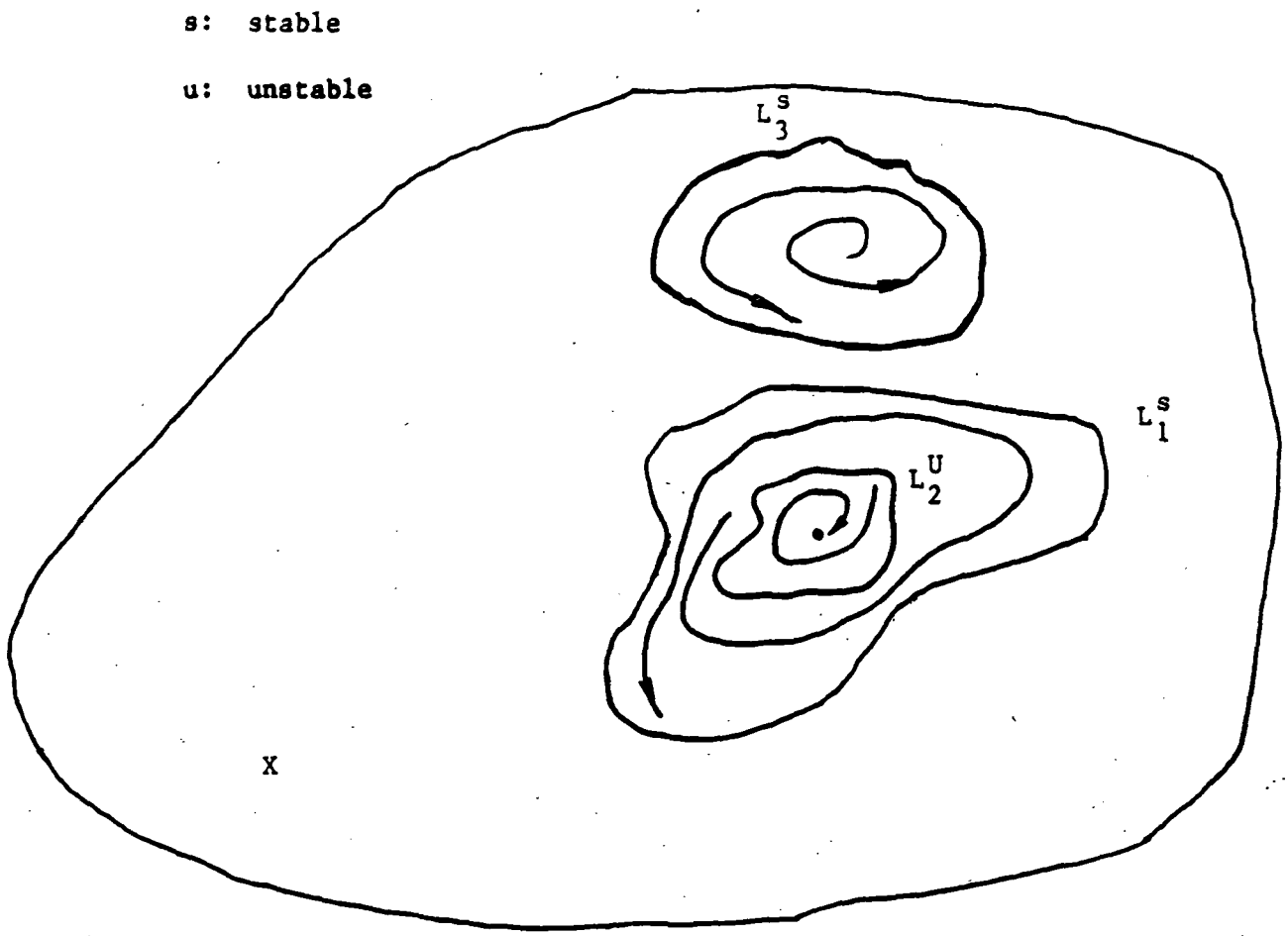

Figure 6.5 Several Limit Cycles Contained in Space X for a Critical Value μ_c of Parameter μ

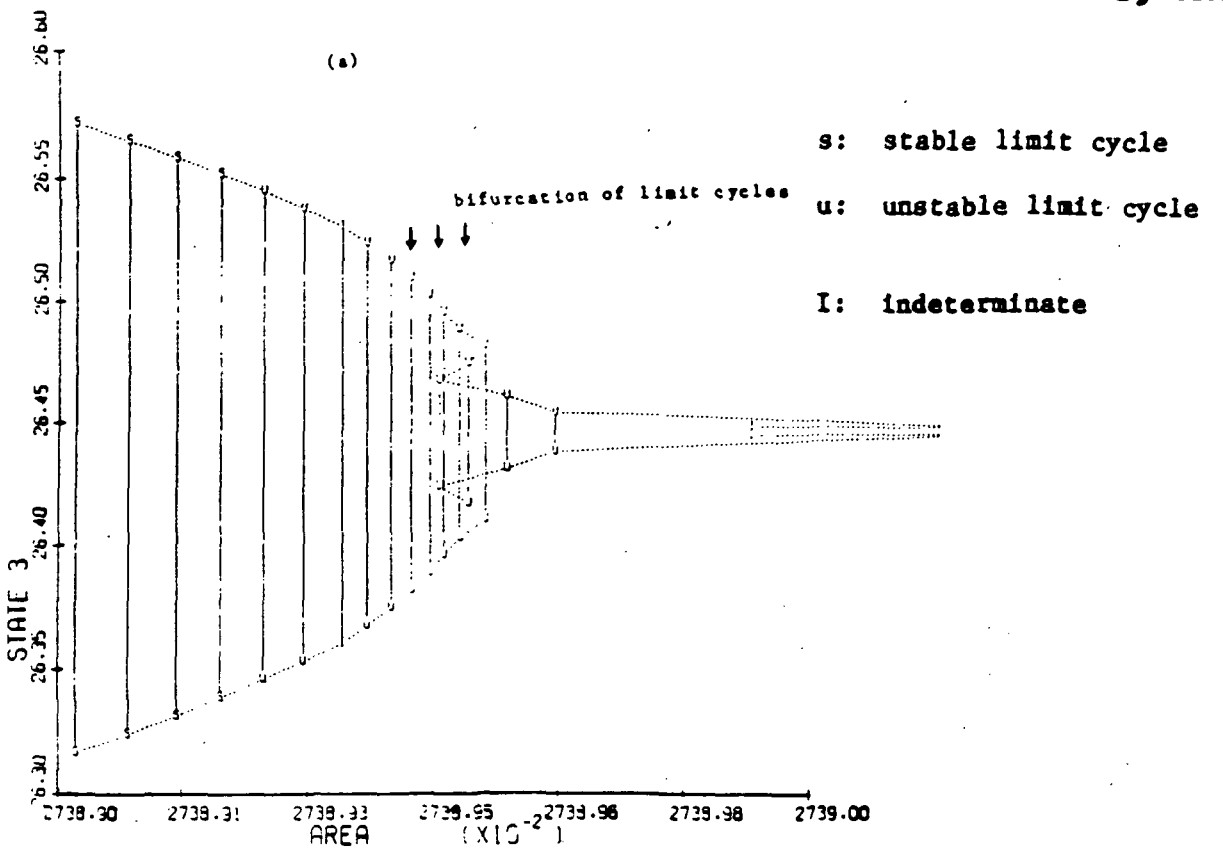

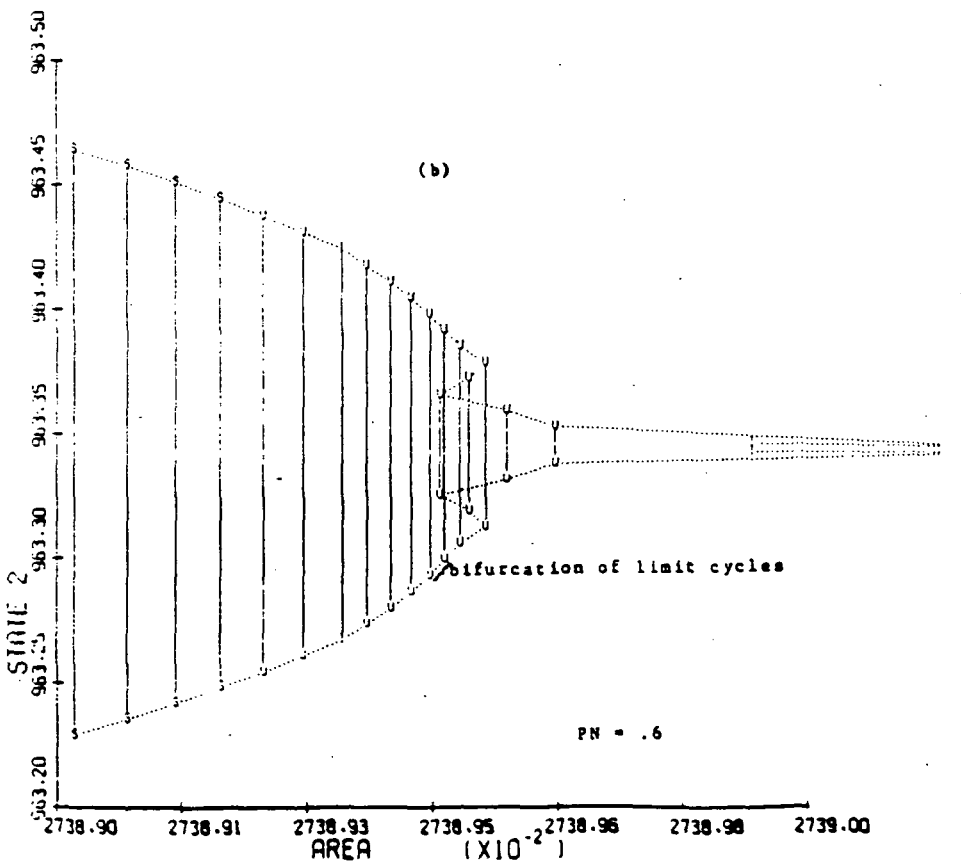

Figure 6.6(a), (b). A Family of Stable Limit Cycles Gives Rise to an Unstable Family. The Unstable Family Splits Off into 3 Families, As Shown.

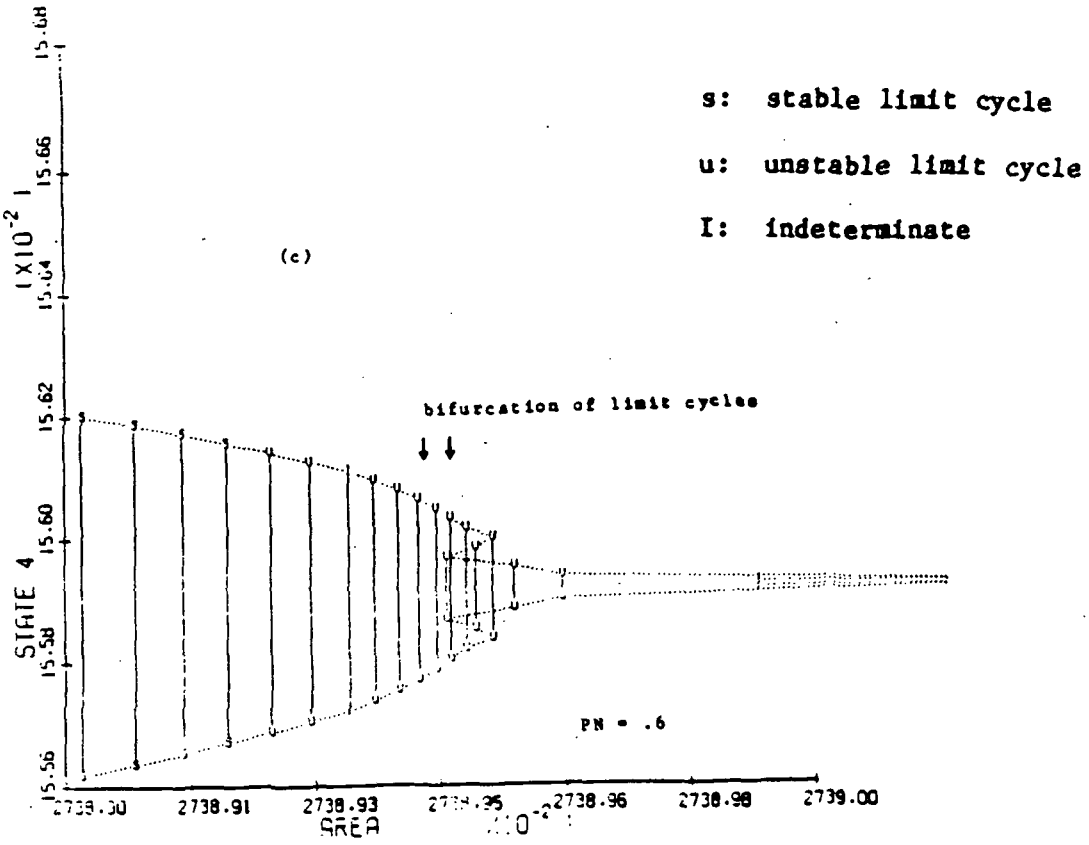

Figure 6.6(c). Limit Cycle Propagation as in Figure 6.6(a),(b) on (x_4,A) plane $(x_4) = W_3$

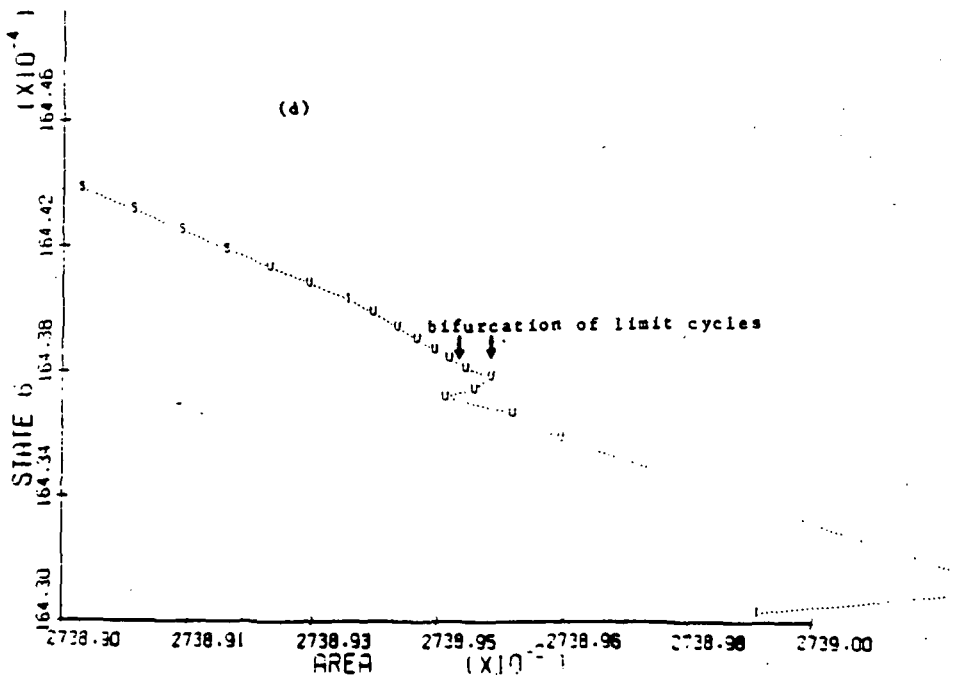

Figure 6.6(d). Period $T = x_6$ of Limit Cycles as a Function of the Parameter A.

parameter A is increased from its initial value of about 27.3890 the amplitude and the period of the stable limit cycles continues to shrink. Approximately at A = 27.3892 and beyond the limit cycle becomes unstable while decreasing in amplitude. Further, increase in A to a value of approximately 27.3895 causes an increase in the number of limit cycles (from 1) to 3. As can be seen from the Figures, this condition persists until A exceeds a value of approximately 27.38955. At that point and beyond once again a unique (unstable) limit cycle family is generated. It can be seen from Figure 6.6(d) that the three limit cycles not only have different amplitudes and "locations" but that their periods are also different. We note that the above graduations in A are too small to be experimentally verifiable, even though the software was calibrated for a 10^{-5} precision level. The point of the above discussion is to point out the theoretical possibility of obtaining 'multiple surge cycles' for some critical parameter values. In fact we do not claim to have discovered <u>all</u> such cycles. A further investigation is warranted to either validate or refute this possibility in a number of realistic models.

We close by noting that the above solution classes represent a fairly complex dynamic phenomenon, involving stable and unstable limit cycles of varying quantity, amplitude, period, and location — all derived as a function of the parameter A. In this way it can be observed that the usual one-to-one association of the values A with "stability" or "instability" is at best an ambiguous notion. This same observation can be expected to extend to other parameters.

6.5 Time Simulations

Here we will present several simulations of the process for various values of the parameters PN and A. This will also serve as a confirmation of some of the results obtained in previous sections by other means.

Figures 6.7(a),(b),(c), and (e) present the time profile of three variables: state variable $x_3 := \frac{dW_2}{dt}$, output variable $F_1 := \frac{P_3^*}{P_2}$, and output variable $F_2 := \frac{T_3}{T_2}$. Other variables have similar properties and have not been sketched, for the sake of brevity.

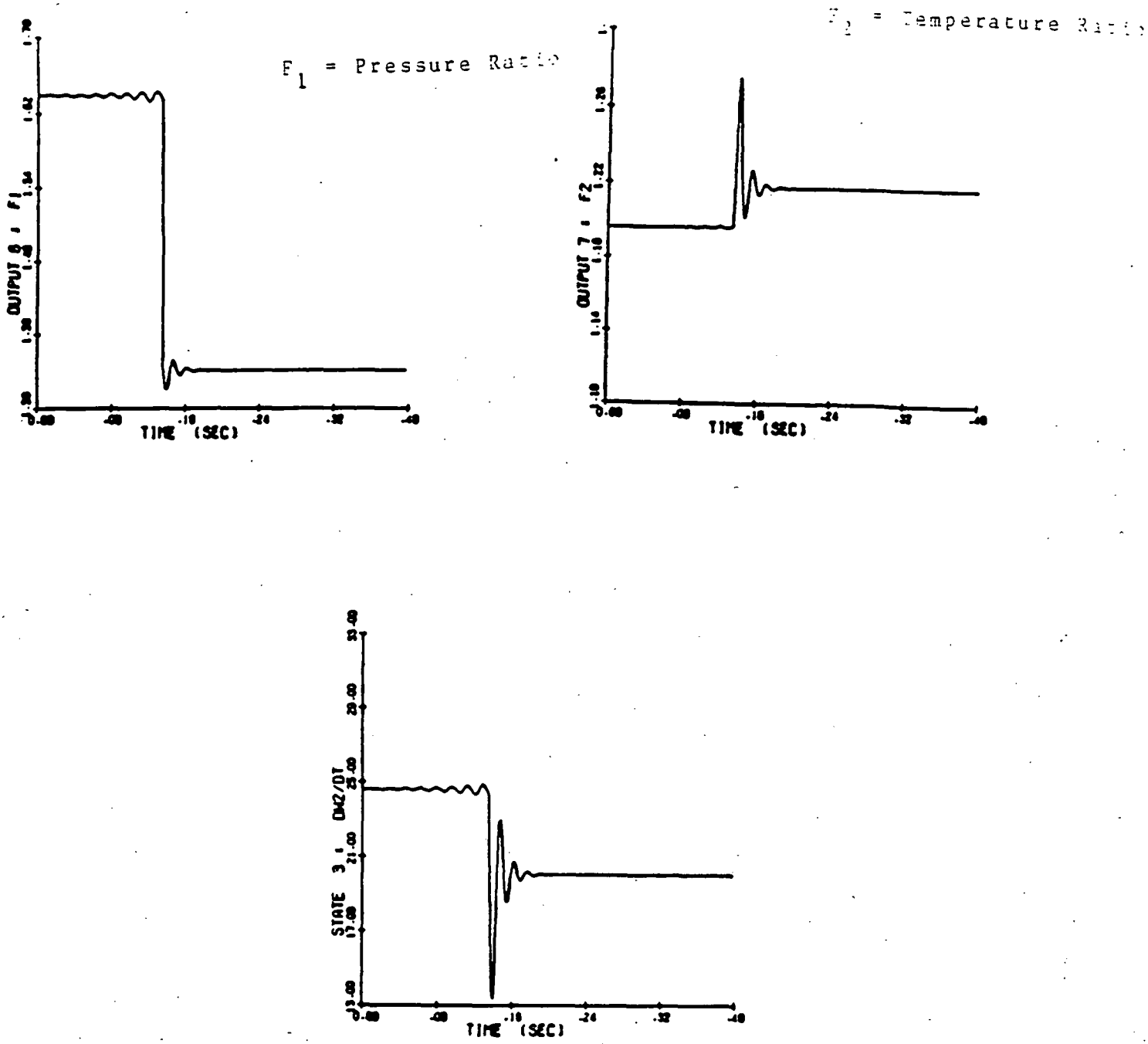

Figure 6.7(a). Growing Oscillations in Unstalled Compressors Lead to (Rotating) Stall. PN = .6 and A = 25.94.

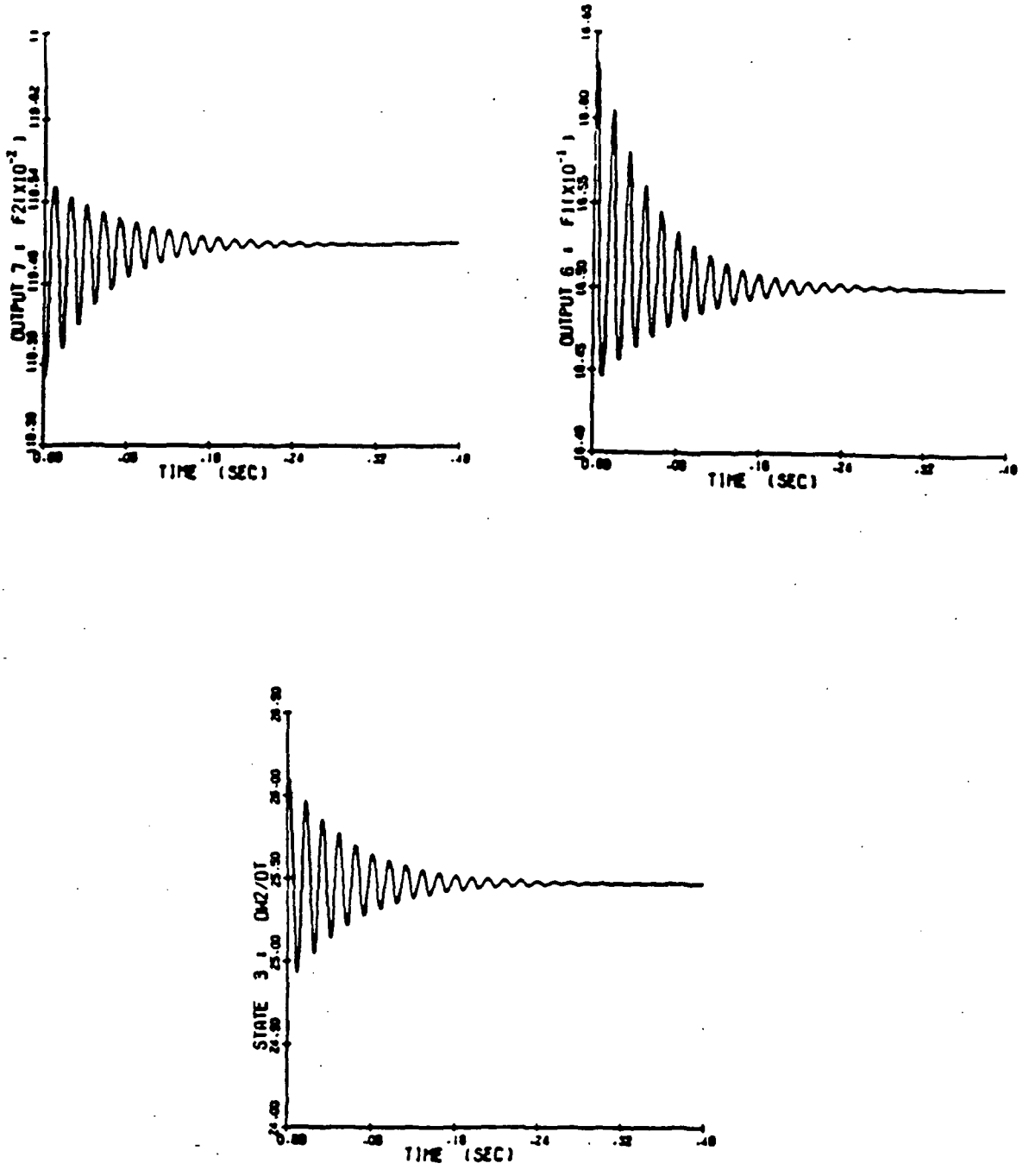

Figure 6.7(b). An Increase in A from its Value in (a) to A = 26.7 Leads to Unstalled Equilibrium

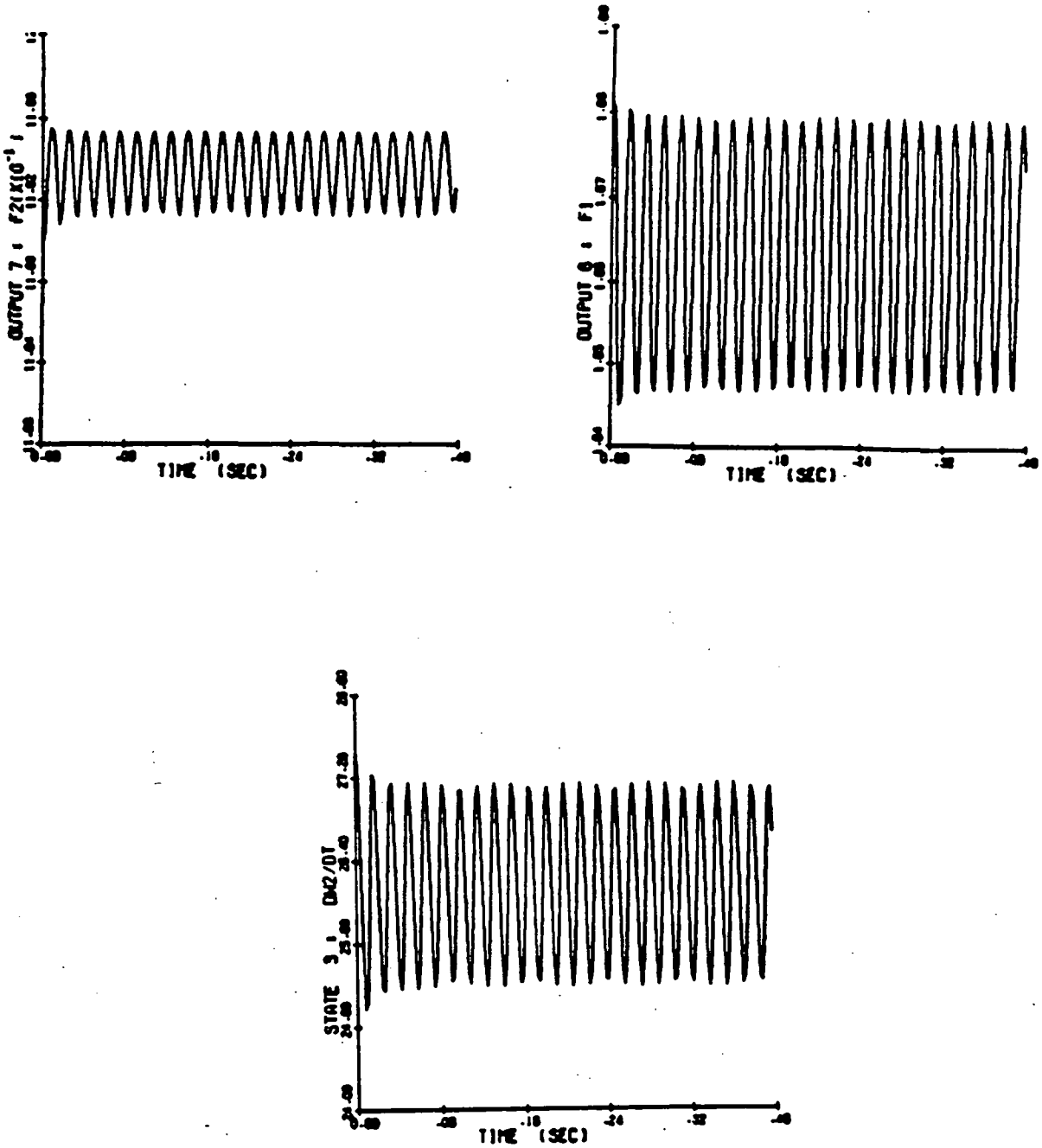

Figure 6.7(c). A Further Increase in A from its Value in (b) to A = 27.2 Leads to Sustained Limit Cycle

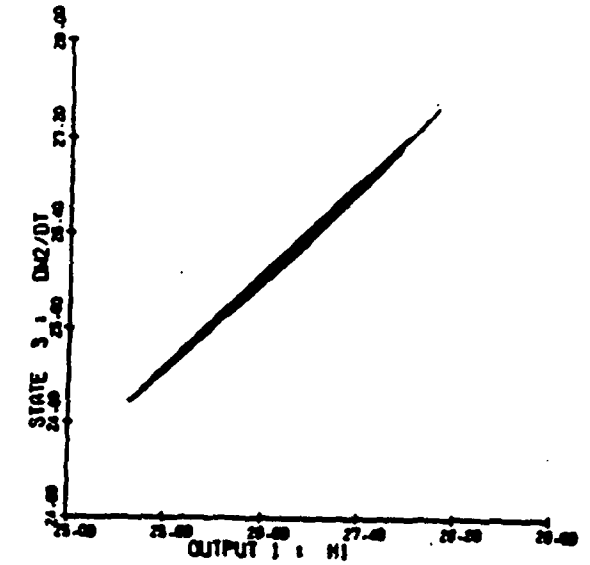

Figure 6.7(d). Phase Portraits of the Stable Limit Cycle in Figure 6.7(c). Cycle is Projected on (x_i, H_1) Planes for $i = 1,5$ H_1 = Corrected Flow Rate Through Compressor.

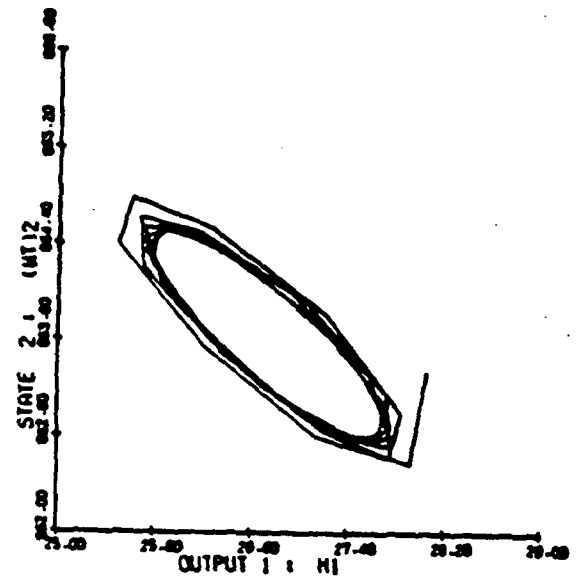

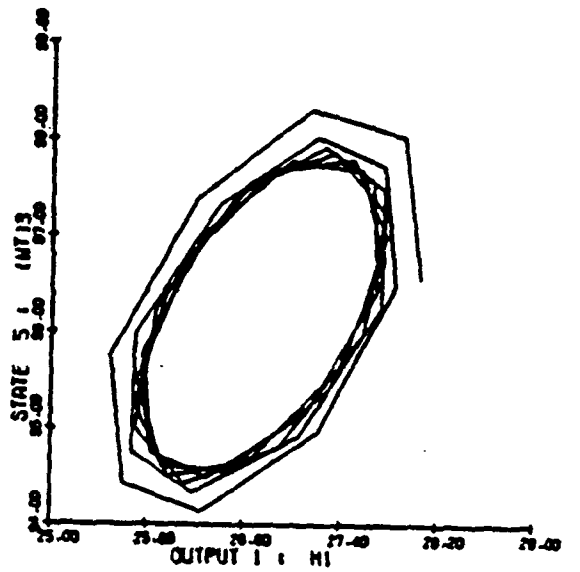

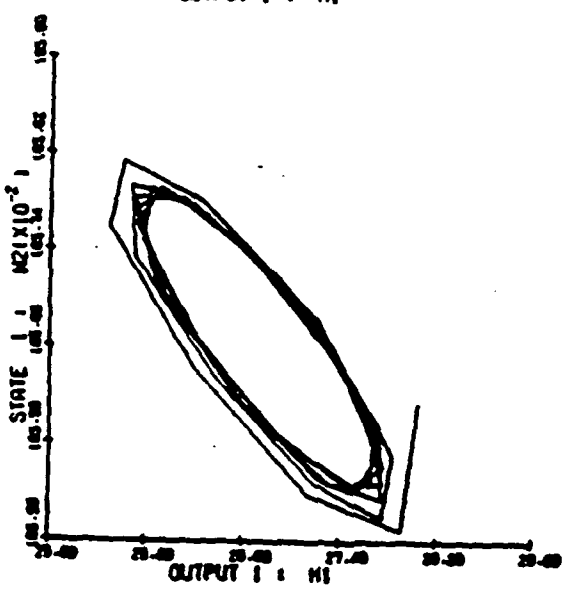

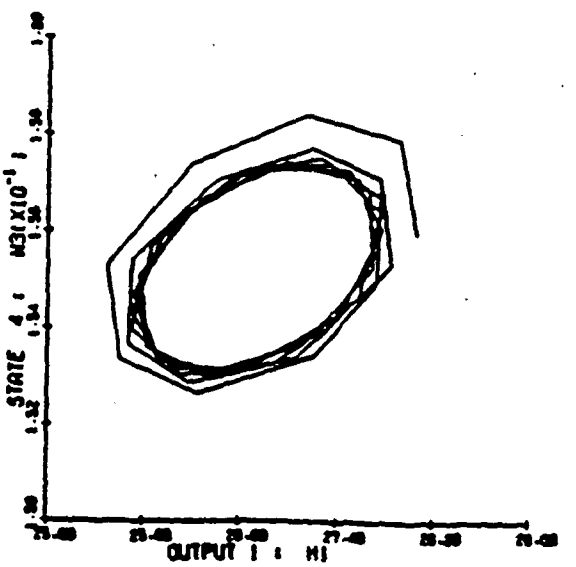

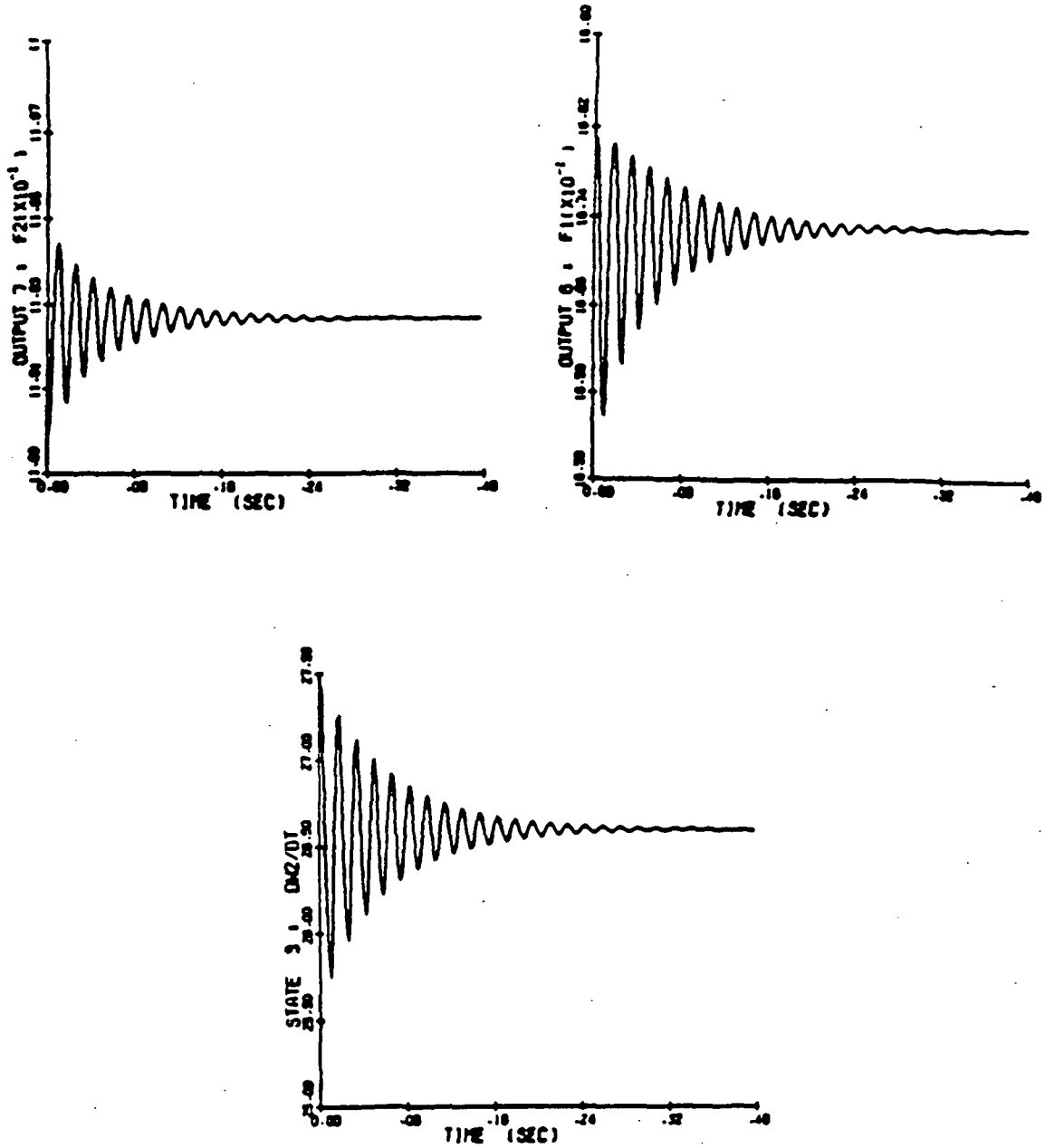

Figure 6.7(e). A Still Further Increase in A From its Value in (d) to A = 27.5 Yields Unstalled Equilibrium.

Figure 6.7(a) presents a trajectory with growing oscillations which begins in (US) and ends in rotating stall (PS). An increase in A to the value of 26.7 restores equilibrium in the unstalled region; this is shown in Figure 6.7(b). A further increase in A, however, brings about oscillatory behavior. Comparing this case with that illustrated in Section 6.5 (e.g., Figures 6.4(a) through 6.4(f)), we see that these oscillations are indeed limit cycles produced by Hopf bifurcation of equilibrium solutions. It can be observed from the plots that both amplitude and frequency of oscillations agree very closely.[5] A Phase Plot of the time function of Figure 6.7(c) is shown in Figure 6.7(d); it shows how a trajectory approaches the (stable) limit cycle. A still further increase in A to the value of approximately 27.5 further restores the unstalled equilibrium.

Thus from the point of view of recoverability it makes a difference by how much a certain nominal value of A is changed and in what direction. Both decreases and increases in appropriate ranges can remove surge type oscillatory behavior. It should be observed that the implications for surge/recovery due to area changes described in the previous paragraphs (or changes in any other parameters) are dependent on the particular trajectory in question, with respect to its location in the trajectory space. Thus further characterization and analytical machinery is required. In the next chapter we will address this problem in part. Finally, surges in the state variables rate for corrected speeds PN of .7, .8, .9 and 1 are listed in Figures E(a) through E(d) in Appendix E.

[5]It is clear that not every oscillatory motion corresponds to a limit cycle.

7. DOMAINS OF ATTRACTION FOR OFF-DESIGN STABILITY, STALL/RECOVERY, AND SENSITIVITY ANALYSIS

7.1 Introduction

The problem of compressor stall is ultimately related to the stability behavior of the compression system under conditions other than the normal steady-state operating environment. In Section 5 we discussed the loci of solution equilibria; and the stability issues that were discussed referred to the local properties of equilibria. However, a given trajectory may or may not be 'near' any equilibria; its stability behavior depends on its overall position, in a global sense.

In order to obtain a complete classification of trajectories we need to compute the **domains of attraction** of equilibria. This problem, however, is beyond the scope of this investigation. But in order to highlight its usefulness for stall/recovery we discuss the issue in Section 7.3. In Section 7.5 we show the applicability of the domain of attraction for use as a criterion of stall. This appears to offer a natural generalization of the notion that the (low) values of corrected flow can be used as proxy for entering stall, e.g., Section 7.4. Partial computations of domains of attraction are presented in Section 7.6. However, in Section 7.2 we first define three types of trajectories according to the 'severity' of their stall/recovery, and give some examples.

7.2 First Stage, Second Stage, and Third Stage Stall/Recovery

We have seen that the total dynamic behavior of the compressor in various conditions can be modeled as three interlocking dynamic models (US), (PS), and (RS). Let's start with a compressor in normal steady state unstalled condition and perturb the steady state operating point, say x_0, to that of $x_1 = x_0 + \delta x_0$ to create an off-design condition. A trajectory based at x_1 and under the control regime $U(\cdot)$ is defined as $\phi_t(x_1,u)$. Depending on the stability properties of x_0 and the amount of perturbation, the resulting trajectory may (i) only involve (US), or (ii) involve (US) and (PS), or (iii) involve (US), (PS), and (RS).

One can think of off-design transient conditions which, using the available control action u, can be cleared without having the compressor enter into either of the two stall conditions as being somewhat benign. We define such trajectories as being **first stage recoverable.**[6] On the other hand, if despite all the available control action the trajectory still enters stall but can be cleared without entering reverse stall, such a stalling trajectory is defined to be **second stage recoverable.** Finally, if the stalling trajectory can be cleared only upon entering (and leaving) both stall conditions, the stalling trajectory is defined as **third stage recoverable.**

The above terminology can be justified by noting that (i) physically, every time a compressor stalls it stands a certain chance of being damaged, perhaps due to some unmodeled factors and, (ii) from a modeling point of view a first stage recoverable trajectory will involve only one dynamic model, thus involving the least amount of dynamic complexity, etc.

Figure 7.1(a) shows a trajectory that begins in the unstalled region and eventually settles in a rotating stall equilibrium.[7] This stalling trajectory can be cleared by a combination of a decrease in PN (to 60%) and an increase in A (to 32). Figure 7.1(b) shows that the trajectory is first stage recoverable. On the other hand, Figure 7.2(a) shows a different stalling trajectory. It turns out that for this trajectory no combination of parameter setting exists that can keep it from entering stall. Figure 7.2(b) shows that this trajectory is second stage recoverable.[8]

---

[6] These terms are defined intuitively only; one can refine these definitions by introducing a mathematical notation.

[7] For the sake of brevity only x_3 component of the trajectory is shown.

[8] Here we limit ourselves to fixed parameter settings.

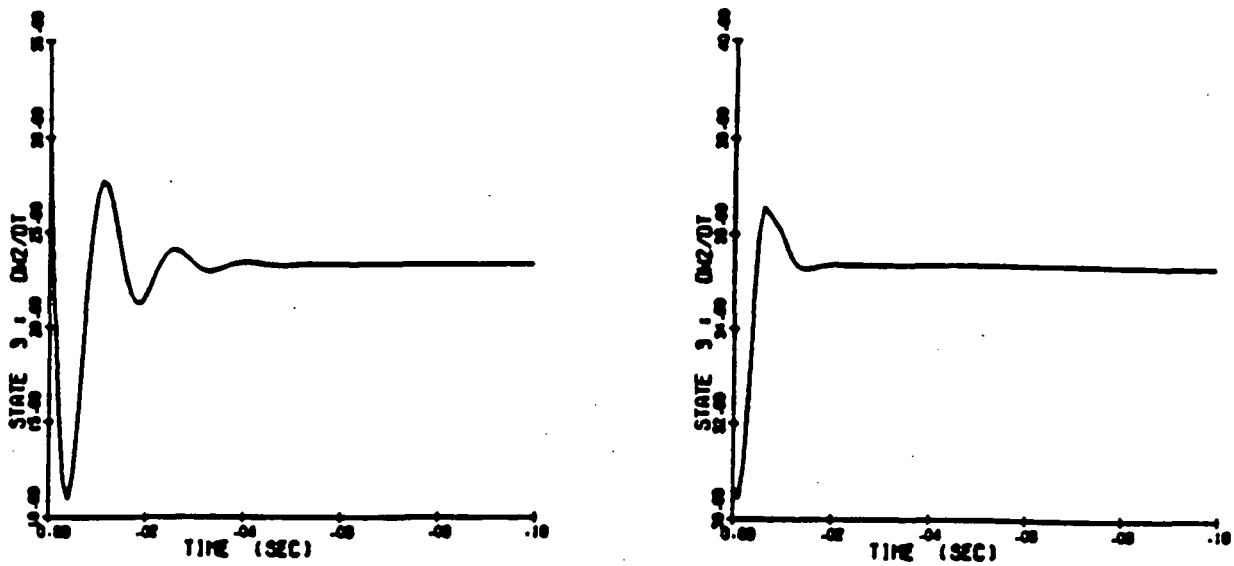

(a): PN=.7, A=30.25, $x_3(0)$=30.0 (b): PN=.6, A=32.0, $x_3(0)$=30.0

Figure 7.1. Example of first-stage recoverable trajectory. Using combination of PN and A, a stalling trajectory (a) is recovered without entering stall (b).

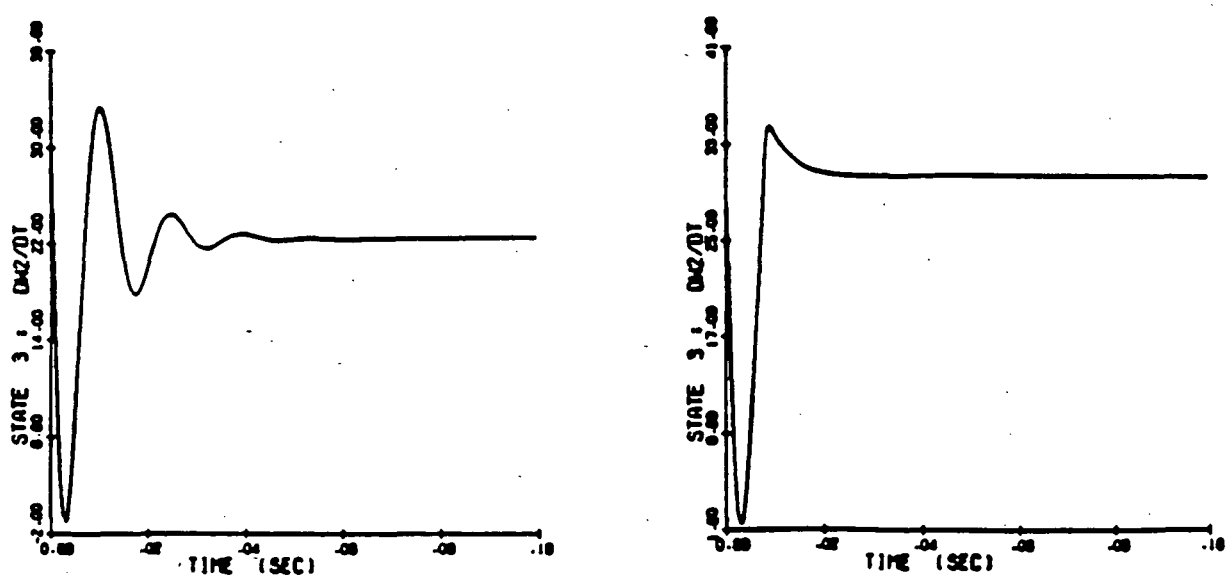

(a): PN=.7, A=29.5, $x_3(0)$=29.3 (b): PN=.7, A=32, $x_3(0)$=29.3

Figure 7.2. Example of second-stage recoverable trajectory. No combination of PN and A exists which can keep trajectory from entering stall before recovery.

7.3 Domains of Attraction

Intuitively an attracting set A for a point x is that which 'attracts' the trajectory $\phi_t(x,\mu_0)$ based at x as time increases.[9] Accordingly, the domain of attraction of A is made up of all those xs which will eventually end up (under the action of the system) at A. A little more notation makes this more precise. A closed invariant set $A \in R^n$ is called an attracting set if there is some neighborhood V of A such that $\phi_t(x) \to A$ as $t \to \infty$, for all $x \in V$. The set $D := \bigcup_{t<0} \phi_t(V)$ is said to be the domain of attraction of A. (The set A may be just one (equilibrium) point.)

These simple ideas can be used to advantage for the analysis of stall and recovery. Let a normal operating condition of the compressor be denoted by x_0, corresponding to the nominal parameter μ_0. The elements of μ_0 may be some design parameters (such as the downstream volume V_3), and some adjustable parameters (such as the throttle area or the rotor speed). Let D_{μ_0} denote the corresponding domain of attraction. Figure 7.3 illustrates this.

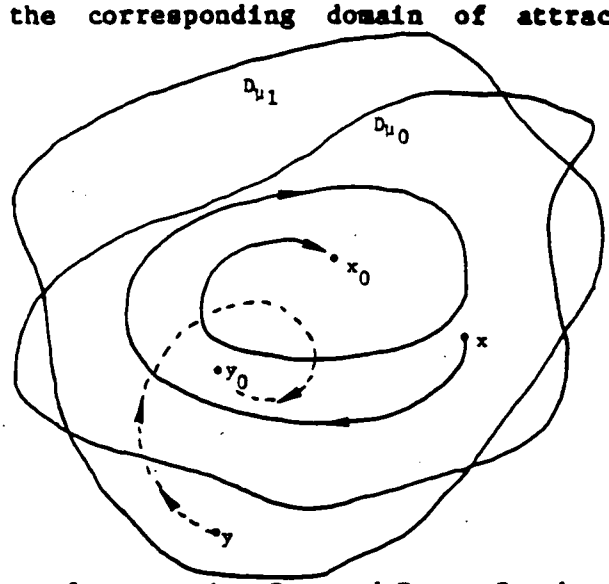

Figure 7.3 Domains of attraction D_{μ_0} and D_{μ_1}. By changing the parameter μ_0 to μ_1, an otherwise stalling trajectory based at y settles at y_0.

It is observed from Figure 7.3 that trajectories based at points outside D_{μ_0} will stall. (For the sake of argument, assume that all those points

[9]Assume that the parameter μ is fixed at μ_0.

not converging to x_0 will end up in rotating stall.) However, by manipulating the parameter μ, say resetting it to μ_1, the shape of D_{μ_0} will change to that of D_{μ_1}. It is observed that in this case an otherwise stalling trajectory such as one based at y will now approach the unstalled stationary operating point y. In this way be varying the parameter μ over the entire feasible parameter space U one obtains the overall recoverability domain $\mathscr{D}$ as

$$\mathscr{D}_{\upsilon} := \bigcup_{\mu \in \upsilon} D_{\mu} \tag{7.1}$$

In this way $\mathscr{D}_{\upsilon}$ represents the set of all trajectories that can be recovered, using the feasible parameter set υ.

The set $\mathscr{D}$ can be computed and stored off-line, once for a given dynamic system. Now if we can pinpoint the location of the state x, the question of whether the trajectory based at x can be recovered reduces to a table look up probelm: determine if the trajectory belongs to $\mathscr{D}$; if so, the trajectory is recoverable - otherwise it is not.

We can utilize the definition of recoverability types (e.g., 1st, 2nd, and 3rd stage recoverability) to obtain three types of recoverability domains: $\mathscr{D}^1_{\upsilon}$, $\mathscr{D}^2_{\upsilon}$, and $\mathscr{D}^3_{\upsilon}$.

7.4 Transient Analysis and Corrected Flow

(a) In this section we first note that in non-transient situations the uncorrected flow rate through the unstalled compressor is a good proxy for its state. In fact in steady state, the uncorrected flow rate x_3 by itself determines the remaining state variables and the corrected flow. This will in turn determine various pressure and temperature ratios. This can be seen by solving the steady-state state vector in (US)

$$0 = F(x,\mu) \tag{US}$$

where F represents the RHS of Equations (U1)-(U5) in Chapter 4.

The particular form of functional relationship is somewhat complicated as it involves a series of substitutions involving nonlinear relationships.[10]

On the other hand, as far as stability is concerned, we have seen that there is no one-to-one (monotone) relationship between the value of the corrected flow h_1 (or the flow area A) and the local stability of equilibria. Thus even for local stability determinations the corrected flow value does not contain the necessary information. The reason is that the corrected flow variable h_1 is an output variable of the system (US) the value of which is determined in a unique casual fashion, by the state vector x.

The question of whether a trajectory is in-stall must therefore be related to the location of the state vector x in the state space rather than that of the output level(s) in the output space. It is clear from Equation (4.10) that there are many state vectors x that will give rise to the same h_1. This is depicted in Figure 7.4.

[10]This was done in SSI's Progress Report (Jan. 1 through May 1, 1984) to NASA Lewis.

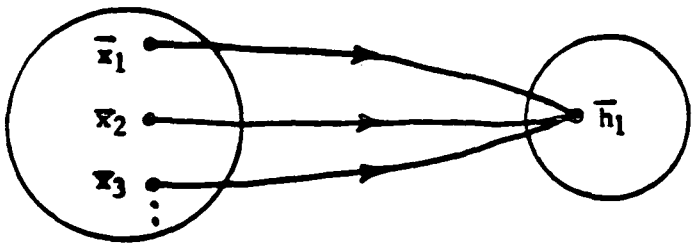

set of admissible x set of admissible h_1

Figure 7.4 The corrected flow h_1 does not uniquely determine the state x.

Therefore the output value h_1 does not give complete information about the state x.

(b) It can be noted (for example, from the analysis of Section 7.6) that the situation is even more complicated in case of off-design (non-steady state) conditions. In particular, no one state variable can be used to determine the remaining state variables; knowledge or estimation of individual state variables is required. Furthermore, the exclusive use of corrected flow rate (or A) for stability rating in this transient case is even less acceptable.

7.5 Domain of Attraction as Stability Set and Criterion for Stall

The definition of stall used in this work[11] is that spelled out in Section 4.6. In particular, for a given corrected speed PN there is a threshold stall value, t_s(PN) for the corrected flow. As the trajectory of the system evolves over time so does the corrected flow h_1. If at any point in time h_1 falls below t_s the unstalled compressor model (US) is replaced by (PS), and whenever h_1 equals or exceeds the recovery threshold

[11]This definition is the same as that spelled out in the Statement of Work (e.g. Wenzel, Bruton (1982)).

$t_r(PN)$ the compressor becomes unstalled. Thus the models are switched based on the **scalar output variable** h_1 - even though, as we have seen, this variable does not contain the entire stability information. In this way this choice of stall criterion may for example lead to stalling of some trajectories that would otherwise recover, or in some cases may provide a 'late' signal of oncoming stall.

Based on the earlier discussions, it appears that a more general and reliable criterion of stall would be provided by the domain of attraction of some 'normal' operating point (or operating region.)

Let x_0 denote some nominal steady state vector corresponding to the corrected spped PN_0, and flow area A_0. Let $D(PN_0, A_0)$ denote the corresponding domain of attraction for x_0. Then one way to decide how to switch the models is as follows:

(i) If $x(t) \in D(PN_0, A_0)$, the trajectory will recover, approaching x_0 as time increases.

(ii) If $x(t) \notin D(PN_0, A_0)$, then replace (US) by (PS) provided $h_1 > 0$.

(iii) If while using (PS) at any time $h_1 < 0$, switch to (RS) until the flow becomes nonnegative again at which time switch to (PS).

(iv) If while using (PS) the trajectory enters $D(PN_0, A_0)$, then switch to (US).

Figure 7.5 illustrates the procedure.

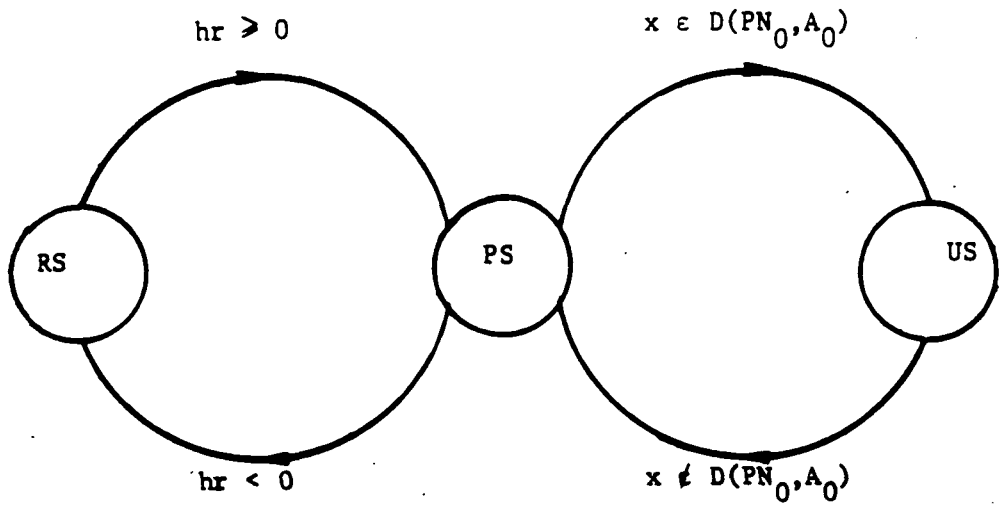

Figure 7.5 Switching of Models Based on Domain of Attraction.

The previous rule may be viewed as being applicable to passive stall/recovery. That is, in this case no control action is taken when the trajectory goes outside $D(PN_0, A_0)$. As we illustrated previously, one may manipulate the control parameters to obtain D_v so as to attempt to recover a particular trajectory. Then the switching rule may be based on this new set or some variation of it. We will not elaborate on this point here. Furthermore, we have not made any distinctions about different stages of recovery here although this can be easily incorporated.

In closing we note that the set $D(PN_0, A_0)$ is contained in R^n. This is in contrast to the scalar output $t_s(PN)$ rule of Wenzel, Bruton (1980). It appears that the use of the set D(PN) in place of the scalar threshold value $t_s(PN)$ represents a natural generalization of the latter approach.

7.6 Some Experimental Results for Stall/Recovery and Sensitivity Analysis

Some partial computations of the domain of attraction were carried out to illustrate the usefulness of the approach. The five dimensional space was projected on the (x_3, x_5) plane. The state variables x_1, x_2, x_4 were fixed at values 1.8, 940, and 0.2, respectively. These values are different from their corresponding equilibrium values; they correspond to some arbitrarily chosen 'off-design' condition. This may represent some perturbed values of some normal operating condition. The nominal area A was fixed at 30.25.

The computations were carried out for two sets of parameters: (i) nominal, and (ii) perturbed (increased from nominal value by 10% in most cases). The particular parameter nominal values chosen and their perturbed values are:

$$\left.\begin{array}{l} A = 30.25 \\ R = 639.6 \\ L = 9.64 \times 10^{-4} \\ \eta_0 = 0.1 \end{array}\right\} \quad \text{nominal parameter values}$$

$$\left.\begin{array}{l} A = 27.5, \text{ and } 27.3 \\ R = 703.56 \\ L = 1.0604 \times 10^{-3} \\ \eta_0 = 0.05 \end{array}\right\} \quad \text{perturbed parameter values}$$

(For definition of parameters see Appendix A and Wenzel, Bruton (1982).)

Figure 7.6 shows the domains of attraction for the unstalled system equilibrium (USE) and stalled system equilibrium (SE)[12]. In each diagram USE1 and SE1 refer to the two equilibrium values for the nominal case (shown in solid lines), while USE2 and SE2 refer to the perturbed case (shown in dotted lines.) The arrows on the figures point to the stall region. It is seen from Figure 7.6 that the domains of attraction of the two equilibria split the (x_3, x_5) plane into several regions. For example Figure 7.6(b) shows the stall and recovery regions for the zero flow efficiency values $\eta_0 = 0.1$ and $\eta_0 = 0.05$. Focusing on the nominal case $\eta_0 = 0.1$ (solid separatrix lines), let's fix attention on the 'horizontal' line: $x_5 = 60.0$ and x_3 free. We see that for the flow rate x_3 between about 5 and 25 the resulting trajectories will all end up in stall. Both higher and lower values of x_3 with respect to this range will result in recovering trajectories. We can also see that by fixing $x_3 = 30.0$ and allowing x_5 to vary, five different regions can be very complicated. We may have various 'pockets' of stall scattered around the recovery regions - a situation which may not be discernable from equilibrium or local stability analysis.

---

[12]Here we make no distinction between various types of stall and recovery discussed in the previous section; only the final point of convergence is considered.

Now by varying the parameters, the shapes and sizes of various regions change - providing information on which a set of trajectories may be recovered by changing the parameters in their feasible sets. For example by changing the zero flow efficiency variable η_0 from its value of 0.1 to that of 0.05 we obtain the new separatrix shown by the dotted lines. In this case we note that the parameter change increases the stall region, but slightly. This provides a method of sensitivity analysis for the impact of various parameters on the stall/recovery regions. Due to the fact that, in general, as a result of parameter changes we obtain a complicated pattern of change in the various regions, sensitivity ranking of the parameters is at best an ambiguous notion. Wenzel and Bruton (1982) provides a sensitivity analysis of some parameters but their method of analysis uses the turbine area A as the stability ranking mechanism. However, as can be seen from Figure 7.6(d), the value of the area A does not seem to provide a clear cut measure of recoverability - especially in some critical ranges.

Figures 7.6(a), and (c) provide the sensitivity of the stall/recovery regions to the changes in the parameters L and R. They have both been computed based on a 10% increase in the nominal parameter values. Of the two, it appears that increases in R have a greater impact on increasing the stall region.

In closing we note that the above analysis is not intended to provide specific recommendations for stall and recovery; rather, our goal has been to highlight the potential usefulness of the techniques for providing specific strategies for stall avoidance and recovery.

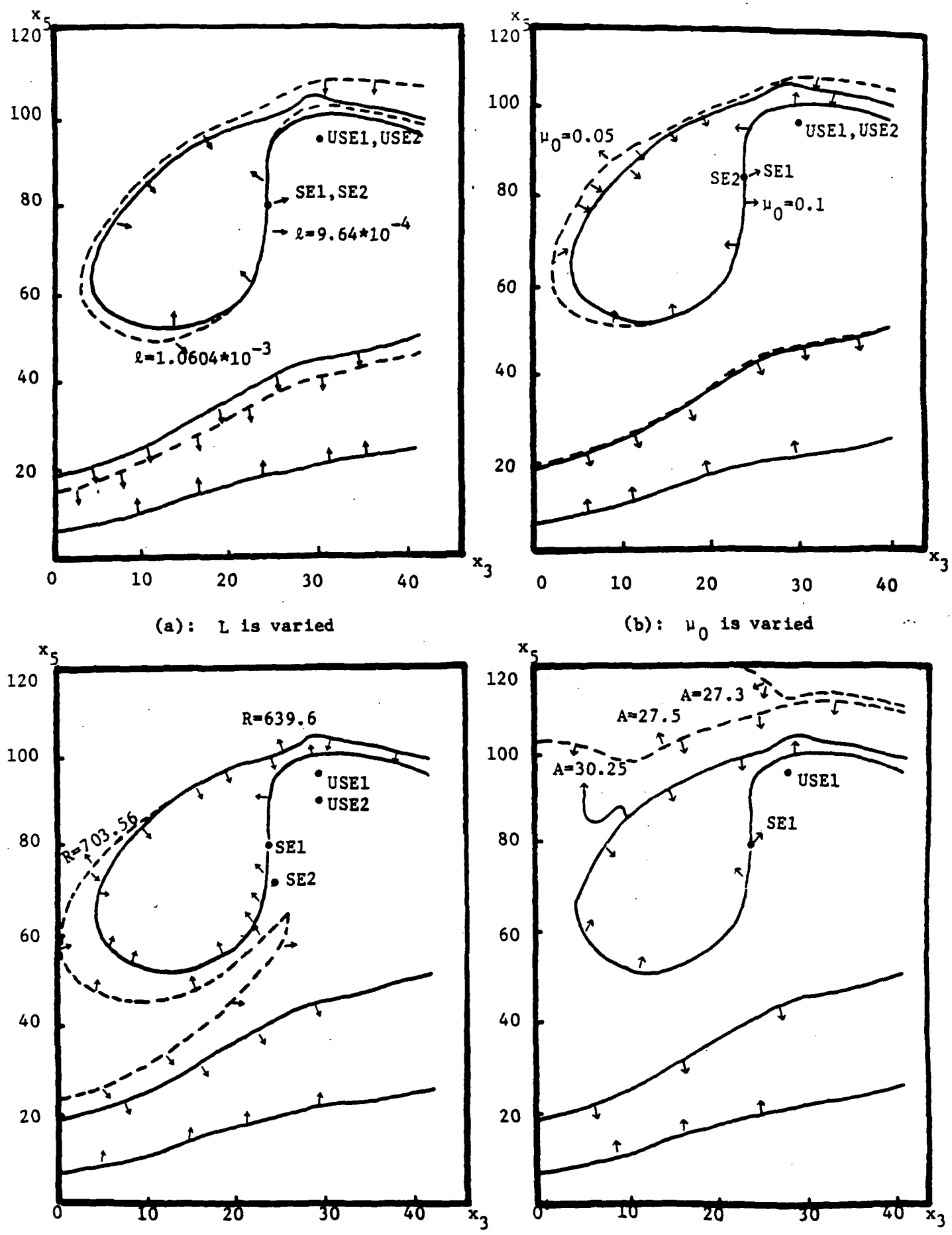

(a): L is varied

(b): μ_0 is varied

(c): R is varied

(d): Area is varied

Figure 7.6 Domains of attraction of stall and unstall equilibria. (Solid and dotted lines refer to nominal and perturbed values of parameters. Arrows point into stall region.)

8. CONCLUDING REMARKS AND SUGGESTIONS FOR FURTHER RESEARCH

This investigation illustrates that analytical methods employed in nonlinear control theory are quite appropriate for the analysis of compressor stall phenomena. In particular the methods of bifurcation and catastrophe theory when combined with a state variable formulation can help formulate a general purpose methodology which provides insight into the stall problem. The approach can provide an across-the-board understanding of various models - all within the same analytical framework.

Though we have presented some sample computations of domains of attraction of equilibria, this objective was beyond the scope of this investigation and therefore remained incomplete. As the discussion of Chapter 7 indicates, the accomplishment of this objective will provide valuable insight into questions of: parameter sensitivity analysis, regions of stall and recoverability from stall, types and availability of feasible control action, just to mention a few.

Switching of the models in this report was based on the threshold stall values $t_s(PN)$ of the corrected flow rates. As we argued in Chapters 6 and 7 this criterion may lead to incorrect conclusions. As a result in Chapter 7 we proposed a new procedure for switching of the models - involving the use of domains of attractions. Further investigation into this approach should be carried out. In particular, a careful matching of the domains of attraction of the stalled and unstalled models must be made. Otherwise a constant back and forth switching of the models in some regions may result. On the other hand if the models are treated as given, then these potential collisions of the attraction domains may result in a new type of 'surge' phenomena.

The development of state space models invariably brings about the question: are the state variables directly measurable quantities? Typically state variables represent important 'internal' variables, not all of which are measurable. Other related variables (e.g. output variables), usually smaller in number than the state variables, may be directly and accurately measurable. In our case, various temperature and pressure

ratios and/or absolute quantities may be good candidates for measurement. Thus observer-estimator type approaches must be adopted to provide closed loop estimation of the state vector. (It would be desirable to construct a special type of observer for this problem: that which would be 'sensitive' to the boundary of the stall region.)

The last but by no means the least recommendation is that modern control theoretic identification techniques should be brought to bear on (i) identification of in-stall characteristics, and (ii) identification of model parameters in the face of noisy data.

BIBLIOGRAPHY

Andronov, A., Poutryagin (1937), "Coarse Systems," Dokl. Akad. Nak USSR, 14.

Andronov, A., and Khaykin (1966), Theory of Oscillations, Pregmon Press, New York.

Arnold, V.I. (1981), Singularity Theory: Selected Papers, London Mathematical Society Lecture Notes, vol. 53.

Chua, L.O., and P.M. Lin (1975), Computer-Aided Analysis of Electronic Circuits, Prentice-Hall, Englewood, NJ.

Day, I.J., EM.M Greitzer and N.A. Cumpsty (1978), "Prediction of Compressor Performance in Rotating Stall," ASME Journal of Engineering for Power, vol. 100.

Emmons, H.W., C.E. Pearson, and H.P. Grant (1955), "Compressor Surge and Stall Propagation," Trans. ASME, vol. 77.

Greitzer, E.M. (1976), "Surge and Rotating Stall in Axial Flow Compressors, I," J. of Eng. Power, no. 98.

Greitzer, E.M. (1980), "Review - Axial Compressor Stall Phenomena," J. of Fluids Eng., vol. 102.

Greitzer, E.M. (1981), "The Stability of Pumping Systems," J. of Fluids Eng., vol. 103.

Hopf, E. (1942), "Abzweigung einer periodischen Losung von einer stationen Losung eines differential systems," Ber. Math. Phys. Kl. Sachs Acad. Wiss. Leipzig, vol. 94, pp. 1-23 (English tr. below).

Hartman, P. (1964), Ordinary Differential Equations, Wiley, New York.

Kelley, A. (1967), "The stable, center stable, center, center unstable and unstable manifolds," J. Diff. Eng., vol. 3, pp. 546-570.

Kubicek, M. (1976), "Dependence of Solution of Nonlinear Systems on a Parameter," ACM Transactions on Mathematical Software, vol. 2, no. 1.

Marsden, J. and M. McCracken (1976), The Hopf Bifurcation and Its Applications, Springer-Verlag, New York.

Moore, F.K., "A Theory of Rotating Stall of Multistage Axial Compressors: Part I — Small Disturbances," Trans. of ASME, paper no. 83-GT-44.

Moore, F.K., "A Theory of Rotating Stall of Multistage Axial Compressors: Part II — Finite Disturbances," Trans. of ASME, paper no. 83-GT-45.

Moore, F.K., "A Theory of Rotating Stall of Multistage Axial Compressors: Part III -- Limit Cycles," Trans. of ASME, paper no. 83-GT-46.

Mehra, R.K., and J.V. Carroll (1982), "Bifurcation and Limit Cycle Analysis with an Application to Aircraft at High Angle-of-Attack," Automatic Control Conf., Arlington, VA.

Mehra, R.K. et al. (1977-79), "Global Stability and Control Analysis of Aircraft at High Angle-of-Attack," Report ONR-CR215-248-1,2,3.

NASA Lewis Stall Recovery Workshop, February 8-9, 1983, Cleveland, OH.

Patterson, G.T. (1983), "Techniques for Determining Engine Stall Recovery Characteristics," AGARD, North Atlantic Treaty Organizations.

Rabinowitz, P.H. (1977), Applications of Bifurcation Theory, Academic Press, Inc.

Seldner, K., J.R. Mihaloew and R.J. Blaha (1972), "Generalized Simulation Technique for Turbojet Engine System Analysis," NASA Tech. Note D-6610.

Stetson, H.D. (1983), "Designing for Stability in Advanced Turbine Engines," in AGARD CP-324 Engine Handling.

Szuch, J.R., and K. Seldner (1975), "Real Time Simulation of F100-PW-100 Turbofan Engine Using the Hybrid Computer," NASA Technical Memorandum X-3261.

Szuch, J.R., K. Seldner and D.S. Cwynar (1977), "Development and Verification of Real Time, Hybrid Computer Simulation of F100-PW-100 (3) Turbofan Engine," NASA Technical Paper 1034.

Szuch, J. (1978), "Model for Jet Engine Systems, Part I: Techniques for Jet Engine Systems Modeling," Control and Dynamic Systems, vol. 14.

Takens, F. (1980), "Introduction to Global Analysis," Comm. Math.Inst. Rijksuniversiteit, Utrecht, vol. 2.

Takens, F. (1980), "Notes on Force Oscillations," Comm. Math. Inst. Rijksuniversiteit, Utrecht, vol. 3.

Thom, R. (1974), Structural Stability and Morphogenesis, Addison Wesley, Reading, MA.

Wenzel, L.M. and W.M. Bruton (1982), "Analytical Investigation of Nonrecoverable Stall," NASA Technical Memorandum 82792.

Wood, E., J. Kempf, and R.K. Mehra (1984), "BISTAB: A Portable Bifurcation and Stability Analysis Package," Appl. Math. and Comp., vol. 15.

APPENDIX A
(Provided by NASA Lewis)

$$P_1 = 14.8 \tag{A1}$$

$$T_1 = 519 \tag{A2}$$

$$\dot{W}_1 = \frac{P_1 - P_2}{R_0} \tag{A3}$$

$$W_2 = \int_0^t (\dot{W}_1 - \dot{W}_2)dt + W_{2,i} \tag{A4}$$

$$(WT)_2 = \gamma \int_0^t \left(\dot{W}_1 \left\{\frac{T_1}{T_2}\right\} - \dot{W}_2 \left\{\frac{T_2}{T'_2}\right\} \right) dt + (WT)_{2,i} \tag{A5}$$

$$P_2 = \frac{R(WT)_2}{V_2} \qquad T'_2 = T_3\left(1 - \frac{\phi}{.7972}\right) \tag{A6}$$

$$T_2 = \frac{(WT)_2}{W_2} \tag{A7}$$

$$\theta_2 = \frac{\begin{Bmatrix} T_2 \\ T_3 \end{Bmatrix}}{519} \tag{A8}$$

$$\delta_2 = \frac{\begin{Bmatrix} P_2 \\ P_3 \end{Bmatrix}}{14.7} \tag{A9}$$

$$PN = \frac{N/\sqrt{\theta_2}}{16042} \tag{A10}$$

$$\phi = 7.972 \times 10^{-3} \frac{\dot{W}_2\sqrt{\theta_2/\delta_2}}{PN} \tag{A11}$$

$$\psi = \begin{Bmatrix} KP \\ KN \end{Bmatrix} \phi^2 + 0.33 \tag{A12}$$

UNSTALLED	STALLED	
$P_3^* = P_2 \cdot F_1\left(\frac{\dot{W}_2\sqrt{\theta_2}}{\delta_2}, PN\right)$	$P_3^* = \frac{P_2}{.837}(1 + .7746\ \psi\ PN^2)$	(A13)
$T_3^* = T_2 \cdot F_2\left(\frac{\dot{W}_2\sqrt{\theta_2}}{\delta_2}, PN\right)$	$T_3^* = T_2 \quad 1 + \left(\frac{\left(\frac{P_3^*}{P_2}\right)^{.286} - 1}{\eta}\right)$	(A14)
	$\eta = \eta_0 + F_4(PN, \eta_0)\phi$	(A15)

$$\dot{W}_{ST} = F_3(PN) \tag{A16}$$

$$\text{STALL IF } \frac{\dot{W}_2\sqrt{\theta_2}}{\delta_2} \quad \dot{W}_{ST}$$

$$\text{RECOVER IF } \frac{\dot{W}_2\sqrt{\theta_2}}{\delta_2} > 1.1\ \dot{W}_{ST}$$

$$W_3 = \int_0^t (\dot{W}_2 - \dot{W}_3)dt + W_{2,i} \tag{A17}$$

$$\dot{W}_2 = \frac{1}{L} \int_0^t (P_3^* - P_3)dt + \dot{W}_{2,i} \tag{A18}$$

$$(WT)_3 = \gamma \int_0^t \left(\dot{W}_2 \left\{ \frac{T_3^*}{T_3} \right\} - \dot{W}_3 T_3 \right) dt + (WT)_{3,i} \tag{A19}$$

$$\dot{W}_3 = A \frac{P_3}{\sqrt{T_3}} \tag{A20}$$

$$P_3 = \frac{R(WT)_3}{V_3} \tag{A21}$$

$$T_3 = \frac{(WT)_3}{W_3} \tag{A22}$$

$$\begin{aligned} A &= A_i && \text{for } t \quad t_1 \text{ and } t \quad t_3 \\ &= A_i - a(t - t_1) && \text{for } t_1 < t < t_2 \\ &= A_i - a(t - t_1) + 2a(t - t_2) && \text{for } t_2 < t_1 < t_3 \end{aligned} \tag{A23}$$

STALL THRESHHOLD VALUES $t_s(PN)$

PN	$t_s(PN)$
0.6	24.8
0.7	31.2
0.8	42.3
0.85	47.1
0.90	51.2
0.95	55.3
1.00	59.5

$$t_r(PN) = 1.1\ t_s(PN)$$

APPENDIX A
SYMBOLS

A	area	in^2	m^2
dt	time increment	sec	sec
f_i	performance function (i=1,4)	-	-
KN	constant describing in-stall compressor performance at negative flow	-	-
KP	constant describing in-stall compressor performance at positive flow	-	-
L	fluid inertance, length/(area g)	sec^2/in^2	sec^2/m^2
N	rotational speed	rev/min	rev/min
p	static pressure	lbf/in^2	N/m^2
P	total pressure	lbf/in^2	N/m^2
PN	fractional corrected compressor speed	-	-
R	flow resistance, Δ (pressure drop)/ Δ (flow)	lbf sec/lbm in^2	N sec/KG m^2
T	temperature	°R	K
t	time	sec	sec
V	volume	in^3	m^3
W	weight	lbm	kg
$\dot{W}$	weight flow	lmb/sec	kg/sec
α	constant	-	-
γ	ratio of specific heats	-	-
δ	rati of total pressure to standard atmospheric pressure	-	-
Δ	incremental change	-	-
η	efficiency	-	-
θ	ratio of total temperature to standard atmospheric temperature	-	-
φ	flow parameter	-	-
ψ	pressure parameter	-	-

Subscripts:

0	ambient
1	fan inlet
2	compressor
3	compressor discharge
i	initial
*	denotes quasi-steady parameter at compression component discharge

The terms within braces { } in the equations are switched when flow reverses as follows: If flow is positive, in the normal sense, the upper term within the braces are used.

APPENDIX B

STATE SPACE REPRESENTATION FOR STALLED MODEL (PS)

The state vector x that we have chosen is

$$x = \begin{bmatrix} W_2 \\ (WT)_2 \\ \dot{\omega}_2 \\ W_3 \\ (WT)_3 \end{bmatrix}$$

We have from Appendix A

$$\dot{W}_1 = \frac{P_1 - P_2}{R_o} \tag{A3}$$

$$W_2 = \int_o^t (\dot{W}_1 - \dot{\omega}_2)\, d\tau + W_{2,i} \quad . \tag{A4}$$

Upon differentiation and substitution, equations (A3) - (A4) yield

$$\dot{W}_2 = \frac{P_1}{R_0} - \frac{R}{R_0 V_2} (WT)_2 - \dot{\omega}_2$$

or

$$\dot{x}_1 = \frac{P_1}{R_0} - \frac{R}{R_0 V_2} x_2 - x_3 \quad . \tag{B1}$$

Given

$$(WT)_2 = \gamma \left(\int_o^t \dot{W}_1 \begin{Bmatrix} T_1 \\ T_2 \end{Bmatrix} - \dot{\omega}_2 \begin{Bmatrix} T_2 \\ T_2' \end{Bmatrix} \right) d\tau + (WT)_{2,i} \tag{A5}$$

we obtain

$$(\dot{WT})_2 = \gamma \left(\frac{P_1 - P_2}{R_0} \begin{Bmatrix} T_1 \\ T_2 \end{Bmatrix} - x_3 \begin{Bmatrix} T_2 \\ T_2' \end{Bmatrix} \right) \quad .$$

But

$$T_2 = \frac{(WT)_2}{W_2} = \frac{x_2}{x_1} \tag{B2}$$

and

$$P_2 = \frac{R(WT)_2}{V_2} = \frac{R}{V_2}\, x_2 \tag{B3}$$

yields

$$\dot{x}_2 = \gamma\left(\frac{P_1}{R_0}\begin{Bmatrix} T_1 \\ x_2/x_1 \end{Bmatrix} - \frac{R}{R_0 V_2}\, x_2 \begin{Bmatrix} T_1 \\ x_2/x_1 \end{Bmatrix} - x_3 \begin{Bmatrix} x_2/x_1 \\ T_2' \end{Bmatrix}\right) \quad . \tag{B4}$$

Now

$$W_3 = \int^{t} (\dot{\omega}_2 - \dot{\omega}_3)\, d\tau + W_{3,i} \tag{A17}$$

$$\dot{\omega}_3 = A\,\frac{P_3}{\sqrt{T_3}} \tag{A20}$$

with

$$P_3 = \frac{R(WT)_3}{V_3} = \frac{R}{V_3}\, x_5 \tag{B3'}$$

$$T_3 = \frac{(WT)_3}{W_3} = \frac{x_5}{x_4} \tag{B2'}$$

yield

$$\dot{W}_3 = \dot{\omega}_2 - \dot{\omega}_3$$

$$= \dot{\omega}_2 - A\,\frac{\frac{R}{V_3}\, x_5}{\sqrt{x_5/x_4}}$$

or

$$\dot{x}_4 = x_3 - \frac{AR}{V_3} \sqrt{x_4 x_5} \quad . \tag{B5}$$

Equation

$$\dot{\omega}_2 = \frac{1}{L} \int_0^t (P_3^* - P_3)\, d\tau + \dot{\omega}_{2,i} \tag{A18}$$

upon differentiation and substitution obtains

$$\dot{x}_3 = \frac{1}{L} \left(P_3^* - \frac{R}{LV_3} x_5 \right) \tag{B6}$$

At this point we shall concentrate on the stalled dynamics in the positive flow direction. Thus

$$P_3^* = \frac{P_2}{0.837} (1 + .7746\ \psi\ PN^2) \tag{A13}$$

where

$$\psi = KP\ \phi^2 + 0.33 \tag{A12}$$

$$\phi = 7.972 \times 10^{-3} \frac{\dot{\omega}_2 \sqrt{\theta}/\delta_2}{PN} \quad . \tag{A11}$$

Using (A-11), (B2), (B3), and

$$\theta_2 = \frac{T_2}{519} \tag{A8}$$

$$\delta_2 = \frac{P_2}{14.7} \tag{A9}$$

we obtain

$$\phi = \frac{g_1}{PN} \frac{x_3}{\sqrt{519\ x_1 x_2}} \tag{B7}$$

where

$$g_1 \triangleq \frac{7.972 \times 10^{-3} \times 14.7\ V_2}{R} \quad . \tag{B8}$$

Substituting (B7) in (A-12) yields

$$\psi = KP \left(\frac{g_1}{PN}\right)^2 \frac{x_3{}^2}{519\ x_1 x_2} + 0.33 \quad . \tag{B9}$$

Thus

$$P_3^* = g_2 x_2 + g_3 g_1^2\ KP\ \frac{x_3^2}{x_1} \tag{B10}$$

$$g_2 = g_2(PN) \triangleq \frac{R}{0.837\ V_2} + 0.305\ \frac{R}{V_2}\ PN^2 \tag{B11}$$

$$g_3 \triangleq 0.925\ \frac{R}{519\ V_2} \quad . \tag{B12}$$

Finally (B6) becomes

$$\dot{x}_3 = \left(\frac{1}{L}\ g_2 x_2 + g_3 g_1^2\ KP\ \frac{x_3}{x_1} - \frac{R}{V_3}\ x_5\right) \quad . \tag{B13}$$

Equations (A-20), (B2)', (B3)', and

$$(WT)_3 = \gamma \int_0^t (\dot{\omega}_2\ T_3^* - \dot{\omega}_3\ T_3)\ d\tau + (WT)_{3,i} \tag{A19}$$

yield

$$\dot{x}_5 = \gamma\left(x_3 T_3^* - \frac{AR}{V_3}\ x_5\ \sqrt{x_5/x_4}\right) \quad . \tag{B14}$$

Now

$$T_3^* = T_2\left(1 + \frac{\left(P_3^*/P_2\right)^{.286} - 1}{\eta}\right) \tag{A14}$$

together with Equations (A13) and (A22) obtain

$$T_3^* = \frac{x_2}{x_1}\left(1 + \frac{\left[1.19 + 0.925\left(KP\,\frac{(g_1x_3)^2}{519x_1x_2} + 0.33\ PN^2\right)\right]^{.286} - 1}{\eta}\right). \tag{A28}$$

Furthermore

$$\eta = \eta_0 + F_4(Pn,\eta_0)\phi \quad . \tag{A15}$$

Using (B7), (A15), and (A28),

$$T_3^* = \frac{x_2}{x_1}\left(1 + \frac{\left[1.19 + 0.925\left(KP\,\frac{(g_1x_3)^2}{519x_1x_2} + 0.33\ PN^2\right)\right]^{.286} - 1}{\eta_0 + F_4(PN,\eta_0)\frac{g_1}{PN}\,\frac{x_3}{\sqrt{519\ x_1x_2}}}\right).$$

Upon substitution for T_3^* in (B14)

$$\dot{x}_5 = \gamma\,\frac{x_2x_3}{x_1}\left(1 + \frac{\left[1.19 + 0.925\left(KP\,\frac{(g_1x_3)^2}{519x_1x_2} + 0.33\ PN^2\right)\right]^{.286} - 1}{\eta_0 + F_4(PN,\eta_0)\frac{g_1}{PN}\,\frac{x_3}{\sqrt{519\ x_1x_2}}}\right).$$

$$- \frac{\gamma AR}{V_3}\,x_5\sqrt{x_5/x_4} \tag{B16}$$

deriving the last state equation. Specializing Equation (B4) to the positive flow case we collect the equations for easy reference.

Summary of State Space Systems for Positive Flow Stalled Dynamics (PS)

$$\dot{x}_1 = \frac{P_1}{R_0} - \frac{R}{R_0 V_2} x_2 - x_3 \tag{PS1}$$

$$\dot{x}_2 = \gamma\left(\frac{P_1}{R_0} T_1 - \frac{R}{R_0 V_2} T_1 x_2 - x_2 \frac{x_3}{x_1}\right) \tag{PS2}$$

$$\dot{x}_3 = \frac{1}{L} g_3 g_1^2 KP \frac{x_3^2}{x_1} + \frac{1}{L} g_2(PN) x_2 - \frac{1}{L}\frac{R}{V_3} x_5 \tag{PS3}$$

$$\dot{x}_4 = x_3 - A\frac{R}{V_3}\sqrt{x_5 x_4} \tag{PS4}$$

$$\dot{x}_5 = \gamma \frac{x_2 x_3}{x_1}\left(1 + \frac{\left[1.19 + 0.925\left(KP\frac{(g_1 x_3)^2}{519\ x_1 x_2} + 0.33\ PN^2\right)\right]^{0.286} - 1}{\eta_0 + F_4(PN,\eta_0)\frac{g_1}{PN}\frac{x_3}{\sqrt{519\ x_1 x_2}}}\right)$$

$$- \frac{\gamma A R}{V_3} x_5 \sqrt{\frac{x_5}{x_4}} \tag{PS5}$$

where

$$x = \begin{bmatrix} x_1 \\ x_2 \\ x_3 \\ x_4 \\ x_5 \end{bmatrix} = \begin{bmatrix} W_2 \\ (WT)_2 \\ \dot{W}_2 \\ W_3 \\ (WT)_3 \end{bmatrix}$$

APPENDIX C

STATE SPACE REPRESENTATION FOR THE UNSTALLED MODEL (US)

Equations defined in Appendix A will be referred to as A1, A2, ... etc. Any new notation introduced shall be defined accordingly.

We have from Appendix A

$$\dot{w}_1 = \frac{P_1 - P_2}{R_o} \tag{A3}$$

$$w_2 = \int_0^t (\dot{w}_1 - \dot{\omega}_2)\, d\tau + w_{2,i} \tag{A4}$$

(A3)-(A4) yield

$$\dot{x}_1 = \frac{P_1}{R_o} - \frac{R}{R_o V_2} x_2 - x_3 \tag{C1}$$

Equation (B4), specialized to the positive flow region yields:

$$\dot{x}_2 = \gamma \left(\left(\frac{P_1}{R_o} - \frac{R}{R_o V_2} x_2 \right) \quad T_1 - \frac{x_3 x_2}{x_1} \right) \tag{C2}$$

Equation (A18) obtains the third dynamic relation in the form

$$\dot{x}_3 = \frac{1}{L} \left(P_3^* - \frac{R}{L V_3} x_5 \right) \tag{C3}$$

Here P_3 is obtained from the unstalled case of Equation (A13):

$$P_3^* = P_2 \; F_1\left(\frac{\dot{\omega}_2 \sqrt{\theta_2}}{\delta_2}, \; PN \right) \tag{A-13}$$

Let

$$h_1 \overset{\Delta}{=} \frac{\dot{\omega}_2\sqrt{\theta_2}}{\delta_2} \tag{C4}$$

denote the corrected flow.

We have, from Appendix A and definition of x:

$$\theta_2 = \frac{x_2}{519\ x_1} \tag{C5}$$

$$\delta_2 = \frac{R}{14.7\ V_2}\ x_2 \tag{C6}$$

yielding

$$h_1 = g_4\ \frac{x_3}{\sqrt{x_1 x_2}} \tag{C7}$$

where

$$g_4 \overset{\Delta}{=} \frac{14.7\ V_2}{R\ \sqrt{519}} \tag{C8}$$

(the constants g_1, g_2 and g_3 were defined in previous appendixes.

Equation (C3) thus becomes

$$\dot{x}_3 = \frac{R}{L}\left(\frac{x_2}{V_2} F_1\left(g_4\ \frac{x_3}{\sqrt{x_1 x_2}}, PN\right) - \frac{x_5}{V_3}\right) \tag{C9}$$

The fourth dynamic relation is the same as in Appendix B.

$$\dot{x}_4 = x_3 - \frac{AR}{V_3}\ \sqrt{x_4 x_5} \tag{C10}$$

Finally, the fifth relation is derived from (A19) and

$$(WT)_3 = \gamma \int_0^t (\dot{\omega}_2\ \overset{*}{T}_3 - \dot{\omega}_3\ T_3)d\tau + (WT)_{3,i} \tag{C11}$$

$$\overset{*}{T}_3 = T_2\ F_2\left(\frac{\dot{\omega}_2\sqrt{\theta_2}}{\delta_2}, PN\right) \tag{C12}$$

Substituting for the corrected flow and temperature T_2 in terms of the state variables yields:

$$T_3^* = \frac{x_2}{x_1} F_2 \quad (g_4 \frac{x_3}{\sqrt{x_1 x_2}}, PN) \tag{C13}$$

Thus

$$\dot{x}_5 = \gamma(x_3 T_3^* - \dot{\omega}_3 T_3) \tag{C14}$$

$$= \gamma(x_3 \frac{x_3}{x_1} F_2(g_4 \frac{x_3}{\sqrt{x_1 x_2}}, PN) - \frac{AR}{V_3} x_5 \frac{x_5}{x_4} \tag{C15}$$

where

$$\dot{\omega}_3 T_3 = \frac{AR}{V_3} x_5 \sqrt{\frac{x_5}{x_4}} \tag{C16}$$

Summary of State Space System for Unstalled Dynamics (US)

$$\dot{x}_1 = \frac{P_1}{R_o} - \frac{R}{R_o V_2} x_2 - x_3 \tag{U1}$$

$$\dot{x}_2 = \gamma \left[\left(\frac{P_1}{R_o} - \frac{R}{R_o V_2} x_2 \right) T_1 - x_3 \; x_2/x_1 \right] \tag{U2}$$

$$\dot{x}_3 = \frac{R}{L} \left[\frac{x_2}{V_2} \cdot F_1 \left(g_4 \frac{x_3}{\sqrt{x_1 x_2}}, PN \right) - \frac{x_5}{V_3} \right] \tag{U3}$$

$$\dot{x}_4 = x_3 - \frac{AR}{V_3} \sqrt{x_4 x_5} \tag{U4}$$

$$\dot{x}_5 = \gamma \left[\frac{x_3 x_2}{x_1} \cdot F_2 \left(g_4 \frac{x_3}{\sqrt{x_1 x_2}}, PN \right) - \frac{AR}{V_3} x_5 \sqrt{\frac{x_5}{x_4}} \right] \tag{U5}$$

where the state vector is x

$$x = \begin{bmatrix} x_1 \\ x_2 \\ x_3 \\ x_4 \\ x_5 \end{bmatrix} \triangleq \begin{bmatrix} W_2 \\ (WT)_2 \\ \dot{\omega}_2 \\ W_3 \\ (WT)_3 \end{bmatrix}$$

APPENDIX D

STALLED DYNAMICS (REVERSE FLOW)

Since the procedure is the same as that of the unstalled case or the stalled (positive flow) model, we will derive the five state equations without much explanation.

As before,

$$\dot{x}_1 = \frac{P_1}{R_o} - \frac{R}{R_o V_2} x_2 - x_3 \qquad \text{(B1),(C1)}$$

but

$$\dot{x}_2 = \gamma \left(\frac{P_1}{R_o} \frac{x_2}{x_1} - \frac{R}{R_o V_2} \frac{x_2^2}{x_1} \right) - x_3 T_2' \qquad \text{(D2)}$$

$$T_2' = T_3 \left(1 - \frac{\phi}{0.7972} \right) \qquad \text{(D3)}$$

$$T_3 = \frac{(WT)_3}{W_3} = \frac{x_5}{x_4} \qquad \text{(D4)}$$

$$\phi = 7.972 \; 10^{-3} \; \frac{\dot{\omega}_2 \sqrt{\theta_2}}{\delta_2 \; PN} \qquad \text{(D5)}$$

In-stall $\frac{\dot{\omega}_2 \sqrt{\theta_2}}{\delta_2}$ calculation:

$$\dot{\omega}_2 = x_3 \qquad \text{(D6)}$$

$$\theta_2 = \frac{T_3}{T_1} \tag{D7}$$

$$\delta_2 = \frac{P_3}{P_1} \tag{D8}$$

$$P_3 = \frac{R}{V_3} \; x_5 \tag{D9}$$

$$T_3 = \frac{x_5}{x_4} \tag{D10}$$

Equations (D6)-(D10) yield

$$hr = \frac{\dot{\omega}_2 \sqrt{\theta_2}}{\delta_2} = g_6 \frac{x_3}{\sqrt{x_4 x_5}} \tag{D11}$$

where[1]

$$g_6 = \frac{P_1 V_3}{R\sqrt{T_1}} \tag{D12}$$

Substitution from (D11) into (D5) yields

$$\phi = \frac{g_7}{PN} \; \frac{x_3}{\sqrt{x_4 x_5}} \tag{D13}$$

where

$$g_7 = 7.972 \cdot 10^{-3} \; g_6 \tag{D14}$$

Thus (D3) yields

$$T_2' = \frac{x_5}{x_4} \left(1 - \frac{g_8}{PN} \; \frac{x_3}{\sqrt{x_4 x_5}}\right) \tag{D15}$$

---

[1]Subscripts 6,7,... in g's are the continuations of those used in previous appendixes.

$$g_8 = \frac{g7}{0.7972}$$

Hence,

$$\dot{x}_2 = \gamma\left(\left(\frac{P_1}{R_o} - \frac{R}{R_o V_2} x_2\right) \frac{x_2}{x_1} - \left(\frac{x_3 x_5}{x_4} \quad 1 - \frac{g8}{PN} \frac{x_3}{\sqrt{x_4 x_5}}\right)\right) \tag{D16}$$

As before,

$$\dot{x}_4 = x_3 - \frac{AR}{V_3} \sqrt{x_4 x_5} \tag{D17}$$

Now

$$\dot{\omega}_2 = \frac{1}{L} \int_0^t (P_3^* - P_3)\, d\tau + \dot{\omega}_{2,i} \tag{D18}$$

$$P_3^* = \frac{P_2}{0.837} \quad (1 + 0.7746 \quad \psi \; PN) \tag{D19}$$

ψ is different in reverse flow,

$$\psi = KN\, \phi^2 + 0.33 \tag{D20}$$

From (D13), (D19), and (D20)

$$P_3^* = \frac{R}{0.837\ V_2} x_2 \left(1 + 0.2556\ PN^2 + 0.7746\ KN \frac{(g_T x_3)^2}{x_4 x_5}\right) \tag{D21}$$

From (D9), (D18), and (D21)

$$\dot{x}_3 = \frac{R}{L} \quad \frac{x_2}{0.837\ V_2} \quad (g_9 + KN\ g_{10} \frac{x_3^2}{x_4 x_5}) - \frac{x_5}{V_3} \tag{D22}$$

where

$$g_9 = 1 + 0.2556\ PN^2 \tag{D23}$$

$$g_{10} = 0.7746\ g_7^2 \tag{D24}$$

Now from

$$(WT)_3 = \gamma \int_0^t (\dot{\omega}_2 T_3 - \dot{\omega}_3 T_3)dt + (WT)_{3,i}$$

and Equation (B14),

$$\dot{x}_5 = \gamma \left(\frac{x_3 x_5}{x_4} - \frac{AR}{V_3} x_5 \sqrt{\frac{x_5}{x_4}} \right) \tag{D25}$$

This concludes the derivation of the fifth order reverse flow stalled system Equations.

Summary of Reverse Flow Stalled Dynamics (RS)

$$\dot{x}_1 = \frac{P_1}{R_0} - \frac{R}{R_0 V_2} x_2 - x_3 \tag{RS1}$$

$$\dot{x}_2 = \gamma \left(\left(\frac{P_1}{R_0} - \frac{R}{R_0 V_2} x_2 \right) \frac{x_2}{x_1} - \frac{x_3 x_5}{x_4} \left(1 - \frac{g8}{PN} \frac{x_3}{\sqrt{x_4 x_5}} \right) \right) \tag{RS2}$$

$$\dot{x}_3 = \frac{R}{L} \left(\frac{x_2}{0.837\ V_2} \left(g_9 + KN\ g_{10} \frac{x_3^2}{x_4 x_5} \right) - \frac{x_5}{V_3} \right) \tag{RS3}$$

$$\dot{x}_4 = x_3 - \frac{AR}{V_3} \sqrt{x_4 x_5} \tag{RS4}$$

$$\dot{x}_5 = \gamma \left(x_3 \frac{x_5}{x_4} - \frac{AR}{V_3} x_5 \sqrt{\frac{x_5}{x_4}} \right) \tag{RS5}$$

where

$$\text{corrected flow } h_r = g_6 \frac{x_3}{\sqrt{x_4 x_5}}$$

$$g_6 = \frac{P_1 \; V_3}{R \sqrt{T_1}} \; .$$

APPENDIX E

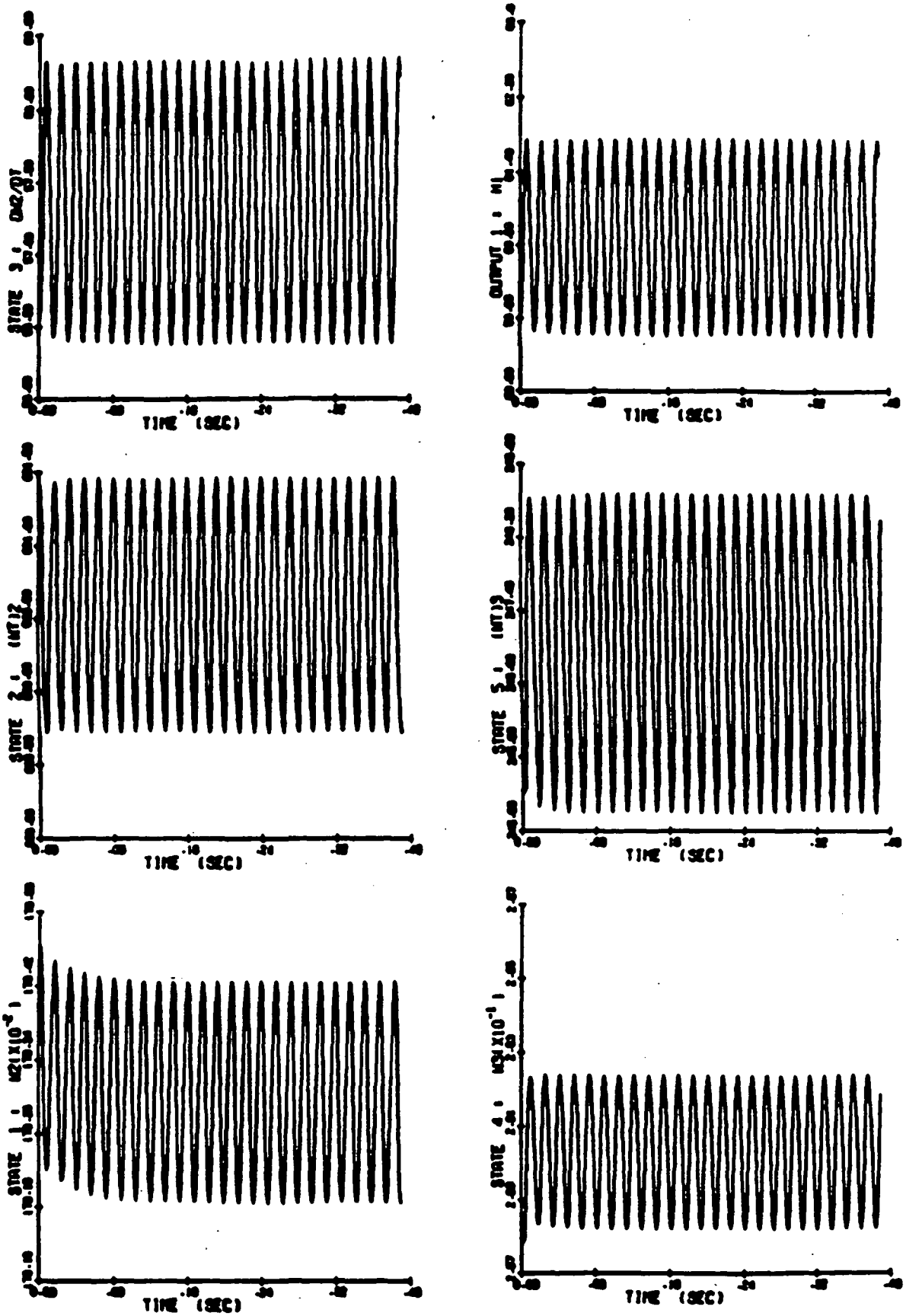

Figure E(a) Surge oscillations for PN=1 occur at A=26.96.
(They also occur at A=27.18; they are not included here.)

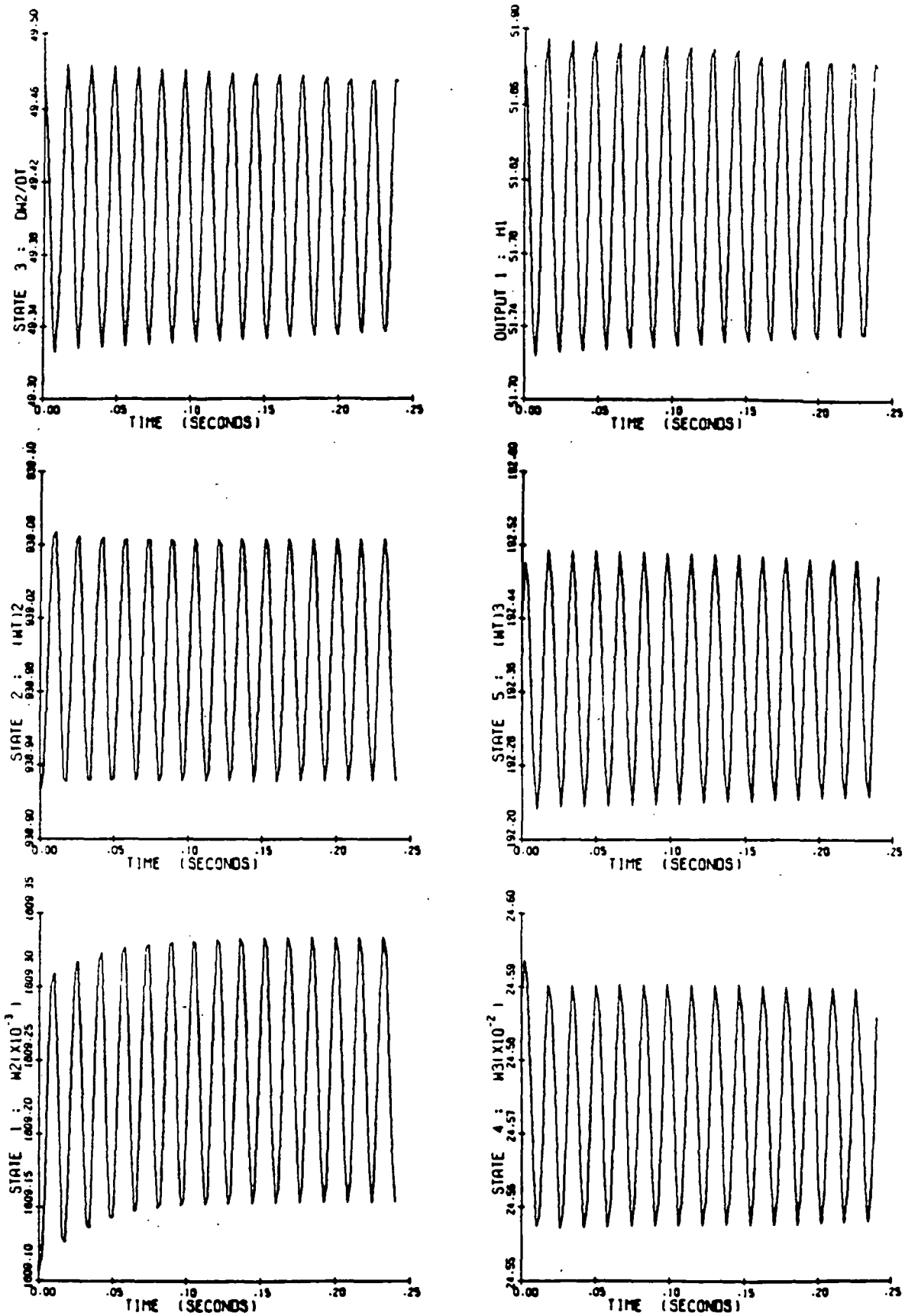

Figure E(b) Surge oscillations for PN=.9 occur at A=28.873

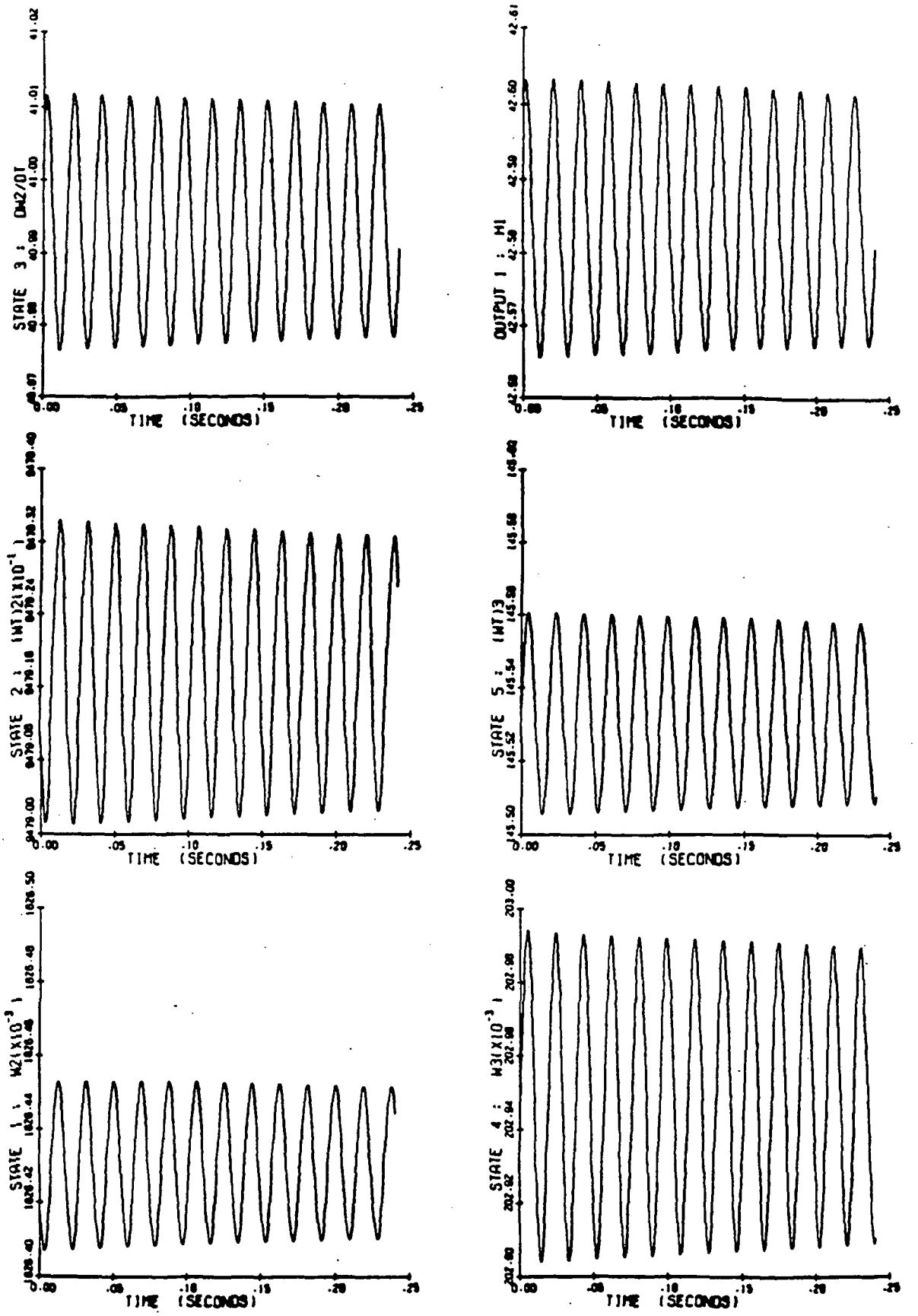

Figure E(c) Surge oscillations for PN=.8 occur at A=30.309

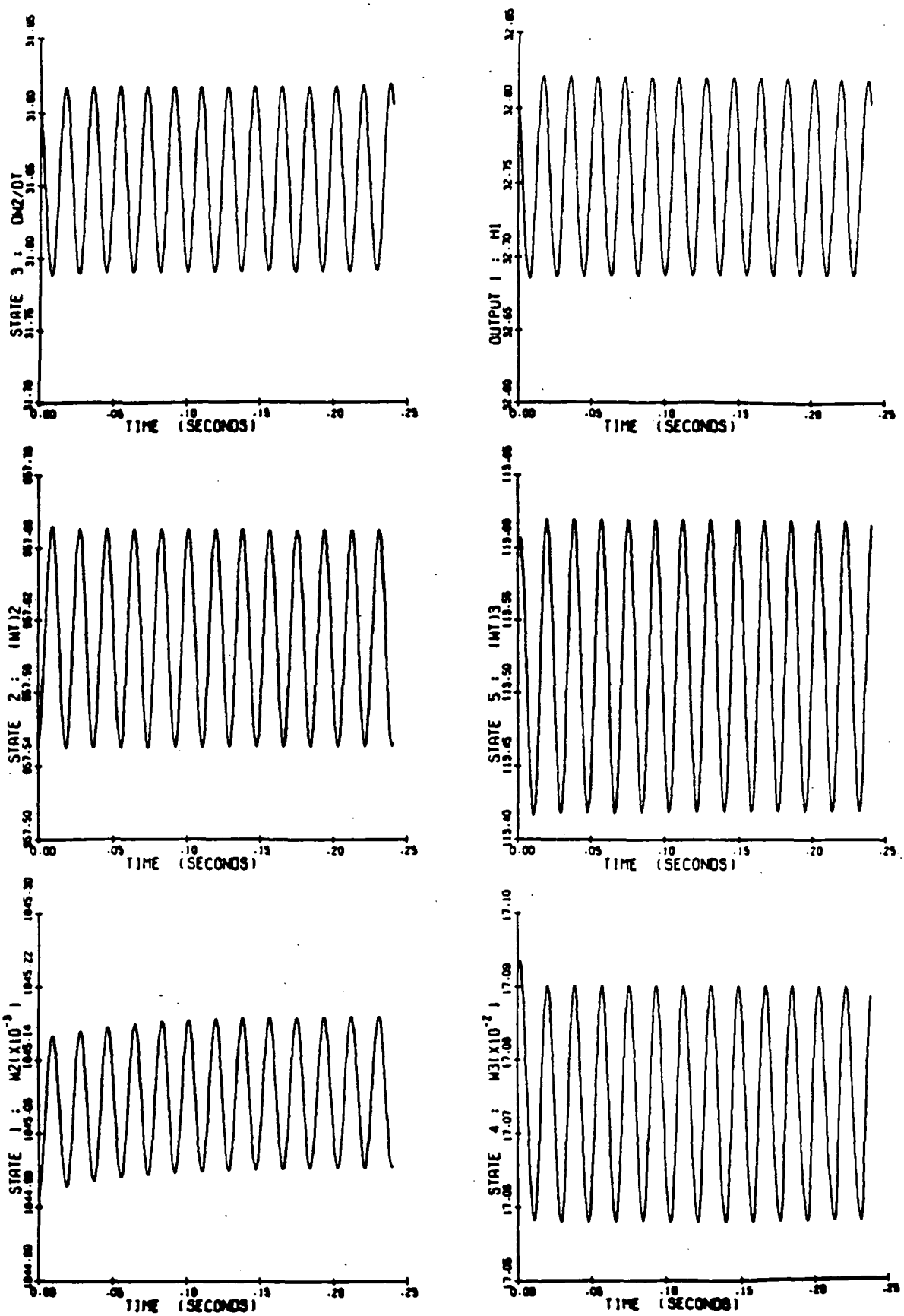

Figure E(d) Surge oscillations for PN=.7 occur at A=29.072

N85-29960

1. Report No.	2. Government Accession No.	3. Recipient's Catalog No.
NASA CR-174908		

4. Title and Subtitle	5. Report Date
NONLINEAR GLOBAL STABILITY ANALYSIS OF COMPRESSOR STALL PHENOMENA	June 1985
	6. Performing Organization Code
7. Author(s)	8. Performing Organization Report No.
Hamid Razavi	SSI-1076
	10. Work Unit No.
9. Performing Organization Name and Address	11. Contract or Grant No.
Scientific Systems, Inc. 54 CambridgePark Drive Cambridge, MA 02140	NAS3-24089
	13. Type of Report and Period Covered
12. Sponsoring Agency Name and Address	Contractor Report
National Aeronautics and Space Administration Washington, D.C. 20546	14. Sponsoring Agency Code

15. Supplementary Notes

Project Manager, Leon Wenzel, Powered Lift Section, Propulsion Systems Div., NASA Lewis Research Center, Cleveland, Ohio

16. Abstract

Compressor stall phenomena are analyzed from the point of view of nonlinear control theory, based on bifurcation-catastrophe techniques. This new approach appears promising and offers insight into such well-known compressor instability problems as surge and rotating stall and suggests strategies for recovery. Three interlocking dynamic nonlinear state space models are developed. It is shown that the problem of rotating stall can be viewed as an induced bifurcation of solution of the unstalled model. Hysteresis effects are shown to exist in the stall/recovery process. Surge cycles are observed for some critical parameter values. The oscillatory behavior is seen to be due to development of limit cycles, generated by Hopf bifurcation of solutions. More specifically, it is observed that at certain critical values of parameters, a family of stable limit cycles with growing and then diminishing amplitudes is generated, then giving rise to an unstable family of limit cycles. This unstable family in turn bifurcates into other unstable families. To further illustrate the utility of the methodology, some partial computation of domains is carried out, and parameter sensitivity analysis is performed.

17. Key Words (Suggested by Author(s))	18. Distribution Statement
Compressor stall, nonrecoverable stall, bifurcation techniques, compressor stability, nonlinear stability and control	Unclassified - unlimited

19. Security Classif. (of this report)	20. Security Classif. (of this page)	21. No. of pages	22. Price*
Unclassifed	Unclassified	78	